Role of the Ste20 like Kinase in Muscle Development and Muscular Dystrophy

Benjamin Pryce

Thesis submitted to the University of Ottawa in partial fulfillment of the requirements for the PhD degree in Cellular and Molecular Medicine

Department of Cellular and Molecular Medicine

Faculty of Medicine

University of Ottawa

Authorization

Much of the work in "Chapter 3 – Results: Effect of SLK Deficiency on Muscle Development and Regeneration" has been adapted from the original article "Deletion of the Ste20-like kinase SLK in skeletal muscle results in a progressive myopathy and muscle weakness" by Benjamin R. Pryce, Khalid N. Al-Zahrani, Sébastien Dufresne, Natalya Belkina, Cédrik Labrèche, Genaro Patino-Lopez, Jérôme Frenette, Stephen Shaw and Luc A. Sabourin. The article was published in as open access in Skeletal Muscle, 2017, **7**:3 (DOI 10.1186/s13395-016-0119-1). Adapted figures form this article are indicated in the Figure legends as "Adapted from Pryce et al, 2017." BioMed Central copyright and license agreement allows for derivative works to be generated from open access publications.

Abstract

Duchenne Muscular Dystrophy (DMD) is a fatal X-linked disorder affecting 1 out of every 3500 male births. The underlying cause of DMD is mutations within the dystrophin gene resulting in loss of protein expression, which leads to myofiber instability and damage. The constant damage of skeletal muscle causes sustained immune infiltration, marked by increased levels of cytokines, such as TGFβ. Interestingly, TGFβ can decrease the myogenic potential of satellite cells, thus preventing muscle regeneration. Previously, our lab has shown that knockdown of the Ste20-Like Kinase, SLK, in normal mammary epithelial cells was sufficient to delay TGFβ induced epithelial to mesenchymal transition. Therefore, we speculated that decreasing SLK levels would be sufficient to decrease the anti-myogenic effects of TGFβ both in cultured myoblasts and in a mouse model of muscular dystrophy. In the first section of this study, we explored the effect of muscle specific deletion of SLK on muscle development and regeneration. Skeletal muscle specific deletion of SLK did not impair muscle development, but caused a myopathy in older mice. Additionally, muscle regeneration was delayed, but not inhibited by SLK deletion. These findings indicated that SLK has beneficial roles in skeletal muscle, but was not absolutely required for optimal muscle development and regeneration. In the second section, we investigated the potential for SLK knockdown to mitigate the anti-myogenic effects of TGFβ *in vitro*. Decreasing levels of SLK restored myoblast differentiation in the presence of TGFβ in a p38 dependent manner. In the final section, we determined that SLK levels are elevated in dystrophic muscle and that subsequent deletion of SLK in the *mdx* mouse enhances terminal differentiation of myoblasts without further exacerbating the pathology of the disease. Collectively, this work demonstrates that SLK inhibition can provide a protective effect against the anti-myogenic effects of TGFβ via upregulation of p38 activity.

Table of Contents

List of Figures

List of Tables

List of abbreviations

°C	degrees Celsius
AAV	Adeno-associated virus
AdCre	Adenovirus for Cre recombinase
AdGFP	Adenovirus for Green Florescent Protein
AdshScr	Adenovirus for scramble short hairpin
AdshSLK	Adenovirus for short hairpin for SLK
ATCC	American Type Culture Collection
AON	Antisense oligonucleotides
ASK1	Apoptosis Signaling Kinase 1
ATH	ATI-46 Homology
bFGF	Basic Fibroblast Growth Factor
bHLH	Basic Helix Loop Helix
BMD	Becker's Muscular Dystrophy
C57	Black coated Inbred Mouse Strain
CD11b	Integrin alpha M
CD45	Lymphocyte common antigen
CD45	Lymphocyte common antigen
cDNA	Complementary DNA
cdc42	Cell division control protein 42 homolog
c-Met-	Tyrosine-protein kinase Met/hepatocyte growth factor receptor
Cre	Cre Recombinase
CTGF	Connective Tissue Growth Factor
CTX	Cardiotoxin
DAB	3,3′-Diaminobenzidine
DAPI	4′,6-diamidino-2-phenylindole
DGC	Dystroglycan Associated Complex
DMD	Duchenne Muscular Dystrophy
DMEM	Dulbecco's Modified Eagles Media
DML	Dorsomedial Lip
DNA	Deoxyribonucleic Acid
DPI	Days Post Injections
E10.5	post coitum day 10.5
E12.5	post coitum day 12.5
E13.5	post coitum day 13.5
E47	Transcription factor 3/E2A immunoglobulin enhancer-binding factor
EBD	Evan's Blue Dye
ECM	Extracellular Matrix
EDL	Extensor Digitorum Longus
eMHC	Embryonic Myosin Heavy Chain
EMT	Epithelial to Mesenchymal Transition
ERM	Ezrin/Radixin/Moesin
F4/80	EGF-like module-containing mucin-like hormone receptor-like 1
FBS	Fetal Bovine Serum
FDA	Federal Drug Administration

FGF	Fibroblast Growth Factor
FITC	Fluorescein isothiocyanate
Frt	flippase recognition target
FVB/N	Albino Inbred Mouse Strain
GAPDH	Glyceraldehyde 3-phosphate dehydrogenase
GRMD	Golden Retriever Muscular Dystrophy
GSK3β	Glycogen Synthase Kinase Beta
H&E	Haematoxylin and Eosin
HGF	Hepatocyte Growth Factor
HRP	Horse Radish Peroxidase
HS	Horse Serum
HSA	Human Skeletal Actin
IF	Immunofluorescence
IHC	Immunohistochemistry
IL-10	Interleukin 10
ILK	Integrin Linked Kinase
iNOS	Nitric oxide synthases
JNK	c-Jun N-terminal kinase
KΔC	Truncated SLK with mutated ATP binding site (lysine 63 to arginine 63)
K63R	Full length SLK with mutated ATP binding stie (lysine 63 to arginine 63)
LacZ	β-galactosidase
LOK	Lymphocyte oriented kinase
LoxP	locus of X-over P1
LPM	Lateral Plate Mesoderm
MEF2C	Myocyte Enhancer Factor 2C
Mdx	Spontaneous dystrophin knockout mouse model
MHC	Myosin heavy chain
MKK6	mitogen activated protein kinase kinase 6
mKO	muscle knockout
mRNA	messenger ribonucleic acid
MRF	myogenic regulatory factor
MST1/2	mammalian sterile 20-like kinase 1/2
MTJ	myotendinous junction
MurF1	Muscle RING-finger protein-1
MyoG	myogenin
mL	milliliter
mg	milligram
mM	millimolar
mm	millimeter
NC	notochord
NMuMG	Normal mouse mammary gland cells
NT	neural tube
Pax3	paired box gene 3
Pax7	paired box gene 7
p38	P38 mitogen-activated protein kinase
PBS	Phosphate Buffered Saline

PCR	polymerase chain reaction
PFA	paraformaldehyde
PKC	Protein kinase C
Postn	Periostin
Po	maximum tetanic tension
Pt	twitch force
PVDF	Polyvinylidene difluoride
QPCR	Quantitative Polymerase Chain Reaction
Rac1	Ras-related C3 botulinum toxin substrate 1
RhoA	Ras homolog gene family, member A
ROCK	Rho-associated protein kinase
RT	half relaxation time
SDS	Sodium dodecyl sulfate
SF	Scatter Factor
shRNA	Short hairpin RNA
SLK/STK2	Ste20-Like Kinase/Serine Threonine Kinase 2
$SLK^{fl/fl}$	Conditional SLK knockout allele
Src	Proto-oncogene tyrosine-*protein* kinase
TA	Tibialis anterior muscle
TEM	Transmission Election Microscope
TGFβ	Transforming Growth Factor Beta
TPT	time-to-peak twitch tension
μg	microgram
μL	microliter
μM	micromolar
μm	micrometer
VLL	Ventral Lateral Lip
YΔC	Truncated SLK with mutated (amino acids 1-373)

Contributions

Submitted Manuscripts

Benjamin Pryce, Khalid Al-Zahrani, Sébastien Dufresne, Natalya Belkina, Cédrik Labrèche, Genaro Patino-Lopez, Jérôme Frenette, Stephen Shaw, Luc A. Sabourin. (2016). Deletion of the Ste20-Like Kinase SLK in Skeletal Muscle Results in a Progressive Myopathy and Muscle Weakness. Skeletal Muscle. 7:3: DOI: 10.1186/s13395-016-0119-1.

Benjamin R. Pryce[*], Sarra Ahmed[*], Khalid N. Al-Zahrani, Luc A. Sabourin (2018). The LIM Domain Binding Protein 1, Ldb1, has Multiple Roles in Neu overexpressing Breast Cancer Cells. BBA Molecular Cell Research. Accepted August 2018. (* authors made equal contributions).

Jillian Conway, Khalid Al-Zahrani, **Benjamin Pryce**, Luc Sabourin (2017). Transforming Growth Factor Beta-induced Epithelial to Mesenchymal transition requires the Ste20 like kinase SLK independently of its catalytic activity. Oncotarget. 19;8(58):98745-98756. DOI: 10.18632/oncotarget.21928.

Khalid N. Al-Zahrani, Prabhjot Sekhon, Daniel R. Tessier, Julien Yockell-Lelievre, **Benjamin R. Pryce**, Kyla D. Baron, Grant A. Howe, Roshan K. Sriram, Kate Daniel, Marlene McKay, Vivian Lo, Jennifer Quizi, Christina L. Addison, Andrée Gruslin and Luc A. Sabourin. (2014). Essential role for the SLK protein kinase in embryogenesis and placental tissue development. Developmental Dynamics. 243(5): 640-641.

Roshan Sriram, Vivian Lo, **Benjamin Pryce**, Lilia Antonova, Alan Mears, Manijeh Daneshmand, Bruce McKay, Simon J. Conway, William J. Muller and Luc A. Sabourin. (2015) Loss of Periostin/OSF-2 in ErbB2/Neu-driven tumors results in Androgen Receptor-positive molecular apocrine-like tumors with reduced Notch1 activity. Breast Cancer Resarch. 17(7): **DOI:** 10.1186/s13058-014-0513-8.

Contributions by Collaborators

Dr Jerome Frenette ..... Isometric and Eccentric Contraction [Fig3.10 & Fig5.7]

Dr Michele Ardolino ..... Flow Cytometry analysis of Macrophages [Fig5.6].

Dr Steven Shaw ..... Assisted in Generating $SLK^{fl/fl}$ Model [Fig3.4]

Contributions by Lab Members

Cedrik Labreche Analysis of Paxillin and FAK activation [Fig3.12]

Core Facilities

CHEO Research Institute ..... Electron Microscopy [Fig3.9]

uOttawa Histology Core ..... Embedding Paraffin Tissue

Funding

Canadian Breast Cancer Foundation ..... Salary Support/Operating Grant

uOttawa Center for Neuromuscular Disease ..... Salary Support

Canadian Institute for Health Research ..... Operating Grant

Thesis Advisory Committee

Dr Robert Korneluk

Dr David Lohnes

Dr Michael Rudnicki

Acknowledgements

Firstly, I would like to thank my supervisor, Dr Luc Sabourin, for all the guidance provided throughout the project. He accepted me in his lab as a Masters student in 2012 and was nice enough to allow me to continue my graduate work as a PhD student under his supervision. His unique balance between optimism and pessimism helped me maintain some sense of sanity within the lab throughout the years. I strongly believe that I would not have been as successful in another environment, and I have Luc to thank for that.

I would also like to thanks my Thesis Advisory Committee, Dr David Lohnes, Dr Robert Korneluk and Dr Michael Rudnicki as well as my external comprehensive exam examiner, Dr Nadine Wiper-Bergeron. These guys have definitely kept me on track throughout the years and gave me a much needed boot in the right direction when it was required the most. They've been more than willing to talk outside of the scheduled TAC meeting to make sure that things stayed on track throughout the project.

A special thanks goes out to my lab mate Khalid Al-Zahrani. Both Khalid and I started our degrees at the same time in Luc's lab and we both faced a lot of challenges together. He's been a very strong person to have around when it comes to learning new techniques, or just talking about project directions. My experience in grad school would surely have been less productive and far less entertaining had he not been here.

Finally, I have to thank everyone else close to me, most especially Elizabeth who, although not understanding most of it, was still willing to listen to me rant and rave about my successes and failures in the lab.

Chapter 1 - Introduction

1.1 Skeletal Muscle Development and Regeneration

Skeletal muscle is a highly complex tissue making up on average 40% to total body mass in humans (Morley, Baumgartner, Roubenoff, Mayer, & Nair, 2001). The majority of skeletal muscles are derived from cells residing in the dorsal portion of the somite, termed the dermomyotome [Fig1.1] (Chal & Pourquie, 2017). These cells express the paired box transcription factors Pax3 and Pax7, as well as low levels of Myf5, a basic helix-loop-helix (bHLH) transcription factor (Gros, Manceau, Thome, & Marcelle, 2005; Kassar-Duchossoy et al., 2005). Cells of the ventrolateral lip of the dermomyotome delaminate from the somite and undergo extensive migration into the developing limb buds and diaphragm [Fig1.1] (Pu et al., 2013). Muscles that compose the body wall are generated by elongation of the dermomyotome from the dorsomedial lip (Christ, Jacob, & Jacob, 1983). Specification of myogenic precursors is controlled by the concentration of secreted morphogens (Bentzinger, Wang, & Rudnicki, 2012). For example, both Wnt1 and Wnt3a, secreted from the neural tube, have been shown to be critical for maximal expression of Pax3 and Myf5 in the developing dermomyotome (Ikeya & Takada, 1998; Parr, Shea, Vassileva, & McMahon, 1993). In contrast to Wnt, bone morphogenetic proteins (BMPs) are secreted in opposing gradient concentrations and maintain the undifferentiated cell state, inducing high levels of Pax3 while also preventing the expression of Myf5 and MyoD (Pourquie, Coltey, Breant, & Le Douarin, 1995). In addition to coordinating spatiotemporal differentiation of myogenic precursors, secreted proteins are also required to mediate cellular migration to the site of skeletal muscle formation. The most notable pro-migratory factor is hepatocyte growth factor, also known as scatter factor (HGF/SF) (Dietrich et al., 1999). HGF binds to the c-Met receptor on myoblasts to stimulate cellular migration in the direction of HGF secretion. This mechanism is involved in the delamination of cells from the

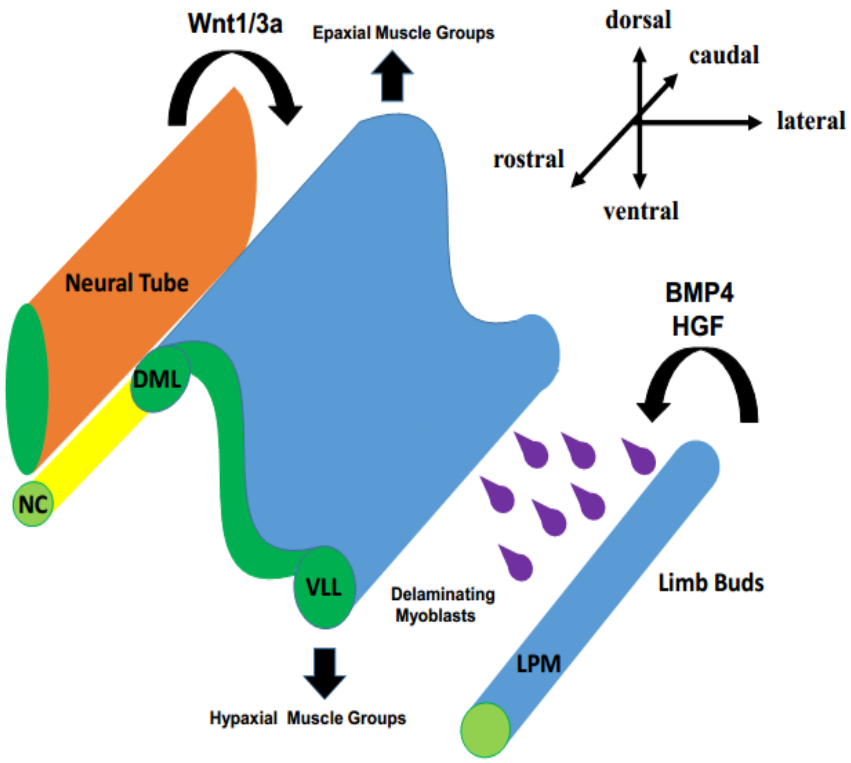

Figure 1.1: Skeletal Muscle Development during Embryogenesis. Embryonic myogenesis is under the control of various molecules secreted by the neural tube (NT) and the notochord (NC). Under the action of Wnt1/3a from the neural tube induce Myf5 expression in the in the dorsomedial lip (DML), which elongate upward from epaxial muscles groups, such as those of the torso. Secretion of BMP4 from the Lateral Plate Mesoderm (LPM) represses differentiation and maintains Pax3 expression, thus allowing cells to expand prior to differentiation. Secretion of HGF from the limb bud acts as a chemoattractant for myoblasts that delaminate from ventrolateral lip (VLL) of the dermomyotome and generate limb muscles.

dermomyotome to the developing limb buds. Mice that lack either HGF or c-Met fail to develop limb muscles due to decreased cellular migration (Bladt, Riethmacher, Isenmann, Aguzzi, & Birchmeier, 1995). Upon their arrival in the developing limb buds these cells begin to differentiate to form functional skeletal muscle.

1.1.1 Myoblast Differentiation

The process of myogenesis is coordinated by a well-defined cascade of myogenic transcription factors beginning with myogenic specification through the expression of either Pax3 or Pax7, members of the paired-homeobox domain transcription factor family [Fig1.2] (Bentzinger et al., 2012). Pax3 is critical for embryonic myogenesis as its inactivation results in embryos lacking hypaxial muscle groups (Tremblay et al., 1998). Additionally, Pax3 is required for MyoD expression during myogenesis (Tajbakhsh, Rocancourt, Cossu, & Buckingham, 1997). Interestingly, Pax7 was determined to be dispensable for the formation of skeletal muscle, but its deletion did result in muscle defects, such as smaller myofibers and the absence of satellite cells (Seale et al., 2000). Myogenesis proceeds past specification through the induction of two basic helix-loop-helix proteins (bHLH); MyoD and Myf5. Both transcription factors require E-protein heterodimerization to mediate target gene activation (Massari & Murre, 2000). Studies using single knockouts of Myf5 or MyoD showed that at least one of these transcription factors is required for myogenesis to proceed (Braun, Bichlmaier, & Cleve, 1992; Rudnicki, Braun, Hinuma, & Jaenisch, 1992). However, deletion of both MyoD and Myf5 results in severe differentiation delays indicating functional overlap between these two proteins (Rudnicki et al., 1993). Interestingly, mice lacking Myf5 or MyoD display muscle development delays in the epaxial and hypaxial groups respectively (Kablar et al., 1998). Developing muscles devoid of MyoD frequently upregulated Myf5 expression, further suggesting that these factors have

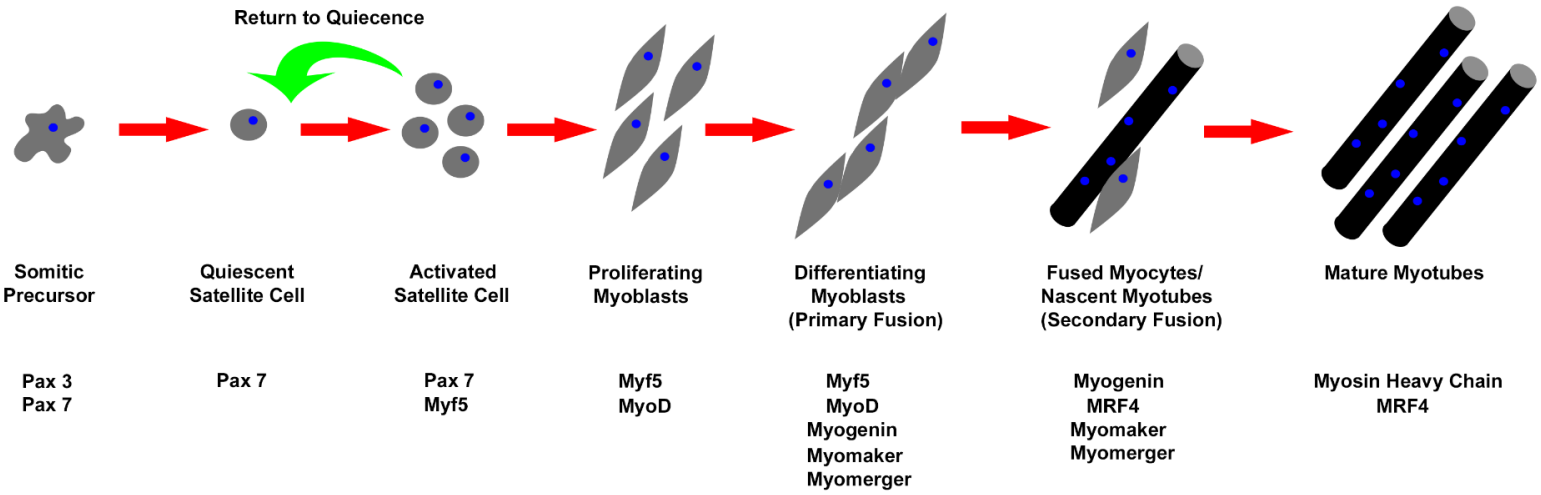

Figure 1.2: Myogenic Transcriptional Program. In the developing somite, myogenic specification is determined by the expression of Pax3 and Pax7. These cells generate the both early skeletal muscle and satellite cells present in adult muscles. Following activation by muscle damage, satellite cells begin to proliferate and differentiate into myoblasts, expressing both Myf5 and MyoD. A fraction of the satellite cells can return to quiescence (green arrow) and replenish the stem cell niche. Differentiating myoblasts begin to express late markers such as Myogenin. Expression of both Myomaker and Myomerger are also required in order to mediate efficient myoblast fusion. Primary myoblast fusion occurs between two mono-nucleated myoblasts. Secondary fusion occurs between myoblasts and nascent myotubes. Following syncytium formation, the expression of terminal differentiation markers, such as Myosin Heavy Chain and MRF4, are increased. These processes are recapitulated *in vitro* with cycling myoblasts.

some functional redundancy (Rudnicki et al., 1992). Following the expression of MyoD and Myf5, myoblasts undergo differentiation, characterized by the expression of the bHLH Myogenin (MyoG) and MRF4/Myf6, as well as terminal differentiation markers, such as myosin heavy chain (MHC) (Bentzinger et al., 2012). The co-ordinated expression of these genes is essential to form fully differentiation and functional myofibers.

Various signaling pathways converge on myogenic transcription factors in order to mediate myoblast differentiation. For example, expression of the dominant negative RhoA-GTPase inhibited the expression of myoblast differentiation markers, such as MyoD (Reuveny, Heller, & Bengal, 2004). These findings suggest that RhoA expression may be required for initiation of myogenesis. However, other reports indicate that inhibition of the Rho-associated kinase (ROCK) resulted in a drastic increase in myoblast differentiation (Iwasaki, Hayashi, Fujioka, & Sobue, 2008). Interestingly, the benefits of ROCK inhibition were only observed if induced after differentiation, whereas inhibition of ROCK in proliferating myoblasts prevented differentiation. These findings suggest that RhoA-ROCK signaling is a finally tuned process required for the induction of differentiation. The p38 MAPK pathway also has a distinct role in myoblast differentiation. Phosphorylation of E47 by p38 enhances the formation of MyoD-E47 heterodimers and is essential for myoblast differentiation to proceed (Lluis, Ballestar, Suelves, Esteller, & Munoz-Canoves, 2005). Furthermore, increased p38 activity is sufficient to drive a myogenic transcriptional program (Puri et al., 2000). However, further research has shown that p38 activity is required to be downregulated in order to form differentiated myotubes, also demonstrating tight regulation of p38 (Weston, Sampaio, Ridgeway, & Underhill, 2003).

1.1.2 Myoblast Fusion and Syncytium Formation

Differentiating myoblasts undergo extensive cell fusion to generate multinucleated functional myofibers. The fusion of differentiating myoblasts requires appropriate cellular migration, cell-cell recognition and cytoskeleton remodeling (Abmayr & Pavlath, 2012). Drosophila models were initially used to characterize myoblast fusion during muscle development due to the rapid progression of myogenesis (Bate, 1990). In contrast to mammals, each muscle in Drosophila is composed of only a single multi-nucleated myofiber (Bate & Rushton, 1993). The process of myotube formation in Drosophila begins with the specification of a single founder cells, which is the fusogenic partner for proliferating myoblasts (Dutta, Anant, Ruiz-Gomez, Bate, & VijayRaghavan, 2004). Both cells types arise from a common progenitor population and develop in close proximity to each other (Tixier, Bataille, & Jagla, 2010). Expression of surface proteins on both the founder cells and the fusion competent myoblasts are required for cell-cell recognition and subsequent fusion. For example, the protein Sticks and Stone (Sns) is expressed on the surface of myoblasts and is required to respond to Kin-of-IrreC/Dumfounded (Kirre/Duf) or Roughest/Irregular-optic-chiasma-C (Rst/Irre-C) expressing founder cells (Bour, Chakravarti, West, & Abmayr, 2000; Strunkelnberg et al., 2001). This cell-cell recognition allows for fusion, which is mediated downstream of Sns by cellular machinery regulating both cellular migration and actin cytoskeleton turnover. Proteins involved in the remodeling of the actin cytoskeleton include the GTPase Rac1 as well its downstream effector, Suppressor of cAMP Receptor/WASp family Verprolin-homologous (Scar/Wave) (Gildor, Massarwa, Shilo, & Schejter, 2009). These steps are precursors for the actual membrane fusion process. Membrane fusion itself is mediated through a variety of factors downstream of the initial cascade. Following cellular recognition, there is a rapid formation of actin rich foci in the myoblasts at the site of cellular contact

(Haralalka et al., 2011). The formation of these foci is mediated by CT10 regulator of kinase (Crk), which localizes actin polymerizing proteins, such as Arp2/3, to the sites of cell-cell contact (Kim et al., 2007). These foci develop into finger like protrusions, which invade the membrane of the founder cell and generate a pore, which are the initial sites of contact between both cell membranes (Gildor et al., 2009). Eventually, this process leads to the engulfment of the myoblasts by the founder cell, thus forming a multi-nucleated myotube.

Similar to Drosophila, mammalian myoblast fusion requires cellular migration and cell-cell recognition in order to proceed correctly (Abmayr & Pavlath, 2012). However, the steps of myoblast fusion do not require the specification of a founder cell. Instead, the fusion process occurs in two phases termed primary and secondary fusion (Hindi, Tajrishi, & Kumar, 2013). Primary fusion occurs between two myoblasts and results in the formation of small nascent myotubes. Secondary fusion occurs between nascent myotubes and myoblasts, which leads to the formation of larger myotubes. In essence, the nascent myotubes take the place of a founder cell once primary fusion has occurred. Much of the knowledge acquired on fusion mechanisms in mammalian models are derived from *in vitro* culture systems, such as C2C12 and primary myoblasts. Knockdown and knockout studies have demonstrated the importance in a variety of genes involved in cytoskeletal dynamics as well as cellular adhesion. For example, removal of β1 integrin results in severe fusion and sarcomeric defects (Schwander et al., 2003). Integrins are clustered at sites of cell-cell contact and recruit downstream factors, such as Src and FAK (Hindi et al., 2013; Lafuste et al., 2005). Deletion of FAK was found to regulate myoblast fusion through the upregulation of β1D integrin and caveolin 3 (Quach, Biressi, Reichardt, Keller, & Rando, 2009). Additionally, deletion of FAK within satellite cells resulted in decreased muscle

regeneration following cardiotoxin (CTX) induced injury (Quach et al., 2009). The Rho GTPase family has also been identified as being critical for myoblast fusion and myotube formation. Deletion of cdc42 and Rac1 both decreased the extent of fusion between myoblasts (Olson, Ashworth, & Hall, 1995). Conversely, RhoA activity is downregulated upon cellular fusion and sustained activity blocks syncytium formation (Charrasse et al., 2006). These findings demonstrate the vast array of signalling that is required to mediate maximal myoblast fusion and that deficiencies in one or more of these proteins can have adverse effects on skeletal muscle formation.

The identification of proteins specifically required for myoblast fusion in mammals has been a subject of much research. Until recently, the existence of muscle specific fusogenic proteins was not known, with regulators of myoblast fusion being expressed in both myogenic and non-myogenic tissue. Therefore, it remained unclear as to how myoblast fusion could be induced by these ubiquitous pathways. However, recent studies have demonstrated that myomaker, a transmembrane protein expressed exclusively in differentiating myoblasts, was critical for the formation of multi-nucleated myotubes (Millay et al., 2013). Myomaker null mice were born with no formed musculature, and satellite cells lacking myomaker were incapable of regenerating damaged muscle (Millay et al., 2013; Millay, Sutherland, Bassel-Duby, & Olson, 2014). Interestingly, differentiated myocytes were present within the myogenic compartments indicating that myomaker deficiency had no impact on differentiation. Furthermore, ectopic expression of myomaker in fibroblasts induced fusion to myoblasts, but not to other fibroblasts (Millay et al., 2013). This suggested that myomaker was acting in concert with additional myogenic factors to mediate a muscle specific cellular fusion mechanism. Indeed, three

independent follow-up studies identified a second muscle specific protein which was termed myomerger (also known as myomixer-minion) that was mediating myoblast fusion (Bi et al., 2017; Quinn et al., 2017; Q. Zhang et al., 2017). When myomerger was expressed in combination with myomaker, fibroblasts readily fused together in multi-nucleated cells. Furthermore, it was found that only one fusion partner required myomerger expression, whereas myomaker was required in both cells. These findings demonstrated that muscle specific fusion proteins exist and are absolutely essential in the mechanisms mediating muscle formation.

1.1.3 Muscle Regeneration and Satellite Cells

Satellite cells are mono-nucleated skeletal muscle stem cells that mediate muscle regeneration. These cells arise from a Pax3 and Pax7 expressing population that is localized to the dermomyotome during embryogenesis (Schienda et al., 2006). They take up residence around differentiated myofibers and continue to express Pax7 (Mauro, 1961; Seale et al., 2000). Satellite cells remain mitotically quiescent until activated by muscle damage (Schultz, Gibson, & Champion, 1978). Skeletal muscle is most often times damaged via mechanical trauma from either normal use or over exertion. During mechanical trauma, the plasma membrane of the myofiber ruptures, leading to spillage of intracellular material (Hamer, McGeachie, Davies, & Grounds, 2002). This causes an acute immune response mediating the removal of cellular debris to stimulate the regeneration process (Tidball, 1995). The secretion of various factors such as FGF and HGF, at or near the damaged muscle contributes to satellite cell activation (DiMario, Buffinger, Yamada, & Strohman, 1989; Tatsumi, Anderson, Nevoret, Halevy, & Allen, 1998). Following activation, the satellite cells undergo extensive proliferation to generate a myoblast population capable of fusing and regenerating damaged muscle. During this phase, satellite cells undergo either a symmetric or asymmetric cellular division (Kuang, Kuroda, Le Grand, &

Rudnicki, 2007). Symmetric cellular division occurs parallel to the plane of the myofiber and leads to two identical Pax7-expressing daughter cells. These cells eventually generate enough Pax7 expressing cells to replenish the stem cell niche upon resolution of muscle damage. In contrast, asymmetric cellular division occurs perpendicular to the plane of the myofiber, and results in two distinct cells; a satellite stem cell and a committed myogenic precursor. Following expansion of these respective cell types, satellite cells return to quiescence in order to replenish the stem cell pool while committed myoblasts fuse to repair damaged muscle.

1.2 Muscular Dystrophy

Muscular dystrophies are a group of related diseases characterised by progressive muscle damage and loss of muscle function (Bertini, D'Amico, Gualandi, & Petrini, 2011). Initially, muscular dystrophies were categorized based on their clinical manifestations as well as the age at which they were diagnosed rather than the underlying mutation in the causative genes. However, with the advent of genetic sequencing, it became clear that mutations in different genes could have similar phenotypic outcomes, such as muscle damage and loss of ambulation (Shin, Tajrishi, Ogura, & Kumar, 2013). Typically, mutations in genes encoding proteins critical for myofiber stability are the underlying cause of most muscular dystrophy subtypes. In some cases, muscular dystrophies are associated with non-skeletal muscle symptoms, such as decreased mental capacity or gastrointestinal dysfunction (Bellini et al., 2006; D'Angelo et al., 2011). The heterogeneity of muscular dystrophies are such that symptoms can manifest early in childhood to late in adulthood (Bertini et al., 2011; Lewis, 1966)

1.2.1 Duchenne Muscular Dystrophy

Duchenne Muscular Dystrophy (DMD) is the most common muscular dystrophy affecting approximately 1 in every 3500 male births (Salmaninejad et al., 2018). DMD arises through mutations within the dystrophin gene, located on the X chromosome (Hoffman, Brown, & Kunkel, 1987). These mutations lead to a frame shift and subsequent disruption of the coding sequence, which results in the loss of functional dystrophin expression (Salmaninejad et al., 2018). Various mutations within the dystrophin gene have been reported to cause DMD with the majority of cases being caused by duplication events. Overall, patients with DMD usually become symptomatic in their early teens and lose ambulation before their twenties. Most DMD patients only survive until their early twenties with the most common cause of death being either respiratory or cardiac failure due to both decreased diaphragm function and an underlying cardiomyopathy (Fayssoil, Nardi, Orlikowski, & Annane, 2010). Currently, no robust therapies, asides from corticosteroids, are readily available to mitigate disease progression (Kim et al., 2015). The closely related Becker's Muscular Dystrophy (BMD) also arises from mutations within the DMD gene (Akita et al., 1987; Flanigan, 2014). However, unlike DMD, the mutations in BMD keep the reading frame intact, which result in truncated dystrophin products due to exon skipping. BMD patients are also less symptomatic and have a longer lifespan compared to DMD patients.

Dystrophin is required for anchoring the dystrophin-associated glycoprotein complex (DGC) to the actin cytoskeleton [Fig1.3] (Hoffman et al., 1987; Hoffman & Kunkel, 1989). When dystrophin is absent, the lack of this attachment makes the myofiber more susceptible to

contraction induced injury. However, other functionally related proteins, such as the dystrophin homologue utrophin or integrin complexes, can partially restore this attachment [Fig1.3] (Heller et al., 2013; Peladeau, Adam, & Jasmin, 2018). Overexpression of these functionally related proteins can restore muscle function and integrity in animal models of DMD. However, the lack of dystrophin is still severely deleterious to myofiber stability, indicating that dystrophin is absolutely essential for mature myofiber integrity. Furthermore, deletion of these compensating proteins severely worsens the pathology of dystrophic mice (Guo et al., 2006; McDonald, Hebert, Kunz, Ralles, & McLoon, 2015). Recent evidence suggests that dystrophin also plays a role in the polarity of satellite cells (Dumont et al., 2015). Satellite cells from dystrophin-deficient mice were incapable of localizing Pard3 properly, thus leading to a lack of polarization and improper asymmetric cell division. This effectively reduces the number of myogenic precursors available to regenerate damaged skeletal muscle, further exacerbating the progression of DMD.

1.2.2 Disease Progression and Aberrant Cellular Signaling in Muscular Dystrophy

In DMD, the breakdown of myofibers causes the release of intracellular material which in turn stimulates an immune response (Jarvinen, Kaariainen, Jarvinen, & Kalimo, 2000; St Pierre & Tidball, 1994). In acute muscle damage, there is a transient inflammatory response that is resolved upon muscle regeneration (Chazaud et al., 2003)
. The initial infiltration consists of M1 (pro-inflammatory, iNOS+) macrophages required to remove necrotic and damaged myofibers and stimulate myoblast proliferation, thus providing the necessary environment for the generation of new myofibers (Villalta, Nguyen, Deng, Gotoh, & Tidball, 2009). Following the initial infiltration there is a subsequent increase in M2 (anti-inflammatory, CD206+) macrophages which have been shown to stimulate muscle regeneration

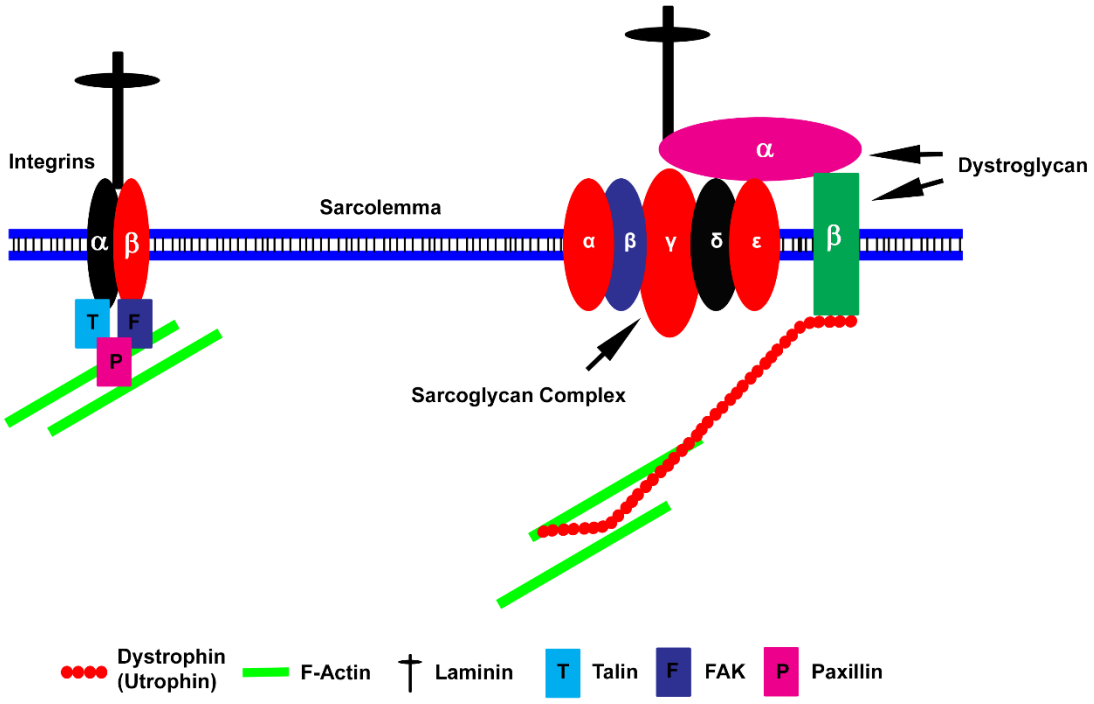

Figure 1.3: Structural Proteins Mediating Myofiber Stability. Schematic drawing of the DGC complex. Dystrophin (or utrophin) complexes with dystroglycan, which binds to extracellular matrix proteins (laminin). Intracellularly, dystrophin binds to actin, thus stabilizing the sarcolemma. In addition to the DGC, integrin complexes can mediate binding to extracellular proteins and similarly stabilize the membrane. Alterations in the composition of the DGC or the integrin complex lead to deficiencies in myofiber integrity and increased muscle damage. This is observed upon the loss of dystrophin or the integrin complexes.

by secretion of cytokines, such as IL-10 (Villalta et al., 2011). However, consistent muscle damage in muscular dystrophy causes a sustained inflammatory response without resolution, as newly regenerated fibers are also susceptible to muscle damage (Porter et al., 2002). The sustained immune infiltration causes an increase in anti-myogenic and pro-fibrotic cytokines, thus leading to increased fibrosis, inhibiting muscle regeneration (N. Deconinck & Dan, 2007). The increased fibrosis further decreases muscle function and worsens the pathology (Desguerre et al., 2009). Interestingly, altering the immune response in favour of regeneration has a significant benefit in reversing disease progression (Capote et al., 2016; Giordano et al., 2015; Serra et al., 2012).

Transforming Growth Factor β (TGFβ) is one of the numerous factors secreted during the initial inflammatory response (Song et al., 2017; Zhou et al., 2006). TGFβ is a member of a family of growth factors that also includes BMPs and activin ligands (Weiss & Attisano, 2013). TGFβ stimulation promotes the expression of extracellular matrix proteins and increases fibrosis in many disease states (Taniguti, Pertille, Matsumura, Santo Neto, & Marques, 2011; Yamazaki et al., 1994). The TGFβ ligand functions by binding to its type 2 serine/threonine kinase receptor, and causes dimerization with the type 1 receptor (Wrana et al., 1992). This leads to direct phosphorylation of the R-Smads (ex. Smad 2/3) by the receptor kinase (Heldin, Miyazono, & ten Dijke, 1997). Subsequent binding of the R-Smads with the Co-Smads (ex. Smad4) leads to nuclear localization of the complex and activation of target genes (Derynck, Zhang, & Feng, 1998). An inhibitory feedback loop exists that consists of inhibitory Smads (I-Smads, Smad7) which inhibits TGFβ signalling by interacting with the receptor and preventing phosphorylation of R-Smads (Nakao et al., 1997). This pathway of activation is similar to other cytokines of the

TGF superfamily, and varies mainly in the receptors that mediate ligand binding, as well as the downstream Smads that are activated. Myostatin, predominantly expressed in muscle tissue, belongs to the TGFβ cytokine superfamily and activates intracellular signalling by binding to the activin type IIA or IIB receptor (Lee & McPherron, 2001; McPherron, Lawler, & Lee, 1997). The intracellular signalling cascade that occurs is similar to that of TGFβ.

TGFβ signalling causes the upregulation of several downstream transcription factors, such as Snai1/2 (Miyazono, 2009). Snail is of particular importance during epithelial to mesenchymal transition (EMT), where it binds to the promoter of E-cadherin and downregulates its expression, leading to the mesenchymal phenotype (Cano et al., 2000). In addition to the canonical Smad signalling pathways, TGFβ can also activate various pathways, such as the RhoA-GTPase (Bhowmick et al., 2001). Treatment of epithelial cells with TGFβ leads to a rapid induction of RhoA activity and subsequent actin stress fiber formation. This was found to be independent of Smad2/3 activation. This is particularly interesting in myoblasts, where decreased activity of RhoA and the downstream Rho-associated protein kinase (ROCK) increased differentiation (Iwasaki et al., 2008). Additionally, TGFβ has been shown to mediate p38 signaling (Yu, Hebert, & Zhang, 2002).

Evidence for TGFβ's anti-myogenic effects was initially shown in cultured myoblasts, where treatment with TGFβ significantly decreased the capacity of myoblasts to differentiate (D. Liu, Black, & Derynck, 2001; D. Liu, Kang, & Derynck, 2004). Furthermore, over-expression of TGFβ in skeletal muscle caused muscular atrophy, fibrosis and stimulation of endogenous TGFβ expression in a feed-forward activation loop (Narola, Pandey, Glick, & Chen, 2013). In addition,

enhanced TGFβ activity causes accumulation of fibrotic material, thus reducing muscle function. Therefore, it is speculated that TGFβ acts in two ways in muscular dystrophy; 1) by increasing the accumulation of fibrotic material and 2) by inhibiting the activation, proliferation and differentiation of satellite cells, thus further impeding muscle regeneration (Burks & Cohn, 2011). Mitigating TGFβ signalling has been effective in restoring muscle function in several models of muscular dystrophy. For example, treatment with TGFβ receptor inhibitors increased the diaphragm function in an animal model of DMD (Nelson et al., 2011). Additionally, the over-expression of a dominant negative TGFβ receptor in skeletal muscle improved the pathology in δ-sarcoglycan deficient mice, a model of limb girdle muscular dystrophy, by both increasing muscle function and decreasing fibrosis (Accornero et al., 2014). Therefore, TGFβ signaling is an important mediator of the downstream pathological features of muscular dystrophy.

1.2.3 Animal models of DMD

Much of the knowledge acquired with regards to DMD was first established in animal models of the disease. The spontaneous dystrophin-null mouse model, dubbed the *mdx* mouse, was discovered and characterized prior to the identification of the dystrophin gene [Fig1.4] (Bulfield, Siller, Wight, & Moore, 1984; Tanabe, Esaki, & Nomura, 1986). The causative nonsense mutation (C→T) is located within exon 23 and prevents full length dystrophin expression (Sicinski et al., 1989). The disease progression parallels some of the pathologies observed in DMD, with increased serum creatine kinase levels and decreased muscle function (Kobayashi, Rader, Crawford, & Campbell, 2012). However, *mdx* mice do not have the dramatic decreased lifespan seen in DMD patients (McGreevy, Hakim, McIntosh, & Duan, 2015). Additionally, the

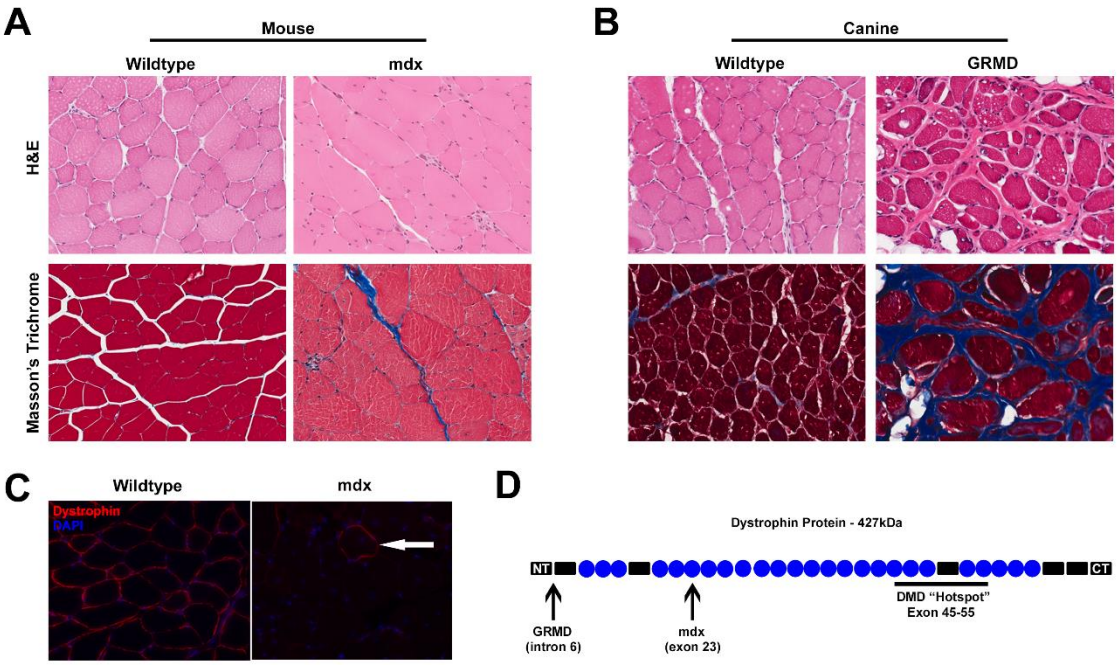

Figure 1.4: Duchenne Muscular Dystrophy (DMD). (A) Muscle sections from the diaphragm of wildtype and mdx mice stained with heamotoxylin and eosin (top) showing a higher proportion of central nuclei, indicating ongoing muscle regeneration. Masson's Trichome staining (bottom) demonstrates fibrosis and collagen deposition (blue) in dystrophic muscle. (B) Muscles sections from wildtype and Golden Retriever Muscular Dystrophy (GRMD) dogs show a more dramatic phenotype compared to the *mdx* mouse, with fibrosis evident in both H&E and Masson's Trichome staining. (C) Staining for dystrophin in wildtype (left) and *mdx* (right) muscle sections. Occasionally, dystrophin staining can be observed due to exon-skipping (white arrow). (D) Schematic of the dystrophin protein, indicating locations of mutations in the *mdx* and GRMD models, as well as the mutation "hot spot" for Duchenne Muscular Dystrophy.

pathological features are much less severe, with lower immune infiltration, fibrosis and muscle necrosis when compared to other animal models of DMD. Functionally homologous proteins, such as utrophin and α7 integrin, are frequently upregulated in *mdx* and DMD in order to compensate for the loss of dystrophin and maintain myofiber integrity (Dowling, Culligan, & Ohlendieck, 2002; Hodges et al., 1997). Nevertheless, there is still a considerable decrease in muscle function in the *mdx* mice, making it a useful model to study DMD. A more severe animal model has been developed in which utrophin knockout mice were crossed with the *mdx* strain, generating the *mdx*/utrophin double knockout model (A. E. Deconinck et al., 1997). Mice lacking both proteins had a more dramatic phenotype and reduced lifespan (Isaac et al., 2013). Similar findings have been found using a dystrophin/α7 integrin double null animal (Guo et al., 2006; McDonald et al., 2015). Additional spontaneous dystrophin mutations have been identified and studied in mice, with variable phenotypic outcomes (McGreevy et al., 2015).

In addition to mouse models there are a number of canine DMD models, the most studied being the Golden Retriever Muscular Dystrophy (GRMD) model [Fig1.4] (Cooper, Valentine, Wilson, Patterson, & Concannon, 1988; Kornegay, Tuler, Miller, & Levesque, 1988). Similar to the *mdx* mouse, the GRMD model was characterized prior to the identification of the dystrophin gene. The GRMD model is caused by a mutation within the intron six of the dystrophin gene, causing an aberrant splice variant that results in an out of frame product (Sharp et al., 1992). However, unlike the *mdx* mouse, the GRMD has a severe pathological phenotype closely related to that of DMD patients. Decreased lifespan is sometimes noted in GRMD dogs compared to wildtype littermates, with cardiac and respiratory failure being the primary cause of death (Ait Mou et al., 2018). The GRMD model has been instrumental in identifying genetic modifiers of DMD, such

as Jagged1, and validating the reproducibility of findings in the *mdx* mouse model (Vieira et al., 2015). Additionally, its use as a preclinical model has been useful in identifying biomarkers of DMD (Barthelemy et al., 2014; Barthelemy et al., 2012).

1.2.4 Treatment Options for Duchenne Muscular Dystrophy

Current therapies for DMD are directed at alleviating some of the more severe pathological side effects of muscular dystrophy that limit muscle function rather than correct the underlying cause of the disease. The most commonly used therapy is corticosteroid treatment (Kim et al., 2015). The mechanism by which steroid treatment can sustain muscle function is not well defined. Some of the possible beneficial effects of steroids have been postulated to be increased myoblast proliferation and decreased proteolysis in myofibers (Guerriero & Florini, 1978; Han, Yang, & Kao, 2017). More well-known is the effect of steroid treatment on reducing the inflammatory response in muscular dystrophy, thus preserving muscle function (Hussein et al., 2006). However, steroid based therapy is prone to side effects, such as the induction of muscular atrophy, and does not completely reverse disease progression (Sassoon et al., 2008; Waddell et al., 2008). Therefore, novel therapeutic targets are required to treat DMD.

The clinical outcome of DMD and BMD differ greatly, with DMD patients showing severe loss of muscle function at an earlier age than BMD patients (Hu et al., 1988). The difference in disease progression is due to the retention of altered dystrophin protein products in BMD patients compared to the complete absence of dystrophin protein expression in DMD patients. These findings indicate that full length dystrophin is not necessarily required to retain muscle function. It is from these observations that treatment options such as mini-dystrophin gene replacement

and exon-skipping, were derived (Cirak et al., 2011; Li et al., 2006; Miskew Nichols et al., 2016). These approaches have been successful in animal models of DMD in rescuing much of the pathology associated with disease progression. For example, mini-dystrophin replacement therapy for *mdx* mice greatly reduced the severity of disease progression (Li et al., 2006). The concept of exon skipping has existed for some time and has been the subject of much research (Miskew Nichols et al., 2016). Numerous studies have demonstrated that directed exon skipping using antisense-oligonucleotides (AON) to remove the portion of the dystrophin gene containing the causative mutation greatly improves disease outcome in animal models. These therapies show promise in clinical trials with Eteplirsen (targeting exon 51 to trigger its excision) being approved for use by the Federal Drug Administration (FDA) (Charleston et al., 2018; Irwin & Herink, 2017; Mendell et al., 2013). This therapy is useful in patients with mutations in exon 51 and accounts for approximately 14% of DMD cases.

Arguably the most direct and possibly the most effective means to treat muscular dystrophy would be the correction of the underlying cause of the disease. In the case of muscular dystrophy, successful correction of the mutation within the *mdx* mouse using Crispr/Cas9 directed methods has been achieved (Long et al., 2016; Xu et al., 2016; P. Zhu et al., 2017). A recent study indicated that targeting the precise mutation within exon 53 in the *mdx*^{4cv} model as well as a strategy to remove exons 52 and 53 was effective in increasing dystrophin expression (Bengtsson et al., 2017). This approach is of particular interest as correcting the mutation would restore dystrophin expression permanently and would not require continued treatment. However, the appropriate delivery method is also required in order to correct the causative mutation in a larger proportion of myogenic cells. Recent studies have taken advantage of a modified

Cripsr/Cas9 system that leads to gene activation as opposed to DNA breaks and repair (Liao et al., 2017). Experiments in the *mdx* model targeted upregulation of utrophin. Delivering this construct using AAV vectors was capable of increasing utrophin expression and rescuing muscle function (Liao et al., 2017). Additional experiments were conducted targeting the over-expression of follistatin and demonstrated similar results. These will undoubtedly be the subject of further investigations in order to restore muscle function in dystrophic patients.

An alternative approach to treat muscular dystrophy is to target upregulated pathways and proteins contributing to disease progression. For example, deletion of several proteins upregulated in muscular dystrophy, such as Periostin, Sacrolipin and Connective Tissue Growth Factor (CTGF), delayed disease progression in animal models of muscular dystrophy (Lorts, Schwanekamp, Baudino, McNally, & Molkentin, 2012; Morales et al., 2013; Voit et al., 2017). These may represent possible therapeutic targets to alleviate the downstream pathology without correcting the underlying defect leading to the disease. Similarly, inhibition of TGFβ signalling in animal models of muscular dystrophy showed drastic increases in muscle function and regeneration making it a valuable therapeutic target (Accornero et al., 2014; Nelson et al., 2011). However, attempts to utilize TGFβ signaling as a clinical target have been unsuccessful (Guiraud & Davies, 2017). Therefore, novel targets controlling TGFβ signaling are required in order to suppress its adverse effects while retaining muscle function.

1.3 The Ste20-Like Kinase

The Ste20-Like Kinase, SLK/STK2, is a ubiquitously expressed serine/threonine kinase which is 1202 amino acids in length and consists of three distinct domains; an N-terminal kinase domain,

a central coiled-coiled domain and a C-terminal "ATH" domain [Fig1.5] (Itoh et al., 1997; Sabourin & Rudnicki, 1999; Yamada et al., 2000). The kinase domain shares extensive homology to the lymphocyte oriented kinase (LOK) and the Ste20 kinases MST1 and MST2 (Sabourin & Rudnicki, 1999). The kinase domain of SLK also contains the Ste20 signature motif TPYWMAPE. SLK has been shown to be phosphorylated at Serine 189 and Threonine 183, both of which are found within the activation segment. The central coiled-coiled domain contains a putative SH3 binding site. The central region also contains a putative caspase 3 cleavage site (DXXD). The C-terminal domain shares homology to the C-terminal portion of LOK. Additionally the C-terminal region of SLK appears to be critical for the binding of co-factors, such as Ldb1/2, which negatively regulate SLK kinase activity (Storbeck et al., 2009). In order to be activated, SLK forms a dimer in a trans-orientation, which leads to phosphorylation on sites S189 and T183 (Delarosa et al., 2011; Luhovy, Jaberi, Papillon, Guillemette, & Cybulsky, 2012).

1.3.1 Cellular Roles of SLK

SLK was initially characterized as a mediator of apoptosis. Over-expression of an active SLK construct resulted in activation of c-Jun N-terminal kinase (JNK1) and actin stress fiber dissolution (Sabourin, Tamai, Seale, Wagner, & Rudnicki, 2000). Additionally, the treatment of multiple cell lines with apoptotic stimuli induced SLK cleavage downstream of caspase 3. SLK's role in apoptosis has also been revealed *in vivo* where overexpression of SLK in kidney glomerular podocytes induced injury and cell death (Hao et al., 2006). Subsequent investigations into SLK's cellular function revealed prominent roles in both proliferation and migration. Overexpression of the truncated dominant negative SLK construct decreased cellular

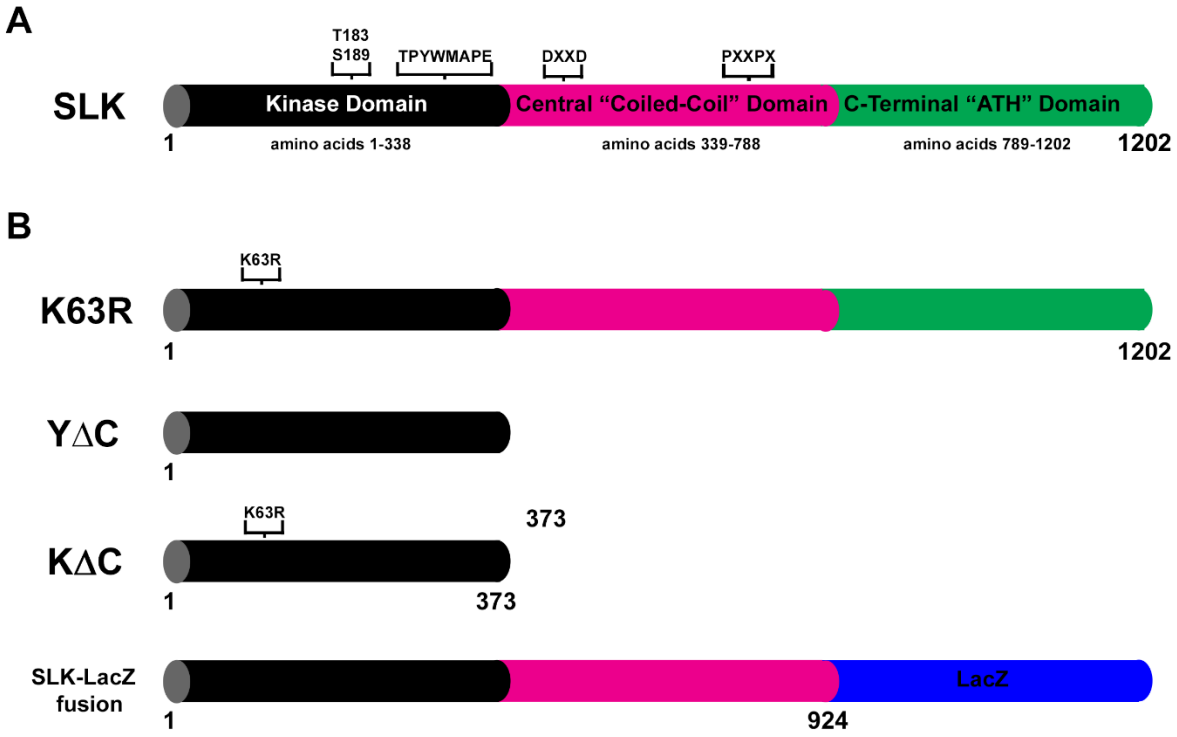

Figure 1.5: Schematic of the Ste20-Like Kinase. (A) Full length SLK contains three domains; an N-terminal Kinase Domain, a Central "Coiled-Coil" region and a C-Terminal "ATH" Domain. The kinase domain contains the ATP binding site at lysine 63 (K63), the auto phosphorylation sites (T183 and S189) as well as the Ste20 consensus sequence (TPYWMAPE). The coiled-coil domain contains a caspase 3 cleavage site (DXXD) as well as the putative SH3 binding domain (PXXPX). The C-terminal ATH domain is critical for binding SLK regulatory proteins, such as Ldb1/2. (B) Mutants used in this study. The K63R mutant replaces the lysine 63 residue with an arginine, preventing ATP binding. The YΔC mutant is the truncated kinase domain comprising amino acids 1-373, and the KΔC is the truncated kinase domain containing the K63R mutation. The SLK-LacZ fusion protein was generated from a gene-trap allele. The C-terminal domain is replaced with LacZ after exon 10 (amino acid 24) of the SLK coding sequence and renders the kinase domain incapable of phosphorylating substrate.

proliferation, caused a G2/M transition block and prevented downregulation of cyclin A (O'Reilly et al., 2005). SLK was also found to be critical for radial array microtubule localization and dynactin localization to the centrosome (Burakov et al., 2008; Zhapparova, Fokin, Vorobyeva, Bryantseva, & Nadezhdina, 2013). The focal adhesion kinase (FAK) was found to be important for SLK kinase activity during cellular migration (Wagner et al., 2008). Paxillin, another integral component of the focal adhesion complex, was found to be phosphorylated directly by SLK (Quizi et al., 2013). This phosphorylation was essential for focal adhesion turnover and cellular migration. Further supporting its role in cytoskeletal dynamics, SLK has been shown to phosphorylate RhoA on serine 188, which mediates RhoA activity and degradation (Guilluy et al., 2008). These findings indicate that SLK is controlling various aspects of cytoskeletal dynamics and critical processes required for cellular function.

Further studies from our lab suggest that SLK has an essential role in ErbB2/HER2+ breast cancer progression (Roovers et al., 2009). SLK activity was upregulated downstream of ErbB2 and was required for heregulin induced cellular migration and invasion. More recently, SLK knockdown was shown to delay TGFβ induced Epithelial to Mesenchymal Transition (EMT) in normal mouse mammary epithelial cells (NMuMGs) (Conway, Al-Zahrani, Pryce, Abou-Hamad, & Sabourin, 2017). This was later determined to be independent of the canonical TGFβ response, as Smad3 activity was unchanged following SLK knockdown. However, the expression of several TGFβ target genes were affected. Additionally, these effects were found to be independent of SLK kinase activity. These findings require further investigation to better understand the role of SLK in breast cancer development.

1.3.2 SLK is Essential for Embryogenesis

A SLK knockout model was generated to better understand SLK's role in development and diseases such as breast cancer. This was generated through a gene-trap allele, where the C-terminal portion of SLK was replaced with LacZ (Al-Zahrani et al., 2014). This fusion protein rendered SLK incapable of phosphorylating exogenous substrates. Heterozygote mice for the SLK-LacZ fusion were phenotypically indistinguishable from wildtype siblings. However, homozygote SLK-LacZ fusion mice developed severe morphological defects between E12.5 and E14.5 and did not survive to birth. Assessments of E14.5 embryos revealed significant lack of expansion of various tissues. Additionally, homozygotes demonstrated decreased angiogenesis in the placenta, which was speculated to be the cause of lethality. Therefore, active SLK appears to be required for embryogenesis to progress normally.

1.3.3 SLK Expression and Function in Skeletal Muscle

Mouse SLK was initially identified in a yeast-two hybrid screen with MyoD (Sabourin & Rudnicki, 1999). However, this interaction was later verified to be a false positive, as SLK and MyoD did not bind directly to each other in subsequent assays. Additionally, it was observed that mature skeletal muscle has lower SLK levels than other tissues (Y. H. Zhang et al., 2002). Nevertheless, a considerable amount of work was conducted on SLK in skeletal muscle and myoblasts. Initial investigations revealed that SLK was predominantly expressed within the slow-twitch type 1 fibers rather than fast-twitch type 2 fibers (Storbeck et al., 2004). SLK was localized with α actinin at the I-band and neuromuscular junctions, possibly implicating it in neurotransmitter signalling and organization of synapses. Expression of a dominant negative/truncated SLK construct (KΔC) in C2C12 myoblasts reduced myoblast fusion and

blocked terminal differentiation. Therefore, it was initially thought that SLK was absolutely required for myogenesis. A transgenic animal model was designed in which the full length inactive kinase was expressed from the human skeletal actin promoter (HSA-K63R) (Storbeck et al., 2013). However, HSA-K63R expressing mice were viable with no overwhelming defects in skeletal muscle development. The HSA-K63R mice also had enhanced muscle regeneration following cardiotoxin (CTX) injections. Primary myoblasts isolated from HSA-K63R mice demonstrated increased myoblast fusion and differentiation. Therefore, a direct role for SLK in myoblast fusion and differentiation could not be determined based on these studies alone.

1.4 Thesis Objectives and Hypotheses

Previous work by our lab demonstrated increased SLK expression in developing skeletal muscle. Additionally, expression of a dominant negative SLK construct blocked differentiation and fusion of C2C12 myoblasts, but did not impair skeletal muscle development in the HSA-K63R (Storbeck et al., 2013; Storbeck et al., 2004). Recently, we observed that SLK knockdown was able to delay TGFβ–induced EMT (Conway et al., 2017). Given that treatment of myoblasts with TGFβ inhibits myoblast differentiation, we speculated that SLK deletion may reverse this effect (D. Liu et al., 2004; S. Zhu, Goldschmidt-Clermont, & Dong, 2004). This is relevant in the context of muscular dystrophy, where increased TGFβ can inhibit satellite cell activation and myoblast differentiation (Burks & Cohn, 2011). To test this hypothesis, we generated a muscle specific SLK knockout using the Myf5-Cre recombinase model to assess muscle function in both a normal and an *mdx* background.

In the first objective, we determined that SLK was not essential for skeletal muscle development or muscle regeneration. However, SLK deletion caused a mild myopathy in older mice suggesting that it was necessary for myofiber integrity. In the second objective, we determined that SLK knockdown was sufficient to render myoblasts resistant to the anti-myogenic effects of TGFβ through upregulation of p38 activity. Finally, in the third objective we found that SLK levels were significantly elevated in dystrophic muscle. Furthermore, we determined that SLK deletion in the *mdx* background increased the expression of terminal differentiation markers. These results suggested that SLK inhibition is a novel means to upregulate muscle regeneration in dystrophic muscle.

Chapter 2 - Materials and Methods

2.1 Antibodies

Antibodies used in this study, along with speci concentrations for experiments used, as well as manufacturer and catalogue numbers, have been listed in Table 1.

2.2 Cell Culture and Treatments

C2C12 myoblasts (ATCC) were cultured at 37ºC and 5% CO2 in DMEM (Dulbecco's Modification of Eagle's Medium, Thermo Fisher), supplemented with 10% fetal bovine serum (FBS) and 200U/mL or streptomycin/penicillin (Invitrogen). For adenovirus infections, equal multiplicity of infection (MOI) were used to infect cells at ~70% density with either AdScramble of AdshSLK virus. Alternatively, stable shSLK lines were made using lentiviral infection and hygromycin selection. Transfections were performed at ~70% density using lipofectamine reagent (Invitrogen). Myoblasts were differentiated in 2% Horse Serum (HS) DMEM media for up to 96 hours. Recombinant TGFβ (Sigma) was used for treatment of cells in either 10% FBS or 2%HS at the concentration indicated. Primary myoblast cultures were isolated as previously described. Briefly, hind leg muscles from 6 week old mice were minced and digested in 0.1% collagenase/dispase solution (Roche). Cells were collected and grown in Ham's F-10 media (Sigma-Aldrich, St Louis MO, USA). Medium was supplemented with 10ng/mL bFGF (Thermo Fisher) and 10% FBS. For proliferation assays, cells were infected with indicated virus and seeded at $5x10^4$ cells/6 cm plate 48 hours post infection (Day 0). Each treatment time point had triplicate biological samples which were counted in duplicate. Proliferation assays were repeated three times and averaged. For Smad4 luciferase assay, the pBV-Luc Smad-Binding Element Reporter (SBE4) or the E-box reporter in combination with the loading control pRL Renilla

Table 1: List of Antibodies and working Dilutions for Specific Applicaitons

Antibody	Manufacturer/Catalogue#	Applications
SLK	Custom Antibody	WB 1:10000, IF 1:1000, IP 1:500
Myogenin	Santa Cruz, sc-12732	WB 1:500, IF 1:100
β Catenin	Sigma, C7082	IF 1:200
MF20	R&D, MAB4470	WB 1:1000, IF 1:200
MHC slow (Type1)	Sigma, M8421	IF 1:1000
MHC fast (Type2)	Sigma, M4276	IF 1:1000
P-GSK3β (S9)	Cell Signalling, 9322	WB 1:1000
GSK3β	Cell Signalling, 9315	WB 1:1000
P-ERM	Cell Signalling, 3141	WB 1:1000
ERM	Cell Signalling, 3142	WB 1:1000
P-Paxillin (S 250)	Custom	WB 1:2000
P-Paxillin (Y 118)	Cell Signalling, 2541	WB 1:1000
Paxillin	BD Bioscience, 610569	WB 1:2000, IF 1:250
P-YAP (S127)	Cell Signalling, 4911	WB 1:1000
YAP	Cell Signalling, 4912	WB 1:1000
P-FAK (Y397)	Cell Signalling, 3283	WB 1:1000
FAK	Cell Signalling, 3285	WB 1:1000, IF 1:200
P-JNK (T183/Y185)	Cell Signalling, 9251	WB 1:1000
α tubulin	Sigma, T9026	WB 1:10000
GAPDH	Cell Signalling, 2118	WB 1:1000

JNK1	**Cell Signalling, 9252**	**WB 1:1000**
P-p38 (T180,Y182)	**Cell Signalling, 9211**	**WB 1:1000**
p38	**Cell Signalling, 9212**	**WB 1:1000**
Dystrophin	**Abcam, ab15277**	**IF 1:500**
Laminin	**Abcam, ab11575**	**IF/IHC 1:500**
Vinculin	**Santa Cruz, sc-25336**	**WB 1:500, IF 1:200**
Pax7	**R&D, MAB1675**	**IHC 1:100**
Myf5	**Santa Cruz, sc-518039**	**IHC 1:100**
CD45	**Biolegend, 103130**	**FC 1:50**
CD11b	**BD, 563015**	**FC 1:50**
F4/80	**Biolegend, 123122**	**FC 1:100**
CD206	**Biolegend, 141719**	**FC 1:50**
iNOS-FITC	**BD, 610330**	**FC 1:50**

IF: Immunofluorescence
IHC: Immunohistochemistry
WB: Western Blot
IP: Immunoprecipitation
FC: Flow Cytometry

(Promega) were transfected into cells and treated with TGFβ for 24 hours. Cells were then lysed in a passive lysis buffer and 20uL aliquots were added to replicate wells in a black bottom 96 well plate (Corning). Cell lysates were incubated with 100μL of luciferase reagent (Promega) and luciferase activity was read on a plate reader. The Stop&Glo (Promega) reagent was added at a volume of 100μL/well. Luciferase activity was normalized to Renilla activity to account for transfection efficiency. Activity of the E-box reporter was transfected into differentiating myoblasts in combination with Renilla and analyzed similarly.

2.3 Western Blot

Skeletal muscle was isolated from mice and homogenized in RIPA buffer (150 mM NaCl, 1% NP-480, 2mM EDTA, 0.5% sodium deoxycholate, 0.1% SDS, 50mM Tris, pH 8.0, 1% Triton-X) containing phosphatase and protease inhibitors. For analysis of utrophin expression in skeletal muscle, samples were homogenized in a UREA buffer with inhibitor cocktail (7M Urea, 2M thiourea, 4M CHAPS, 100mM DTT, 125mM Tris HCl pH 6.8). Lysates were centrifuged at 14000RPM for 5 minutes at 4°C in a micro centrifuge to clear isolated protein. Protein concertation was measured using Bradford reagent (Bio-Rad, Mississauga, ON, Canada). Equivalent amounts of protein were boiled in SDS loading buffer and then run on polyacrylamide gels and subsequently transferred onto a polyvinylidene difluoride (PVDF) membrane (Millipore). Membranes were then probed with indicated primary antibody (Table 1) diluted in 5%BSA/0.1% TBS-T for either 1 hour at room temperature or overnight at 4°C. Membranes were washed with 0.1% TBS-T for 15 minutes and incubated with HRP-conjugated secondary antibodies (Bio-Rad). Following second wash, membranes were incubated with Enhanced chemiluminescence reagent for 1 minutes and exposed to X-Ray film.

2.4 SLK Immunoprecipitation and Autoradiography Kinase Assay

Assessment of SLK activity was performed using *in vitro* kinase assays. 0.4mg of isolated protein was immunoprecipitated using 25μL of protein A beads (GE healthcare) and 1μL of custom SLK antibody (2 hours at 4°C with rotation). Beads were was 3 times with NETN buffer (250mM NaCl, 5mM EDTA, 50mM Tris-HCl, 0.5% NP-40). Following the last wash, cells were incubated in kinase buffer (0.25 mM NaVO3, 20 mM Tris, pH 7.4, 1 mM NaF, 10 mM β-glycerophosphate, 1 mM dithiothreitol, 15 mM MgCl2) and 1μL [32P]γATΠ (5 mCi/mL) for 30 minutes at 30°C. Following incubation, 10μL 4XSDS loading buffer was added to the samples and boiled for 5 minutes. Samples were centrifuged briefly and loaded onto polyacrylamide gel and transferred onto a PVDF membrane. Membranes were exposed overnight to X-ray film for visualization. Following autoradiography, SLK was blotted to ensure even loading.

2.5 RNA Extraction and Quantitative PCR

Skeletal muscle samples or cells were homogenized in Trizol reagent (Life Technologies) and 0.2mL of chloroform was added. Samples were spun at 13000g for 15 minutes. The upper aqueous phase was added to 0.5mL isopropanol, incubated at room temperature for 10 minutes and spun at 13000G for 10 minutes. RNA pellet was washed with 75% ethanol and spun at 8500G. All centrifugation steps were performed at 4°C. RNA was then dissolved in 100uL of RNase Free Water. Samples were then run through an on column RNA cleanup protocol (RNeasy kit, Qiagen) and subjected to on column DNase digestion to remove any contaminating DNA. Concentrations of RNA samples were analyzed using a nanodrop. 500ng of RNA was

Table 2: List of QPCR Targets and Primers

Target	Fwd	Rev
SLK	ACCGAGATCTAAAAGCTGGCA	ACCCAGGGACCAAACATCAG
α7 integrin	ACTGTCCGAGCCAATATCACCGT	ACCAGTAGTCCCGCCAGCACA
β1 integrin	CATCCCAATTGTAGCAGGCG	CGTGTCCCACTTGGCATTCAT
β1D integrin	CATCCCAATTGTAGCAGGCG	GAGACCAGCTTTACGTCCATAG
dystrophin	GTGGGAAGAAGTAGAGGACTGTT	AGGTCTAGGAGGCGTTTTCC
Atrogin1	CGGCAAGTCTGTGCTGGTGGG	GCACACAGGCAGGTCGGTGA
MuRF1	TTTCCGTTGCCCCTCGTGCC	GCACATCGGGTGGCTGCCTT
Periostin	AAGTTTGTTCGTGGCAGCAC	TTCTGTCACCGTTTCGCCTT
eMHC	GCATAGCTGCACCTTTCCTC	GGCCATGTCCTCAATCTTGT
Id3	TGCTACGAGGCGGTGTGCTG	AGTGAGCTCAGCTGTCTGGATCGG
CollagenIII	GCGGAATTCCTGGAAAGGTGATGCTG	GCGGGATCCGAGGGTTCCCCATTATG
CTGF	GCGTGTGCACCGCCAAAGAT	CAGGGCTGGGCAGACGAACG
Fibronectin	GCCCAGTGATT TCAGCAAAGG	ATGTGGACCCCTCC TGATAGT
Vimentin	CACATCGATCTGGACATGCTGT	CGGAAAGTGGAATCCTTGCA
GAPDH	CATCACCATCTTCCAGGAGCG	GAGGGGCCATCCACAGTCTTC

used for cDNA synthesis using SuperSciprt3 (Life Technologies) and oligiodT primers (Invitrogen). Indicated targets were amplified using gene specific primers (Table 2) and SYBR Green Reagent (Bio-Rad). Reactions were carried out on an Applied Bioscience 7500 Fast-Real-Time PCR System. Primers used for Q-PCR are listed in Table 2.

2.6 Immunohistochemistry and Immunofluorescence on Tissue

Muscles were excised from sacrificed mice and either flash frozen in isopentane (cooled in liquid nitrogen) and fixed in OCT or fixed in 10% formalin overnight for paraffin embedding. Following embedding, tissues were sectioned (5μm thick). Paraffin sections with deparaffinised in xylene for 15 minutes, followed by decreasing concentrations of ethanol (2x 100%, 2x 95% and 1X 80% for 5 minutes at each wash). Frozen sections were fixed 10 minutes in 4%PFA. Sections were boiled in pressure cooker for 10 minutes in 10mM citrate buffer for antigen retrieval, followed by 15 minute incubated in 3%H_2O_2 (for histochemistry only). Sections were blocked for 1 hour in 5% donkey serum diluted in PBS. Primary antibody was diluted in 5% donkey serum and left overnight at 4°C. Sections were rinsed 3 times in 1XPBS, and incubated with secondary antibodies for 1 hour (HRP-conjugated for IHC or alexa fluro antibodies for IF, Dako/abcam). For IHC, sections were incubated with DAB reagent to visualize secondary binding, counter stained with haematoxylin and dehydrated prior to mounting in organic mounting media. Slides were scanned using an Aperio imager (ImageScope; Aperio, Vista, CA, USA). For IF, sections were immediately mounted in aqueous mounting media with DAPI and visualized under the microscope. For haemotoxylin and eosin staining alone slides were deparaffinised, incubated in haemotoxylin for 30 seconds and submerged in 0.5% acid alcohol followed by 0.1% ammonia water. Slides were then counter stained in eosin and dehydrated in ethanol and xylene.

2.7 Evan's Blue Uptake

Evan's Blue Dye (Sigma) was dissolved in PBS at a concentration of 10mg/mL. Mice were injected with 0.1mL/10g of body weight of the EBD mixture via intraperitoneal injection. Mice were sacrificed 24 hours later and skeletal muscles were extracted. Muscles were weighed and then homogenized in n n-dimethylformamide and rotated at room temperature for 24 hours. Absorbance of each samples was measured and total amount of EBD in the sample was calculated based on a standard curve. These values were then normalized to muscle weight.

2.8 Cardiotoxin Induced Injury

Mice were given a dose of buprenorphine 1 hour prior to injury. Before cardiotoxin injections, mice with anesthetized with isoflurane. The Tibialis Anterior muscle was injected with 30μL of 10μM cardiotoxin (CTX, Sigma-C9759). Contralateral TA muscles were injected with equivalent volumes of PBS. Mice were sacrificed and muscles were extracted for paraffin sections at 7, 10 and 21 days post injected (DPI). Cross sectional area was measured on H&E stained sections.

2.9 Central Nuclei, Fiber Diameter and Area Calculation

Fiber size was measured using Aperio Imaging software. Cross sectional area and diameter were measured where indicated. For the soleus, the entire muscle section was measured (~100 fibers/muscle). For the diaphragm and TA muscle, >600 fibers/muscle were counted. Central nuclei were quantified by analyzing >600 fibers/muscle and calculating percentage of fibers with a central nuclei in all fields of view analyzed.

2.10 X-gal Staining of Embryo Sections

Embryos were extracted at E12.5 and E14.5 and fixed for 2 hours in 2%PFA/0.2 Glutaraldehyde, 0.01% NP40. Embryos were washed for staining solution for 2 hours at room temperature (2mM $MgCl_2$, 0.01% Sodium deoxycholate, 0.02% NP40 dissolved in 1XPBS). Embryos were then stained in staining solution overnight in the dark (5mM potassium ferrocyanide, 5mM potassium ferricyanide and 1mg/mL of X-gal dissolved in staining buffer). Following staining, embryos were frozen and sectioned. Tail clippings were taken for DNA extraction and genotype analysis.

2.11 Immunofluorescence on Cultured Cells

Cells were cultured on coverslips for the duration of the experiment. Cells were washed in 1XPBS and fixed and 4% PFA for 10 minutes. Cells were washed again and permeablized in 0.3% Triton-X for 5 minutes. Following permeablization, cell were blocked in 5% donkey serum for 1 hour, followed by incubation with primary antibody for 1 hour. Secondary antibody incubations were performed in the dark for 1 hour. Cells were washed and mounted in aqueous mounting media with DAPI. For cellular fusion index, Fusing myoblasts were fixed and stained with MF20 and counter stained with DAPI. The fusion index was calculated by counting the number of nuclei within a cell containing 3 or more nuclei (constituting a syncytium). The number of nuclei within a syncytium were then divided by the total number of nuclei counted to obtain the percentage of fused cells. Three independent samples were taken, and at least 10 fields of view were quantified from each sample.

2.12 Isometric Muscle Contractions

Mice were first injected with buprenorphine (i.p. 0.1 mg/kg) and then anesthetized with pentobarbital sodium (i.p. 50 mg/kg) 15 min later. The right soleus (Sol) and extensor digitorum

longus (EDL) muscles were dissected and incubated *in vitro* in a buffered physiological salt solution (Krebs-Ringer) supplemented with glucose (2 mg/mL) and a constant bubbling of carbogen (5% CO2, 95% O2) at 25^0C. After 15 min of equilibration at optimal length (L0) the following contractile properties were measured: time-to-peak twitch tension (TPT, ms) with 0.2 ms square-wave pulses of supramaximal voltage (~25 V) through two platinum electrodes, half-relaxation time (1/2 RT, ms), twitch tension (Pt, g) and maximum tetanic tension (P0, g) for 700 ms at frequencies of 10, 20, 50, 80, 100 and 120 Hz using the Dual-Mode Lever Arm System 305B-LR controlled by the Dynamic Muscle Control and Data Acquisition software (Aurora Scientific Inc. Aurora, Ontario, Canada). At the end of the contractile properties measurements, tendons were removed and muscles were weighed. The cross-sectional areas were estimated by dividing the wet weight by the optimal muscle length multiplied by the muscle density ($1.06 g/cm^3$) multiplied by the fiber-to-muscle length ratio for Sol and EDL muscles.

2.13 Eccentric Muscle Contractions

Following isometric contractile property measurements, the muscles are subjected to 7 consecutive eccentric contractions. The muscles are stimulated at 150 Hz for 700 ms. Five hundred ms into the tetanic stimulation, the muscles are lengthened to 10% of L_0 at 0.5 L_0/s for 200 ms using the 305B-LR dual mode muscle level system (Aurora Scientific Inc.).

2.14 Transmission Election Microscopy

Skeletal muscle samples were fixed in 2.5% glutaraldehyde for 2 hours, rinsed in 50mM Sodium Cacodylate buffer and incubated in 2% Osmium Tetroixide. Samples were dehydration in ethanol and suspended in acetone, then embedded in Spurr's Resin and polymerized overnight at

65°C. 80nm sections were stained with uranyl acetate and lead citrate and imaged on Hitachi H-7100 TEM. Magnification of images indicated in appropriate figure legends.

2.15 Generation of SLK Knockout Model

The conditional SLK knockout model was generated by inserting a FRT-flanked Neomycin cassette downstream of exon 2 with loxP sites flanking exons 2 and 6 of the murine SLK locus. Chimeras were bred for germline transmission and maintained on a C57 background. Mice were first crossed with β actin-Flp recombinase to remove the neomycin cassette and obtain the SLK flox mice. Mice were bred to the β actin Cre recombinase line and the Myf5-Cre recombinase line to generate a global and muscle specific deletion respectively (Jacksons Lab). Myf-Cre SLK flox mice were bred into the *mdx* strain to generate muscle specific deletion in the dystrophic model.

2.16 Genotyping

Ear clips from weanling mice were subjected to proteinase K digestion and DNA was extracted using an on column method (Qiagen, Mississauga, ON, Canada). SLK flox mice were genotyped using primers flanking the 3' loxP site, where the insertion the loxP sites shifts the wildtype band from 437bp to 471bp. Genetic recombination was analyzed on DNA from skeletal muscle using an additional forward primer upstream of the 5' loxP site. The product size of the uncombined SLK allele was >5000bp, which was not readily amplified. Upon recombination, the product dize was 501bp. Cre was genotyped using sequence specific genes. The *mdx* strain was genotyped using a method previously described using primer competition. Briefly, a common forward

Table 3: Genotyping Primers

Reaction	Forward	Reverse	Size
SLK	TGAGGACCTGGGGAGATTGCT	ATGCAGCTGTATCTTCACAAG	437bp (WT) 471bp (flox)
SLK Recombo	TTGGGGGATGGCTTCGTGCTT	ATGCAGCTGTATCTTCACAAG	471bp (uncombined) 501bp (recombined)
mdx (WT)	GCGCGAAACTCATCAAATATGCGTGTT AGTGT	GATACGCTGCTTTAATGCCTTTAGTCACTCAGATAGT TGAAGCCATTTTG	134bp
mdx (MT)	GCGCGAAACTCATCAAATATGCGTGTT AGTGT	GTCACTCAGATAGTTGAAGCCATTTTA	117bp
Cre	GGATTGCTTATAACACCCTGTTACG	TATTCGGATC ATCAGCTACACCAGAG	213bp

primer was used in conjunction with a wildtype and mutant specific primer. The wildtype specific primer contained a guanine in the last position, in addition to a non-homologous 5' end that was 23bp larger than the mutant primer. The mutant primer contained an adenine in the 3' position to match the mutation in the *mdx* model. The wildtype and mutant bands were resolved on 2% agarose gel. Genotyping primers are listed in Table 3.

2.17 Flow Cytometry

Cells were stained with Zombie NIR Fixable Viability Dye (BioLegend) as per the manufacturer's instructions, followed by incubation with blocking solution (anti-CD16/CD32, BD Biosciences for 20 minutes at 4°C. The cells were then stained with the following fluorescently-labeled antibodies (or appropriate isotype antibodies) for 20 minutes at 4°C in FACS buffer (DPBS + 0.5% BSA): PerCP anti-mouse CD45, Alexa Fluor 647 anti-mouse F4/80, PE-Cy7 anti-mouse CD206 (BioLegend); and BV605 anti-mouse CD11b (BD Biosciences). Cells were fixed and permeabilized using FoxP3/Transcription Factor Staining Buffer Set (eBioscience) as per the manufacturer's instructions. The cells were stained intracellularly with FITC anti-mouse iNOS (BD Biosciences). Stained cells were re-suspended in FACS buffer, and analyzed by flow cytometry. 100,000 – 500,000 events were recorded for each sample on a BD LSR Fortessa. Data analysis was performed using FlowJo software (TreeStar Inc.). Macrophages were classified as $CD45^+$ $F4/80^+$ $CD11b^+$; iNOS and CD206 expression was assessed on this macrophage population. Cells stained with isotype controls were used to set gates.

2.18 Golden Retriever Muscular Dystrophy

Diaphragm lysates from the GRMD model were provided by Dr. Joe Kornegay's laboratory at Texas A&M University, College Station, Texas. The breeding of the GRMD dogs and subsequent necropsy and biopsy procedure were done in accordance with National Research Council Guide for the Care and Use of Laboratory Animals.

2.19 Statistical Analysis and Data Collection

In vitro experiments were conducted in at least three independent experiments and averaged. Errors bars are represented as standard error of the mean. P-values are calculated between groups using two-tailed unpaired student's t-test analysis. Significance was determined by a p-value<0.05 (* $p<0.05$, ** $p<0.01$). For quantification on IHC, multiple muscle samples from individual mice were sectioned and stained with indicated antibody. At least 10 field of views from each section were used for quantification, with the exception of the soleus muscle, in which the entire muscle was analyzed. For force generation, data were analyzed by two-way ANOVA to determine whether the variations among the experimental groups were significant (InStat software, version 3). When a significant F ratio was obtained, a posteriori test was performed (Tukey's protected least-significant differences test) to determine whether there were any specific differences ($p<0.05$).

Chapter 3- Results:

Effect of SLK Deficiency on Muscle Development and Regeneration

3.1 Introduction and Rationale

Previously, our lab has demonstrated a complex role for SLK in myogenesis and skeletal muscle regeneration. The over expression of the truncated kinase dead mutant (KΔC) inhibited C2C12 myoblast fusion and differentiation (Storbeck et al., 2004). Conversely, *in vivo* expression of the full length kinase dead mutant driven by the HSA promoter (HSA-K63R) in FVB/N mice enhanced muscle regeneration and myoblast fusion (Storbeck et al., 2013). These conflicting results suggest specific roles for SLK during the differentiation process. Therefore, to better understand the role of SLK in muscle development, we conducted SLK knockdown studies *in vitro* and generated a muscle specific SLK knockout model using the Myf5-Cre Recombinase strain and a novel SLK conditional knockout mouse.

3.2 SLK Expression, Activity and Localization during Myogenesis

To begin our assessment of SLK's function during myogenesis, we assayed SLK activity by *in vitro* kinase assay as well as expression levels across a differentiation time course in C2C12 myoblasts. SLK expression was similar at each day along the differentiation assay [Fig3.1]. However, SLK kinase activity was decreased as myoblasts differentiated, determined by autoradiography. SLK localized to the lamellipodia and cytosol of proliferating myoblasts and was present throughout the cytosol of fused myotubes [Fig3.1]. Co-staining with β-catenin revealed that SLK was excluded from sites of cellular contact [Fig3.1]. These initial findings alone indicated that SLK activity is decreased during differentiation. Furthermore, localization to the leading edge of proliferating cells suggested that SLK might be regulating focal adhesion turnover and myoblast migration prior to differentiation, similar to its established role in fibroblasts.

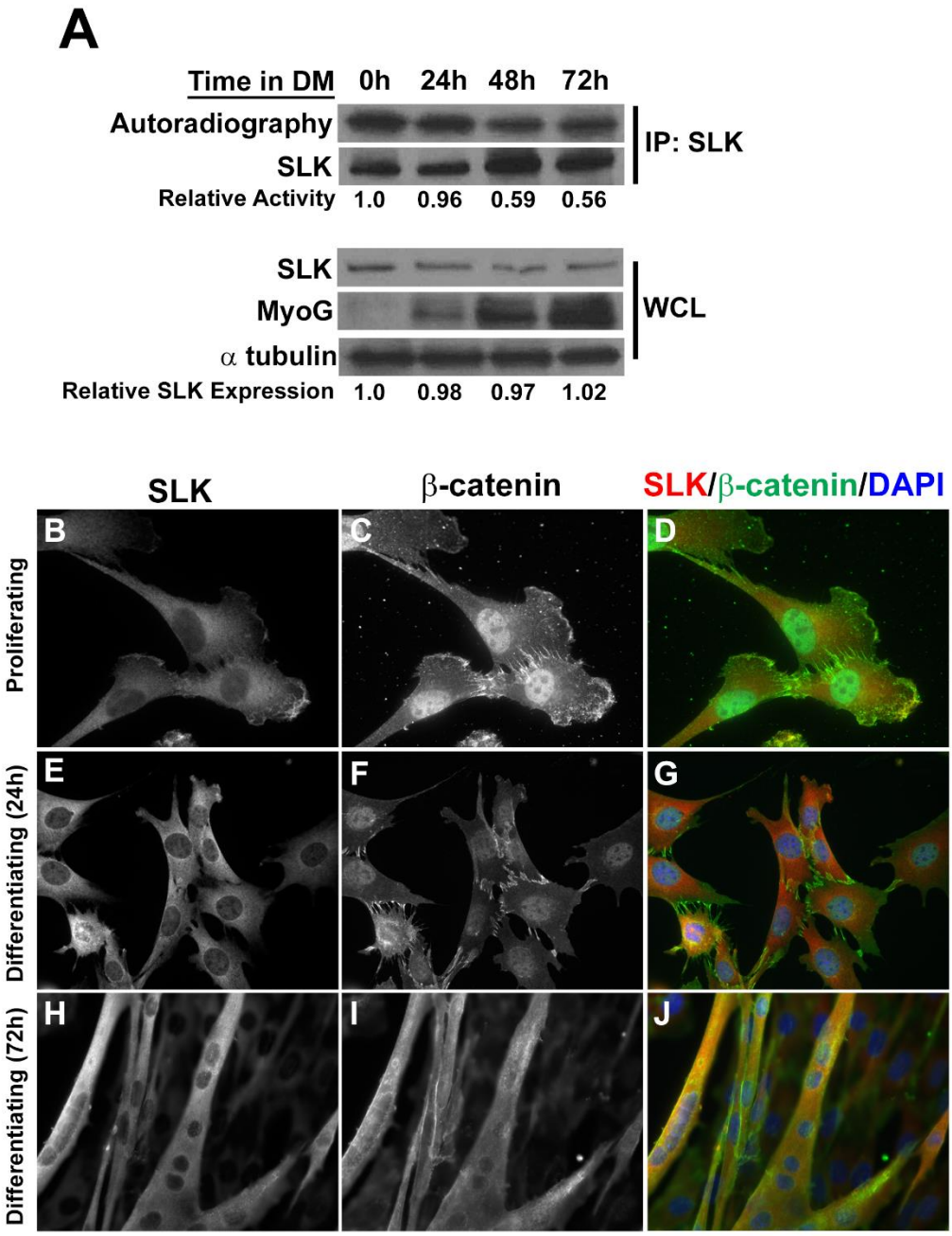
A
Time in DM
0h
24h
48h
72h
Autoradiography
SLK
IP: SLK
Relative Activity
1.0
0.96
0.59
0.56
SLK
MyoG
α tubulin
WCL
Relative SLK Expression
1.0
0.98
0.97
1.02
SLK
β-catenin
SLK/β-catenin/DAPI
Proliferating
Differentiating (24h)
Differentiating (72h)
B
C
D
E
F
G
H
I
J

Figure 3.1: SLK Activity is reduced during Myoblast Differentiation. (A) C2C12 myoblasts were induced to differentiate in 2% Horse Serum. Equivalent amounts of SLK was immunoprecipitated (IP) from samples at each time point and subjected to kinase assays using ^{32}P labelled ATP. Equivalent loading was determined by blotting membrane with SLK. SLK autophosphorylation was reduced as myoblasts differentiated. SLK kinase activity was determined by performing densitometry and calculating the average from three independent experiments. Intensity of autoradiography band was divided by the intensity of the SLK loading band to determine relative activity. Whole cell lysates (WCL) were probed MyoG to assess differentiation and SLK to determine relative expression. SLK expression was determined by normalizing SLK levels to tubulin. No alterations in SLK levels were observed as MyoG levels increased. (B-J) C2C12 myoblasts were plated on coverslips and stained for SLK and β catenin. SLK localized to the leading edge in cycling cells (B-D) and throughout the cytosol in all samples. SLK could not be readily co-localized with β catenin at sites of cellular contact, (E-F).

3.3 Decreased SLK leads to Reduced Cellular Migration and Proliferation

Previously, we have identified that reduced SLK signalling can decrease both cellular migration and proliferation in various cell lines. Both proliferation and migration of myogenic precursors are essential for optimal muscle regeneration, as the progenitor population needs to both expand as well as localize to the site of muscle damage to mediate myofiber repair. We investigated whether SLK was also mediating either these functions in myoblasts. To test this, we knocked down SLK using adenovirus for short hairpin RNA. As in previous studies, we observed a reduction in the number of cells at each time point in a proliferation assay following SLK knockdown [Fig3.2A]. SLK knock down also resulted in a significant decrease in the migratory capacity of myoblasts [Fig3.2B]. Therefore, SLK knockdown decreases both proliferation and migration of myoblasts.

3.4 SLK Knockdown Decreases Myoblast Fusion without Affecting Myoblast Differentiation

Previously, expression of a dominant negative SLK construct resulted in decreased fusion of myoblasts. We predicted that an SLK knockdown would have a similar phenotype. Cells were infected with either a scramble control or a shSLK expressing adenovirus and induced to differentiate for 48 hours. We assessed the levels of myogenic genes for up to 3 days in a differentiation assay by western blot. Interestingly, the myogenic transcriptional program was unaffected by SLK knockdown, as levels of Myogenin and Myosin Heavy Chain (MHC) were comparable between wildtype and knockdown cells [Fig3.3A]. We next assessed myoblast

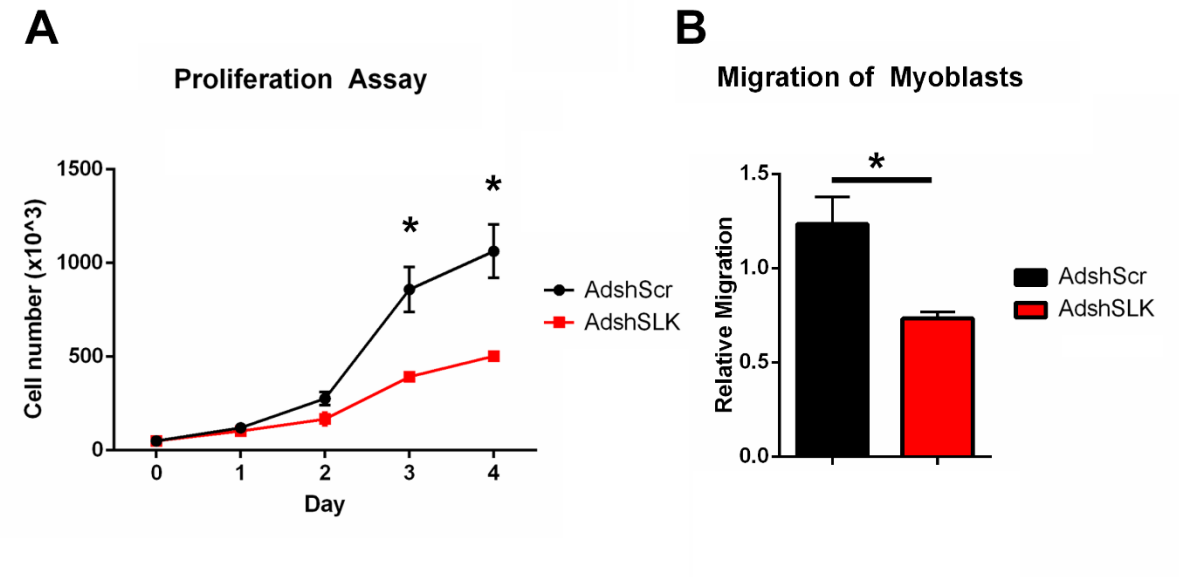

Figure 3.2: SLK Knockdown decreases both Proliferation and Migration of Myoblasts. (A) Myoblasts were seeded at $5x10^4$ cells/plate (D0) and grown for 4 days (D1-D4). Cells were counted at each day across the time course. SLK knockdown significantly decreased the growth rate of myoblasts. A t-test was performed at each timepoint to determine significant differences in the number of cells at each day ($p<0.05$). (B) Myoblasts were plated in serum free media in the top chamber of a transwell plate ($5x10^4$ cells/plate) and 10% FBS was placed in the bottom chamber. Myoblasts were allowed to migrate for 8 hours. Migrated cells were stained with haematoxylin and enumerated. Migrated cells were normalized to AdScr controls. A t-test was used to determine significance ($p<0.05$). SLK deficient cells had significantly reduced migration rate compared to control cells.

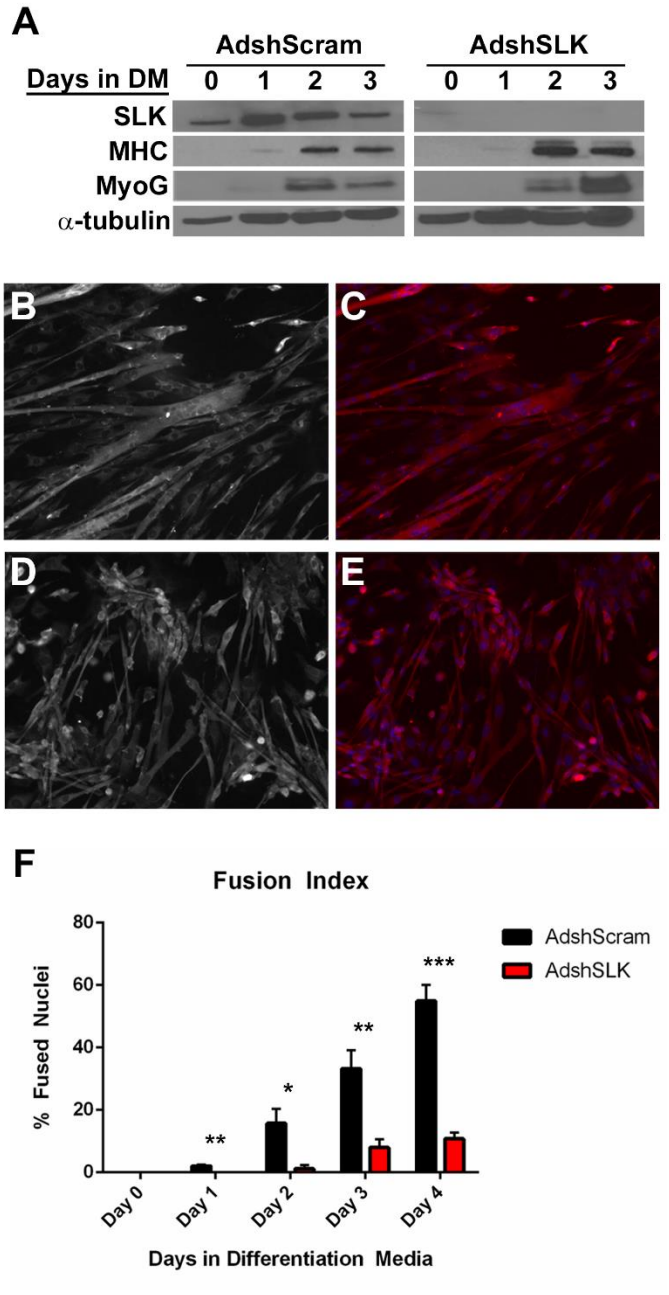
A
AdshScram
AdshSLK
Days in DM
0 1 2 3
0 1 2 3
SLK
MHC
MyoG
α-tubulin
B
C
D
E
F
Fusion Index
% Fused Nuclei
80
60
40
20
0
**
*
**
***
AdshScram
AdshSLK
Day 0
Day 1
Day 2
Day 3
Day 4
Days in Differentiation Media

Figure 3.3: Myoblast Fusion, but not Differentiation, is decreased following SLK Knockdown. (A) AdScramble and AdshSLK infected myoblasts were differentiated for three days and blotted for myogenin (MyoG) and myosin heavy chain (MHC). Loss of SLK did not affect the activation of differentiation markers. (C-G) Myoblasts were stained with MHC and fused cells were enumerated. Fusion was defined as a cell containing three or more nuclei. The number of nuclei in a fused cells was divided by the total number of nuclei counted (n=3 coverslips/timepoint, 10 fields of view averaged for each coverslip for each n value). A t-test was used to determine significant difference in fusion (* $p<0.05$, ** $p<0.01$, *** $p<0.005$). SLK deficient cells showed a significant reduction in myoblast fusion at all timepoints compared to controls.

fusion by staining with MHC and counting the number of nuclei in a fused myotube [Fig3.3B-E]. We observed a significant decrease in the capacity of AdshSLK infected cells to fuse into multinucleated myotubes compared to AdshScramble infected cells. Control cells fused at ~60% and AdshSLK cells displayed less than 10% fusion four days after differentiation was induced [Fig3.3F]. These results suggest that SLK is not required for myogenic differentiation, but does play a role in myoblast fusion.

3.5 Generation of Muscle Specific SLK Knockout Model

Previously, we have shown that SLK expression is elevated within the developing neuronal and myogenic compartments of the embryo. Our early work had showed conflicting results as to the role of SLK signaling in skeletal muscle. Dominant negative SLK expression resulted in opposite phenotypes depending when it was expressed during differentiation. Our attempts to generate a global SLK-null model using our SLK-LacZ gene trap animals demonstrated that global inhibition of SLK signaling was embryonic lethal. Therefore, we generated a conditional SLK knockout model, dubbed $SLK^{fl/fl}$ mice, in order to mediate deletion of SLK in specific tissues. Breeding with the skeletal muscle specific Myf5-Cre recombinase would mediate SLK deletion within the myogenic lineage.

The conditional SLK knockout model was designed by flanking exons 3 and 6 of SLK with LoxP sites [Fig3.4A]. The recombination of exons 3-6 with Cre results in the deletion of a large portion of the kinase domain and causes a frame shift mutation. The resultant frame shift mutation generates a stop codon (TAA) following exon 3 [Fig3.4B]. Genotyping was performed by amplifying a PCR product with primers flanking the 3' LoxP site, causing a band shift in the

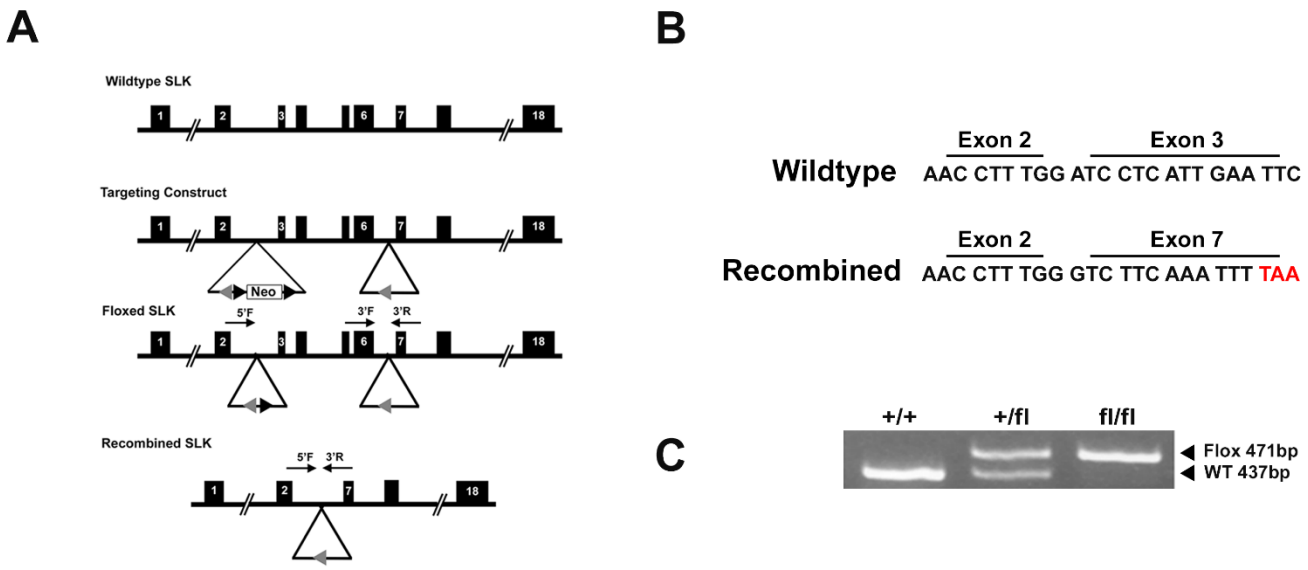

Figure 3.4: Generation of SLK$^{fl/fl}$ Mice. (A) Schematic representation of the SLK locus and the SLK targeted allele showing the Frt (black arrowhead) and loxP sites (white arrowhead). The location of SLK primers (listed in Table 1) are indicated in the Flp-recombined and Cre-recombined alleles. (B) Nucleotide sequence at the 3' end of exon 3 before (top) and after (bottom) genetic recombination. A stop codon (red font) is generated through the frame shift after the recombination of exon2-7. (C) PCR genotyping of genomic DNA from ear clips for the SLK$^{+/+}$, SLK$^{+/fl}$, and SLK$^{fl/fl}$ alleles using 3'F and 3'R primers. Figure adapted from Pryce et al 2017.

presence of the LoxP site [Fig3.4C]. This allows us to correctly identify $SLK^{+/+}$, $SLK^{+/fl}$ and $SLK^{fl/fl}$ mice. The conditional SLK knockout mice were first crossed with the global β actin-Cre recombinase strain. As in the SLK-LacZ gene trap mice, the early global deletion of SLK results in no viable SLK knockout animals, demonstrating a critical role for SLK during embryonic development [Table 4].

3.6 Muscle Specific Deletion of SLK does not Result in Embryonic Lethality

We next crossed the $SLK^{fl/fl}$ mice into a muscle specific Cre recombinase model as well as the Rosa26R-LacZ reporter strain. The Myf-5-Cre knock-in strain was used as a driver of Cre mediated deletion due its expression in embryonic and adult myoblasts. This would recombine the SLK allele during development as well as during muscle regeneration. Due to the decreased fusion of SLK-deficient myoblasts *in vitro*, we initially anticipated a defect in skeletal muscle development in our Myf5-Cre/$SLK^{fl/fl}$ mice. However, analysis of knockout embryos revealed no alterations in the expansion of Myf5-Cre expressing cells or the myogenic compartments, as determined by LacZ and MF20 staining at day E10.5 [Fig3.5A-D]. The formation of nascent myotubes was also similar between wildtype and knockout mice at E13.5, with no obvious decrease in fusion [Fig3.5E&F]. Furthermore, knockout mice were born at expected Mendelian ratios based on genotyping analysis, indicating no decrease in survival in SLK knockout mice. Therefore, we conclude that SLK expression is not absolutely required for the proliferation and fusion of myoblasts during skeletal muscle development.

Adult skeletal muscles from knockout mice were analyzed for Cre mediated deletion of SLK. Recombination of the SLK allele was determined by using the 3' LoxP genotyping primers, in

Table 4: Genotypes from β actin Cre x SLK$^{fl/fl}$. Global β actin Cre expression SLK+/fl males and females were bred together to generate wildtype, heterozygotes and knockout mice. No homozygotes were observed upon weaning.

	Actual	**Expected**
Heterozygote (SLK +/fl)	80/116 (69%)	58/116 (50%)
Wild Type (SLK +/+)	36/116 (31%)	29/116 (25%)
Knockout (SLK fl/fl)	0/116 (0%)	29/116 (25%)

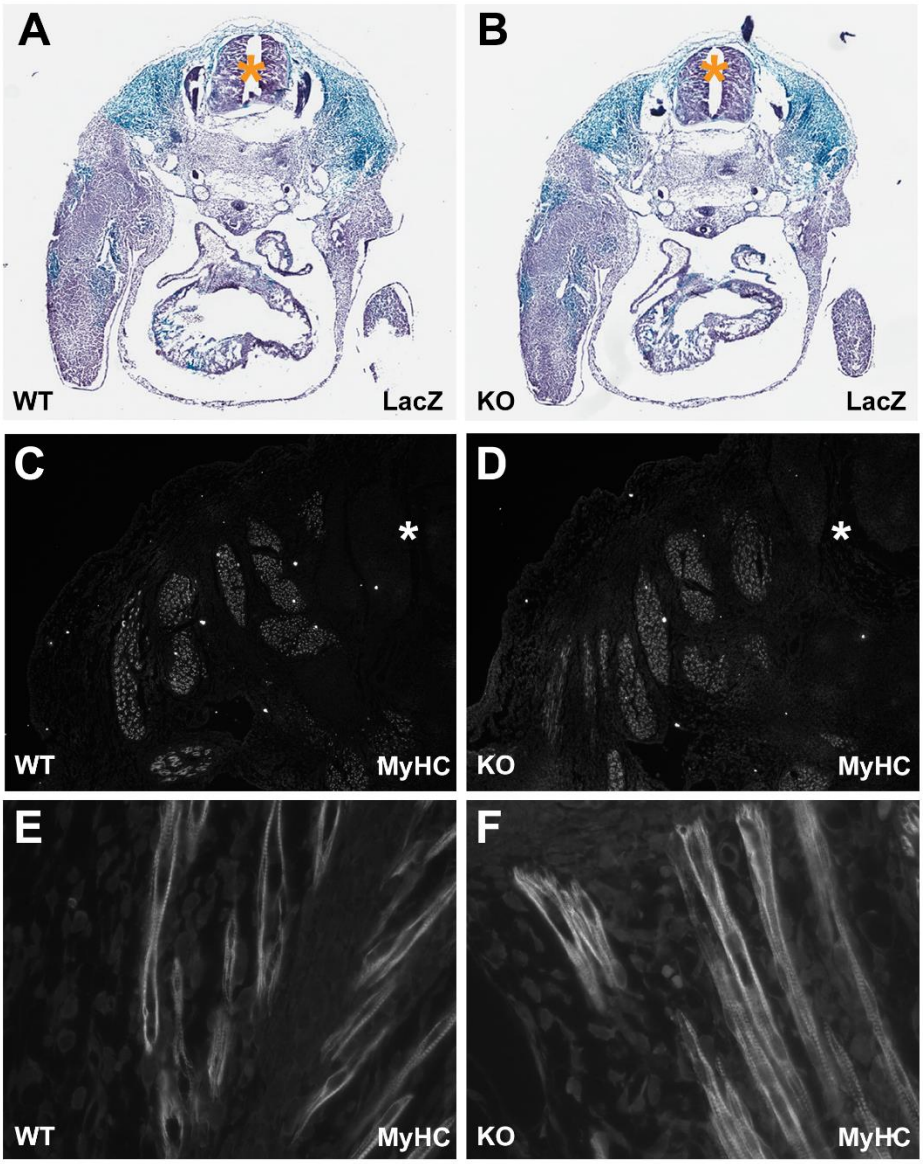

Figure 3.5: Myogenesis occurs normally in SLK Muscle Knockout Embryos. (A&B) β-galactosidase histo-chemistry on cross sections of E12.5 embryos from a wildtype (WT) and SLK-null (KO) embryo into the ROSA26R background. The location of neural tube is indicated (*). (C&D) MF20 immunofluorescence staining to identify differentiated skeletal muscle tissue within developing E12.5 embryos. The neural tube is indicated (*). (E&F) E14.5 embryos were stained for MF20. Differentiated myotubes were observed in both control and knockout muscles. Figure adapted from Pryce, et al 2017.

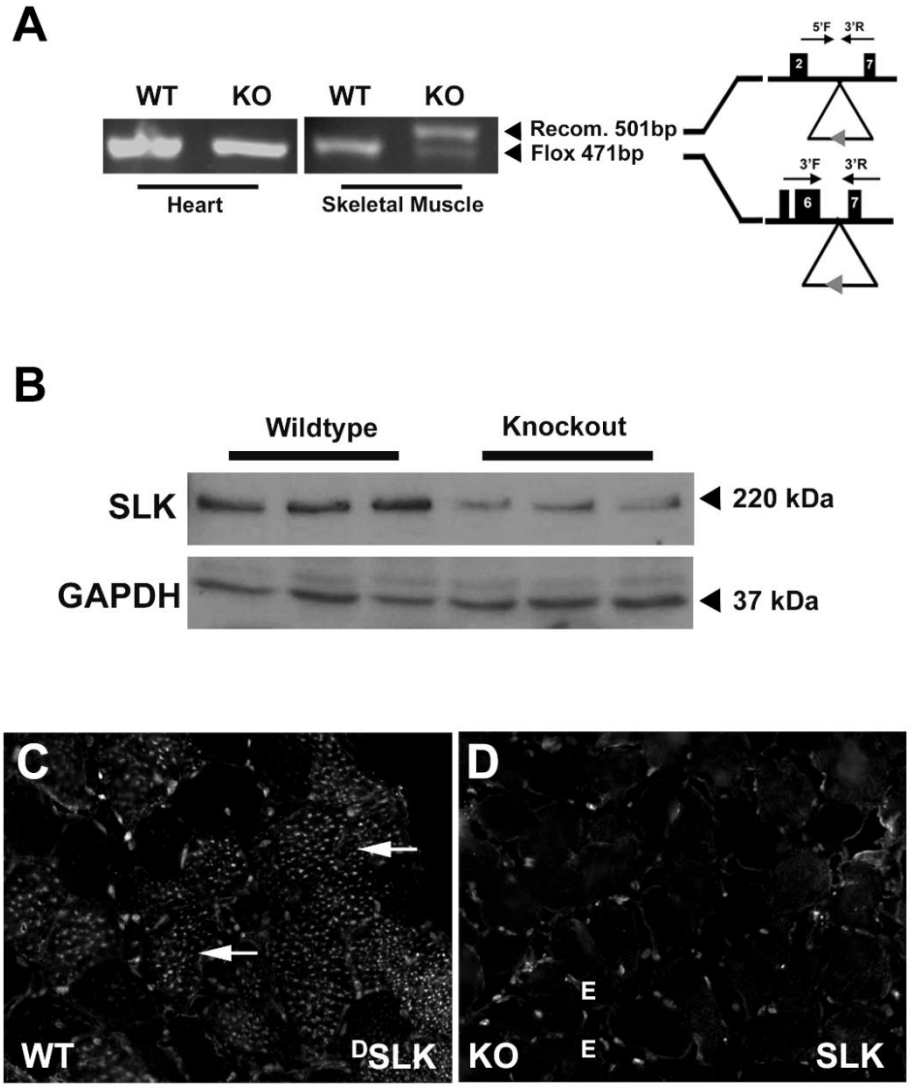

Figure 3.6: Conditional Deletion of SLK in Adult Skeletal Muscles using the Myf5-Cre Recombinase Mice. (A) Genomic DNA PCR on Heart and Skeletal Muscle from wildtype and knockout mice using the primers flanking 3' LoxP sites. Recombination product is only observed following Cre-mediated deletion (500bp). The 3'F and 3'R primers detect the non-recombined DNA strand (471bp). The 5'F and 3'R only generate a product following recombination, whereas the non-recombined allele (>5Kbp) could not be amplified by the 5'F and 3'R primers. (B) Western blot analysis of adult TA muscle lysates from wildtype and knockout mice. Anti-SLK staining of TA muscles from (C) wildtype and (D) knockout mice. Prominent staining was observed in fibers from wildtype (indicated with white arrows) but not in knockout. Figure adapted from Pryce, et al 2017.

addition to a second forward primer upstream of the 5' LoxP site. As expected, the recombination product was only observed in the knockout muscle samples and not in samples from DNA extracted from the heart. The non-recombined product was also observed in DNA extracted from knockout skeletal muscle and was likely being contributed from a non-myogenic cellular population. Additionally, western blot and immunofluorescence demonstrated a reduction in the levels and staining of SLK in knockout muscle fibers. However, a residual SLK signal within knockout muscles was observed, likely being by other cell types, as this has been observed in similar knockout models. Immunofluorescence verified that SLK was deleted within the myofiber.

3.7 Muscle Specific SLK Deficiency Results in Mild Myopathy in Older Mice

We next assessed adult mice for any abnormalities following the deletion of SLK in skeletal muscles. Body weight and muscle fiber diameter was also analyzed at different ages. We observed a slight decrease in body mass in SLK knockout mice as well as a decrease in myofiber size within the TA muscle of 24 week old knockout mice [3.7A&B]. However, there was no upregulation of markers of muscular atrophy, such or active GSK3β or levels of Atrogin-1 and MuRF1, [Fig3.7C&D]. Analysis of fiber type distribution did not reveal any obvious differences between wildtype and knockout mice in either distribution or size of either slow of fast twitch fibers within the Soleus muscle [Fig3.8]. Therefore, we conclude that skeletal muscle does not have any aberrant fiber type distribution or severe atrophy due to SLK deletion.

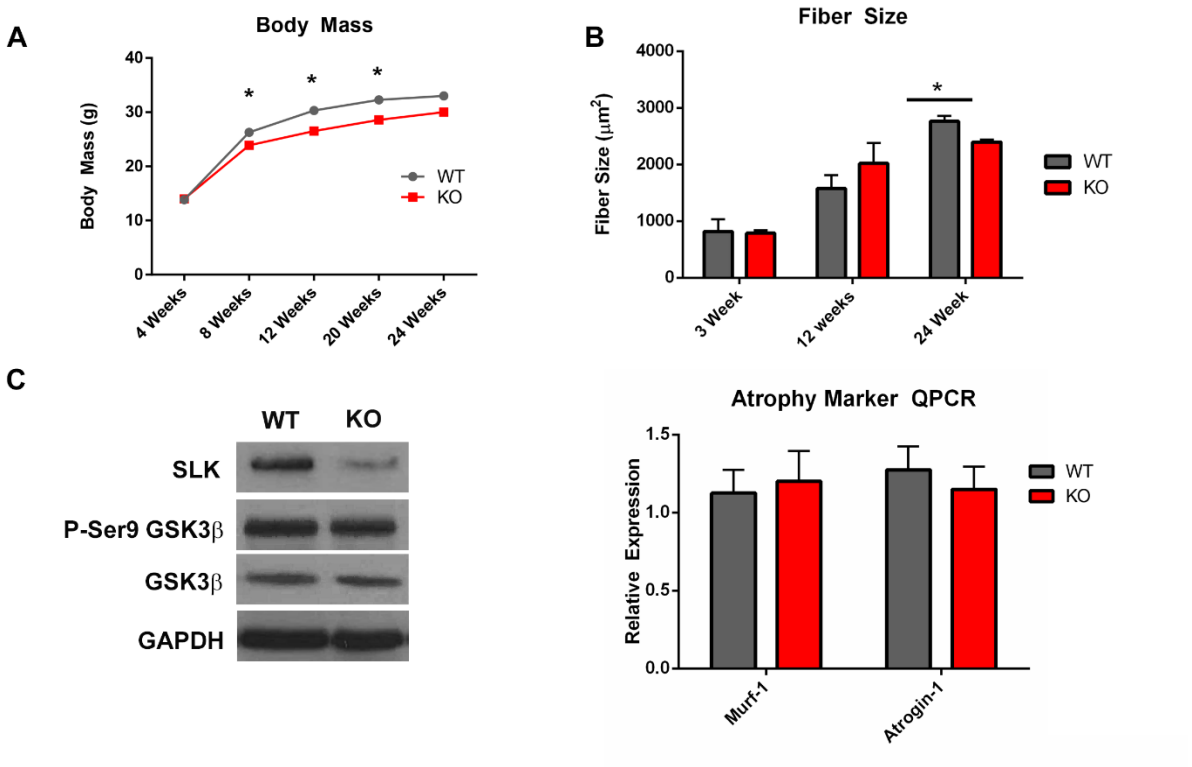

Figure 3.7: Muscle Specific Knockout of SLK Reduces Body Weight and Fiber Size in Older Mice. (A) Body mass of wildtype and knockout littermates was measured from 4 weeks to 22 weeks (n=5/genotype). Knockouts showed a slight decrease in body mass, which was resolved as they aged. (B) Fiber cross sectional area of the TA muscle was measured in wildtype and knockout mice at 3, 12 and 24 weeks (n=5/genotype, students t-test * $p<0.05$). Older mice demonstrated a small but significant decrease in fiber size. (C) Western blot for GSK3β did not show any alterations that would suggest increase atrophy. (D) QPCR for Atrogin1 and MurF were unchanged, indicating no increase in muscle atrophy signalling (n=4/genotype, $p<0.05$).

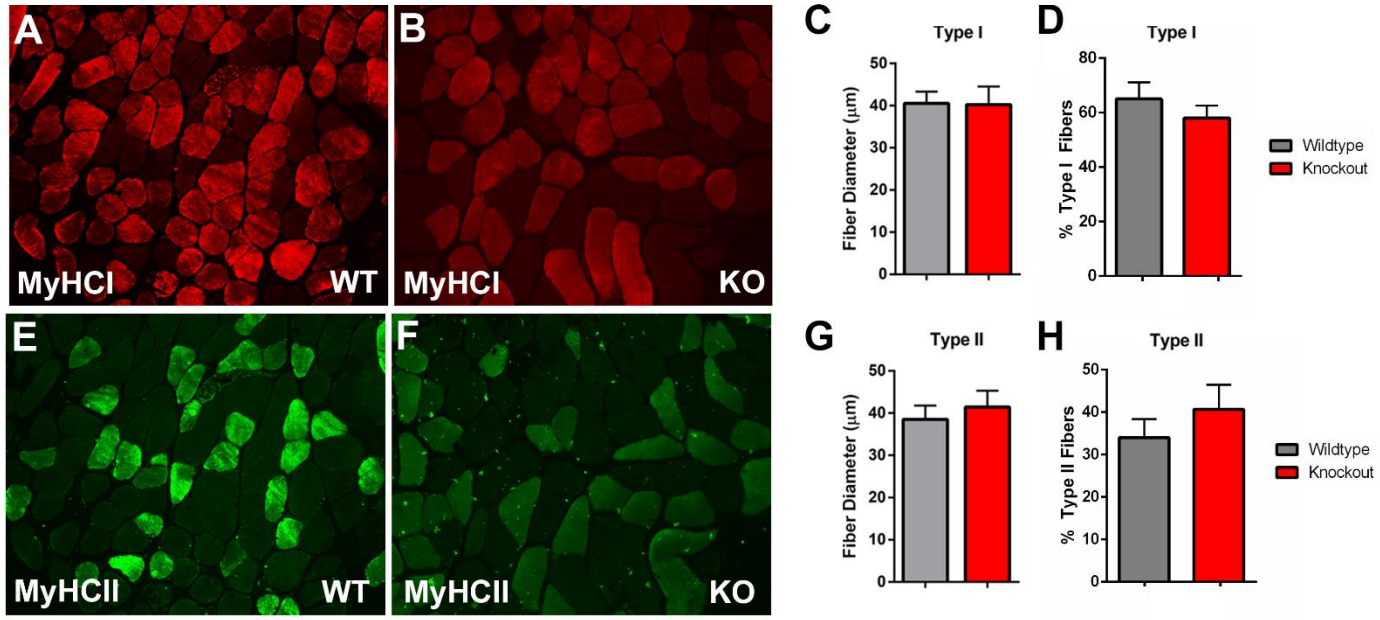

Figure 3.8: Myofiber Type Size and Distribution is unchanged Following SLK Deletion. (A&B) MyHC Type I staining of Soleus muscles (12 weeks) from wildtype (WT) and knockout mice (KO). (C) Minimum Feret's diameter of Type I fibers from each group (n=5/genotype, $p<0.05$). (D) Percentage distribution of Type 1 fibers (n=4/genotype, $p<0.05$). (E&F) MyHC Type II staining and (G) Minimum Feret's diameter of Type II fibers (n=5/genotype, $p<0.05$). Percent Distribution of Type II fibers (n=4/genotype, $p<0.05$) No change in fiber size for specific fiber type or distribution were observed. The distribution of Type 1 and Type 2 fibers was also unchanged. Figure adapted from Pryce, et al 2017.

Interestingly, analysis of skeletal muscle from 6 month old mice revealed an increase of the proportion of centrally located nuclei within the TA muscle of knockout mice that was not observed in 3 month old mice [Fig3.9A-E]. Additionally, electron micrographs revealed alterations in mitochondria stability, as swollen mitochondria were observed throughout the myofibers [Fig3.9F&G]. These results suggest that, although skeletal muscle can develop normally, the deletion of SLK has adverse effects on myofiber integrity. As in the case of muscular dystrophy, muscle damage and central nucleation are often times associated with increase fibrosis and collage synthesis. However, Masson Trichrome staining did not reveal any significant collagen deposition in SLK knockout muscle [FigH&I].

Central nuclear myopathies are commonly associated with decreased force generation. Therefore, we conducted isometric force tests on wildtype and knockout mice. We analyzed both the soleus and EDL muscle, as they are comprised of predominately Type 1 and Type 2 fibers respectively. The average weight of each muscle group was comparable between wildtype and knockout mice [Fig3.10]. Consistent with the central nucleation observed, both muscle groups showed a significant decrease in the maximal force generation, with the soleus muscle having a greater change compared to the EDL [Fig3.10]. These data show that SLK deletion in skeletal muscle is leading to a myopathy in adult mice.

3.8 Alterations in Focal Adhesion Protein Localization in SLK Knockout Muscles

A plethora of signalling pathways can affect muscle stability, as well as be activated downstream of muscle damage. We interrogated a number of these signalling pathways by analyzing the activity of their key regulators. We first assessed several postulated targets of SLK, such as

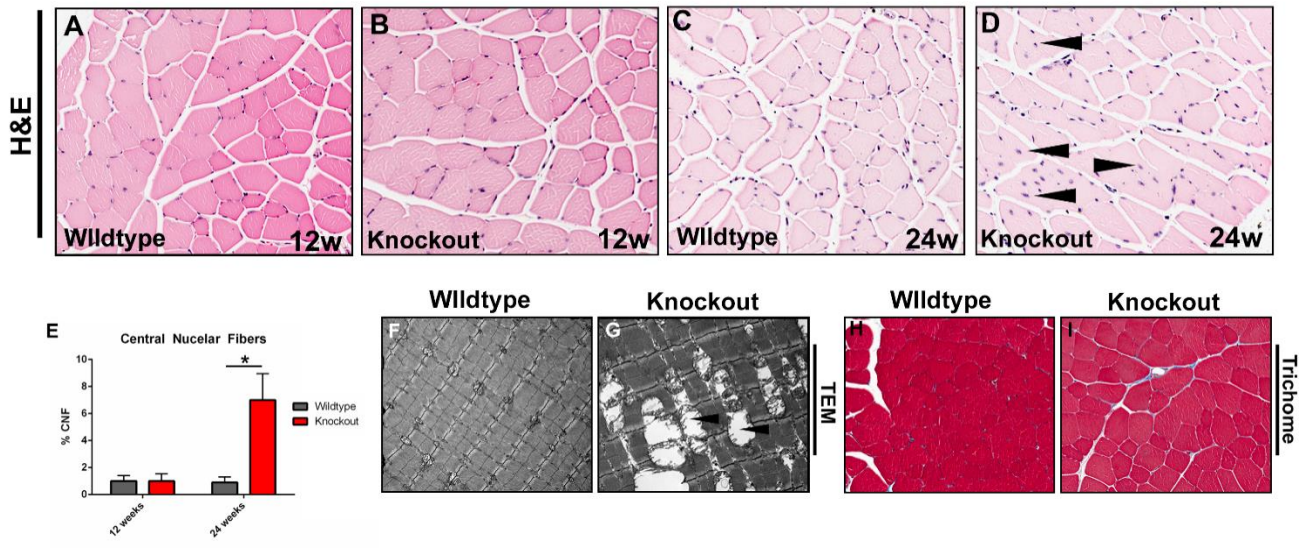

Figure 3.9: SLK Knockout Muscle Display Central Nuclei Myopathy. Haematoxylin and Eosin staining on 12 week old (A&B) and 24 week old (C&D) animals from each genotype. A high proportion of central nuclei (arrow) appeared 24 week old SLK null muscle section. (E) Quantification of central nuclei showed a significant increase in 24 week old SLK null muscles. (n=4/genotype, $p<0.05$). (F&G) Electron photomicrographs from 24 week old skeletal muscles showing enlarged and degenerating mitochondria (arrows). (H&I) Masson's Trichome staining was performed on muscle sections from 24 week old mice. No obvious increase in collagen deposition was observed in knockout mice. Figure adapted from Pryce, et al 2017.

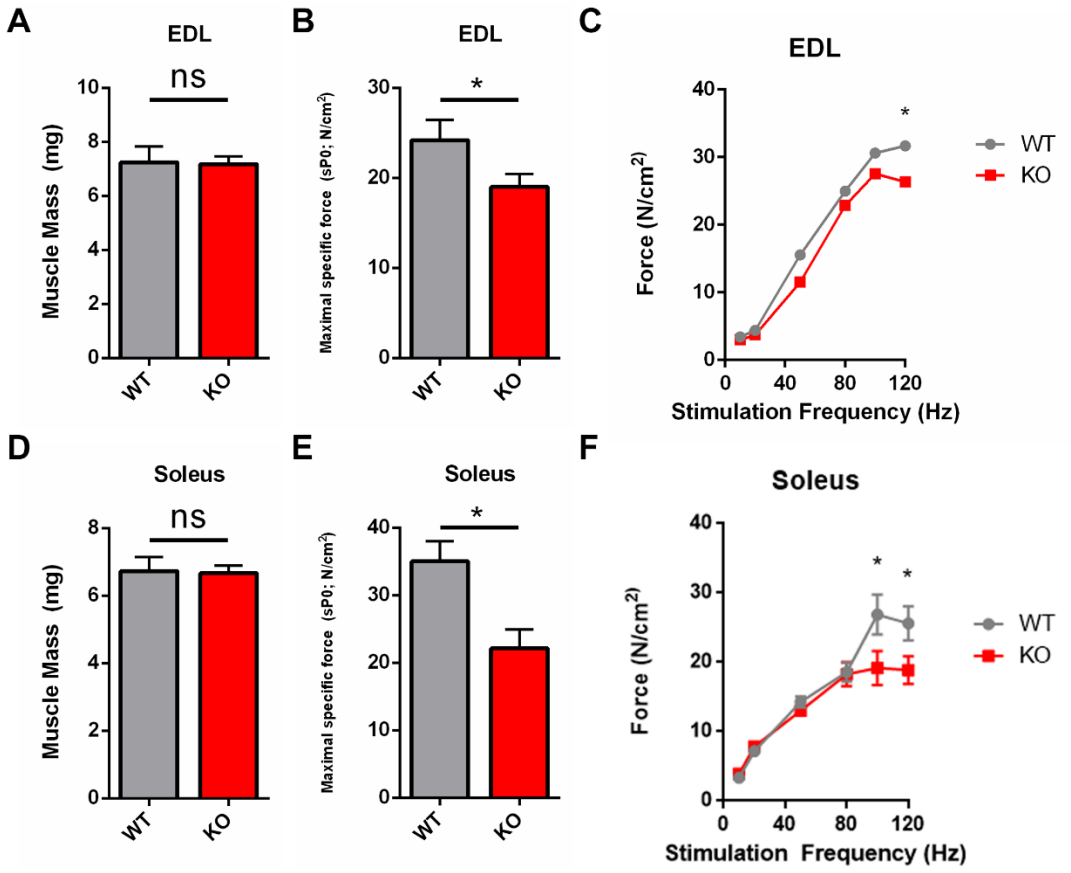

Figure 3.10: Isometric Force is Decreased Following SLK Knockout. The Soleus and EDL muscle fibers were subjected to force measurement assays (7 wildtypes, 10 knockouts). (A) The mass of the EDL was unchanged between groups. (B&C) Maximal specific force was significantly decreased in SLK knockout EDL muscles. (D) Mass of the Soleus was similarly unaffected by SLK deletion. (E&F) Maximal specific force was also significantly decreased in SLK knockout Soleus muscles. The data were analyzed by two-way ANOVA to determine whether the variations among the experimental groups were significant (* $p<0.05$). Figure adapted from Pryce, et al 2017.

ERM, serine 250 on paxillin and serine 127 on YAP. However, none of these markers were changed in SLK null muscles [Fig3.11]. A large body of work performed on SLK by our lab has focused on its role as a mediator of focal adhesion turnover. This is particularly important during myoblast fusion as well as in myofiber integrity. As SLK has been shown to be activated downstream of FAK and functions upstream of Paxillin to mediate turnover, we analyzed the localization and activation status of both of these proteins. The localization of several key mediators of myofiber structural integirty, such as dystrophin, laminin, and vinculin, did not change following SLK knockout [3.11A-F]. However, we observed altered localized of both FAK and Paxillin in a large proportion of myofibers from SLK knockout mice [Fig3.12G-J]. Levels of dystrophin and integrins complexes remain unchanged between the two genotypes as determined by QPCR [Fig3.12K-N]. This suggests that the loss of SLK induces the redistribution of these focal adhesion proteins to the periphery of the fiber. While not as critical for myofiber stability as dystrophin and other members of the DGC, the loss of Paxillin and FAK at the membrane of myofibers can lead to instability and decreased muscle function. Interestingly, activity and levels of both Paxillin and FAK remained unchanged [Fig3.12O]. A more directed approach, such as conditional knockouts of these proteins, would be required to conclusively determine their function in myofiber integrity. Additionally, identification of the mechanisms regulating their localization would also be necessary to further validate this hypothesis.

3.9 SLK Knockout Delays Muscle Regeneration

Another critical component of skeletal muscle homeostasis is the ability to properly regenerate upon damage. Perturbations in the ability of satellite cells to activate, proliferate, migrate and

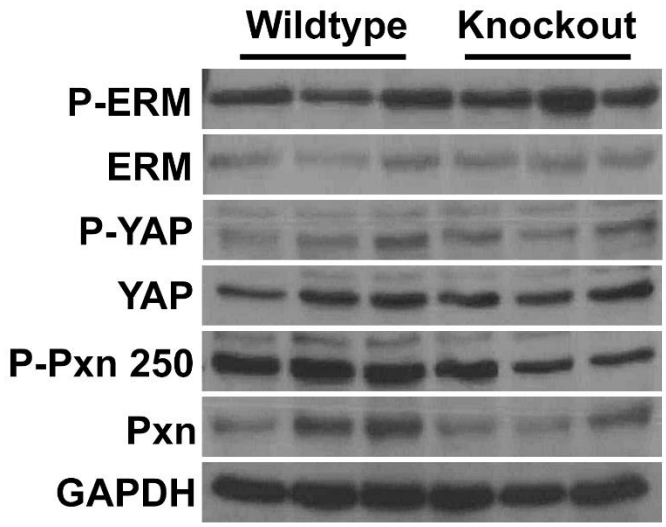

Figure 3.11: Activation Status of Specific Pathways in SLK-null Muscles. Various pathways previously shown to be modulated by SLK, such as Paxillin, and ERM, were analyzed by Western Blot for altered activity in wildtype and SLK knockout muscles. YAP was also assessed due to its activation being modulated by MST1/2, a closely related homologue of SLK.

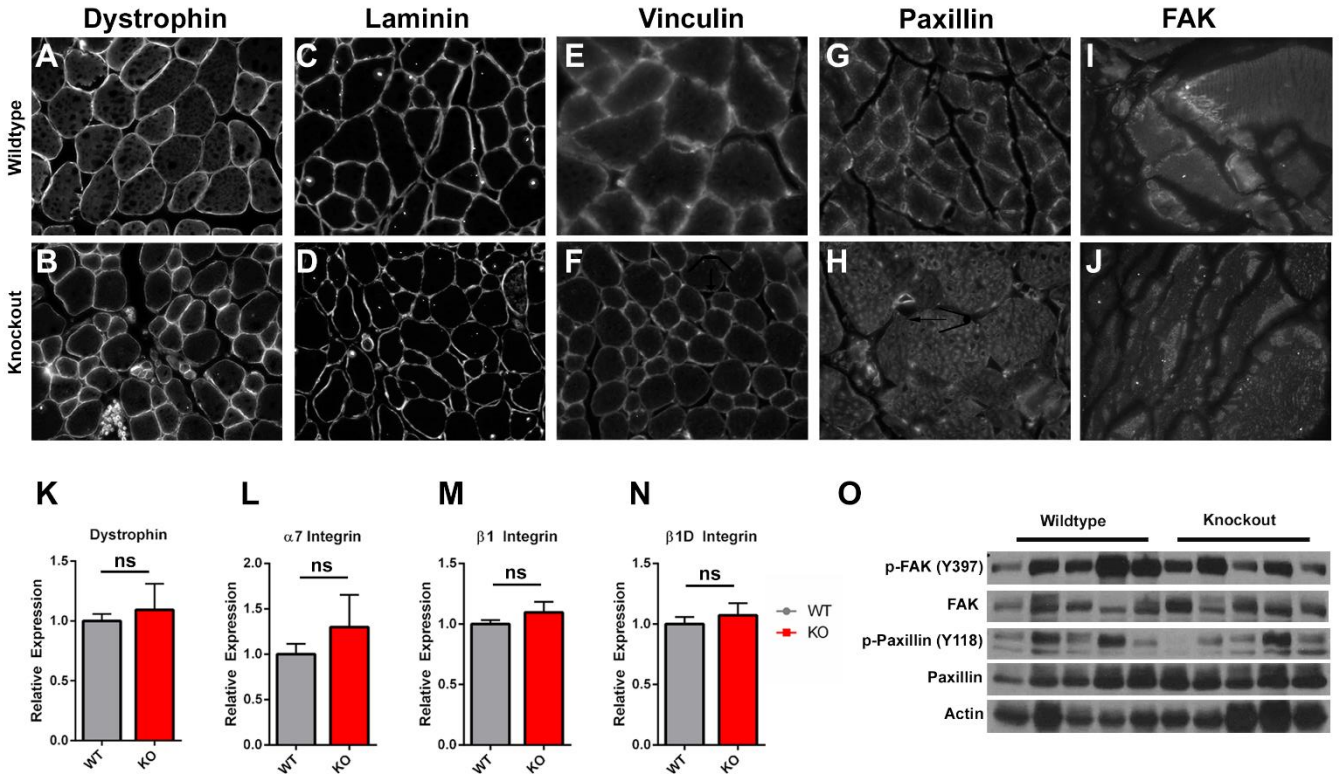
Dystrophin
Laminin
Vinculin
Paxillin
FAK
Wildtype
Knockout
A
B
C
D
E
F
G
H
I
J
K
Dystrophin
ns
Relative Expression
WT
KO
L
α7 Integrin
M
β1 Integrin
N
β1D Integrin
O
Wildtype
Knockout
p-FAK (Y397)
FAK
p-Paxillin (Y118)
Paxillin
Actin

Figure 3.12: Localization of Paxillin and FAK is altered in SLK-null Muscle. Dystrophin (A&B), Laminin (C&D), Vinculin (E&F), Paxillin (G&H) and FAK (I&J) were stained on muscle sections from wildtype and knockout mice. Both Paxillin and FAK showed aberrant localization in SLK knockout muscles. (K-N) Q-PCR analysis was used to determine the relative mRNA levels of dystrophin, α7 integrin, β1 integrin and β1D integrin. (O) Phosphorylation status of FAK and Paxillin were analyzed in both wildtype and knockout samples (n=3/genotype, $p<0.05$). Both proteins were similarly activated in wildtype and knockout muscles. Figure adapted from Pryce, et al 2017.

finally fuse into newly generated myofibers can severely impair the ability to restore muscle function following traumatic injury. Given that SLK deficiency resulted in reductions in proliferation, migration and fusion we hypothesized that muscle regeneration would be impaired following SLK deletion.

We first analyzed SLK expression following muscle damage. Wildtype mice were injected with cardiotoxin in the TA muscle and samples were collected 7 days post injection (DPI). Interestingly, SLK levels were significantly elevated in smaller regenerating myofibers [Fig3.13A-C]. Additionally, we observed an increase in total SLK protein levels at 3 and 7 DPI by western blot [Fig3.13D]. These observations suggest that SLK may be playing a prominent role in muscle regeneration.

In order to assess muscle regeneration in SLK deficient muscles we injected cardiotoxin into the TA muscle of 12 week old wildtype and knockout mice. Mice were then sacrificed at 7, 10, and 21 days post injection and TA muscles were collected and sectioned. Sections were stained with H&E and myofiber cross sectional areas were calculated. Analysis of 7 DPI samples revealed that there was a reduction in fiber size distribution and myofiber size, indicating a decrease in regenerative potential in knockout muscles [Fig3.14A-C]. However, analysis of later time points showed no difference between the two groups [Fig3.14D-I]. Furthermore, assessment of the percentage of Myf5 and Pax7 positive nuclei revealed that satellite cells were activated similarly between the two groups [Fig3.15]. Therefore, although there is an initial decrease in myofiber

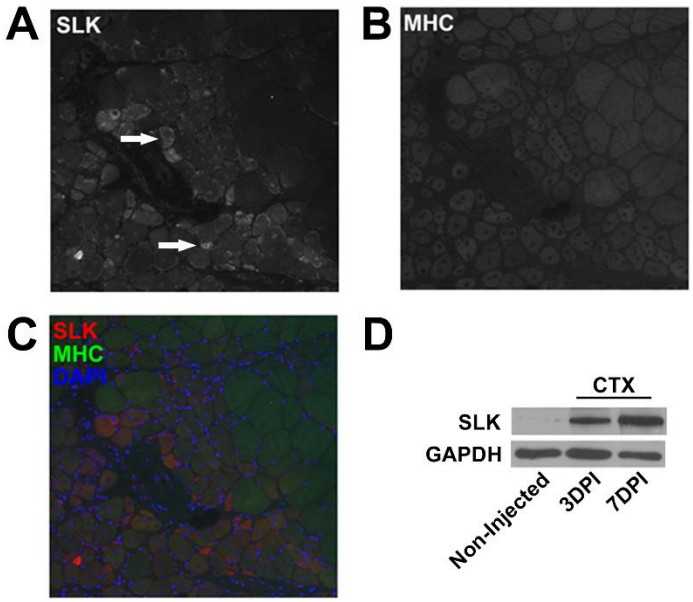

Figure 3.13: SLK Expression is induced in Regenerating Muscles. TA muscle from wildtype mice were injected with cardiotoxin. (A-C) Sections were stained for SLK and MF20. Smaller regenerating fibers had more intense SLK staining (white arrows, A) than neighbouring undamaged fibers. (D) Western blot analysis on whole muscle extracts revealed a significant increase in SLK levels 3 and 7 days post injection of cardiotoxin compared to non-injected controls.

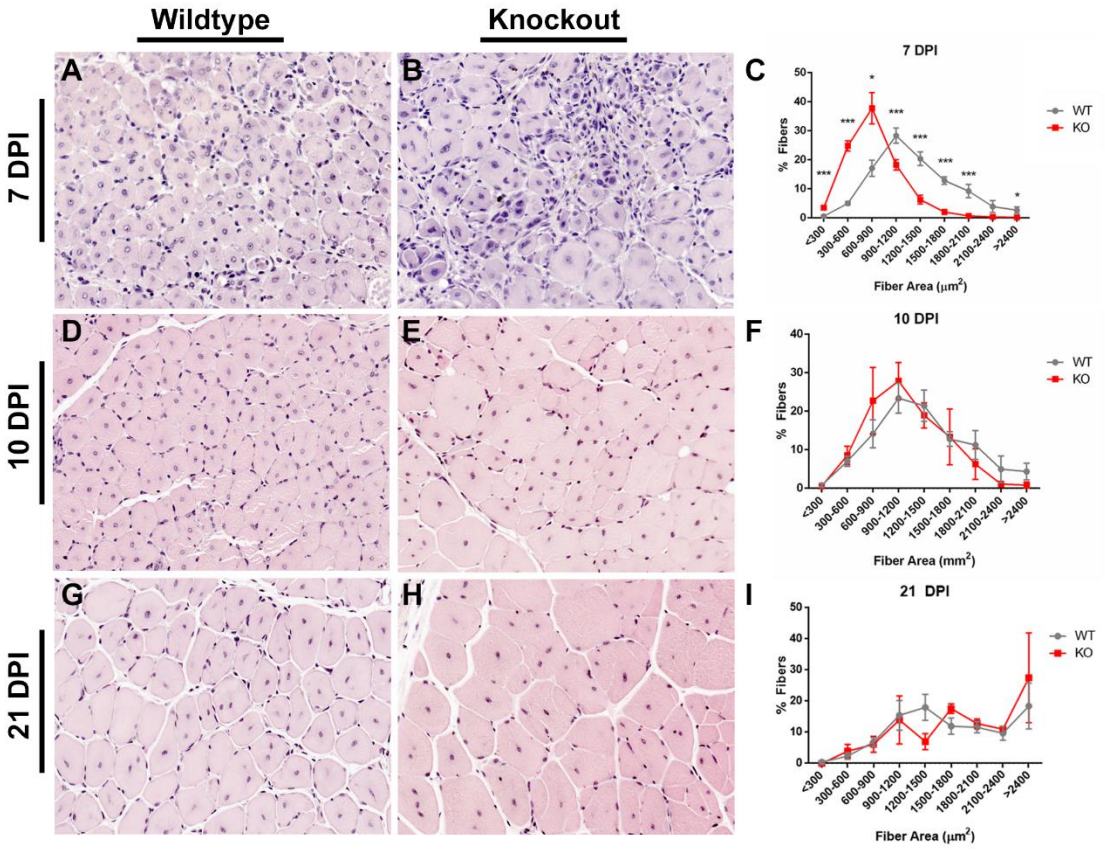

Figure 3.14: Knockout of SLK Results in Delayed Muscle Regeneration. TA muscles from 10-12 week old mice were injected with cardiotoxin. Hematoxylin and Eosin staining was performed on cross sections of cardiotoxin injected TA muscles from 7 (A&B), 10 (D&E), and 21 (G&H) DPI. The myofiber cross sectional area from each time point was calculated (n=5/genotype/day, * $p<0.05$, ** $P<0.01$, *** $P<0.005$,). (C) Day 7 samples showed a significant reduction in the cross sectional area, which was undetectable in 10 (F) and 21 day (I) samples, indicating an initial delay in muscle regeneration. Figure adapted from Pryce, et al 2017.

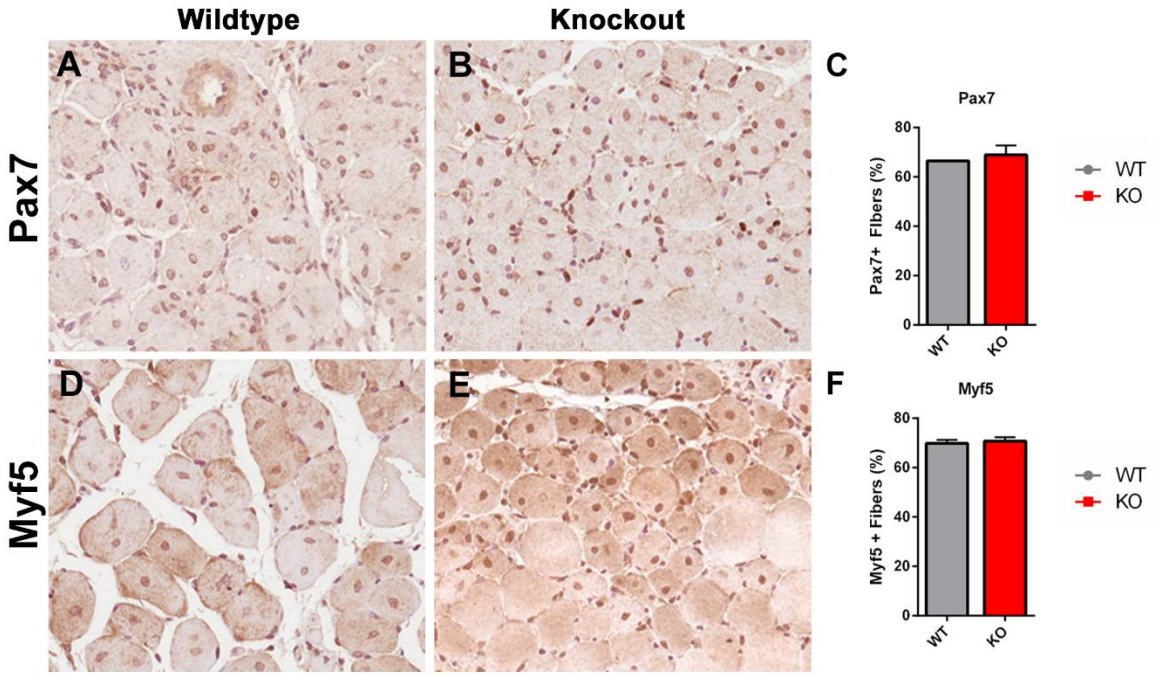

Figure 3.15: Proportion of Myf5 and Pax7 Expressing Cells is unchanged Following SLK Deletion. Cross sections from 7 DPI samples were stained for Myf5 (A&B) and Pax7 (D&E). The percentage of Myf5+ (C) and Pax7+ (F) nuclei were unchanged relative to wildtype controls (n=3/genotype, $p<0.05$). Figure adapted from Pryce, et al 2017.

size, SLK deficient muscles regenerate to the same capacity as wildtype controls, with no apparent inhibition in fusion or decrease in number of activated progenitor cells.

3.10 Discussion and Interpretation of Results

We assessed the role of SLK in myogenesis by performing knockdown studies *in vitro* as well as a skeletal muscle specific knockout of SLK. In our cell culture experiments, we demonstrate a role for SLK in the fusion of myoblasts. Although cellular fusion still occurred, it was greatly reduced across a differentiation time course. Interestingly, this effect was independent of the genetic response, as genes such as myogenin and MHC were still induced in SLK knockdown samples. This phenotype has been reported previously for a number of other proteins. The most striking example of fusion and differentiation decoupling is the deletion of myomaker (Millay et al., 2013; Millay et al., 2014). In myomaker null myoblasts, cellular fusion in completely ablated, but the genetic program is left intact. This leads to fully differentiated mononuclear myocytes comprising the entirety of the muscle compartment. These findings, along with numerous other reports, indicate that myoblast fusion and differentiation are two distinct processes. More relevant to SLK, the deletion of FAK from myogenic precursors also led to a reduction in myoblast fusion, but did not completely inhibit syncytium formation (Quach et al., 2009). Therefore, SLK-deficient myoblasts have a reduced capacity to form multi-nucleated myotubes *in vitro*. However. SLK deletion *in vivo* down not affect myogenesis or muscle repair. Although beneficial to myoblast formation and myofiber integrity, proteins such as SLK and FAK are dispensable for the formation of skeletal muscle. Many loss of function studies have shown a benefit of these proteins in muscle regeneration and myoblast fusion, but few other than studies on myomaker have demonstrated an absolute dependence for myoblast fusion to occur.

Therefore, based on our observations, we conclude that SLK is a dispensable for myogenesis and muscle regeneration but is required for myofiber integrity *in vivo*.

Chapter 4 – Results:

Decreased SLK Signaling can Alter the Anti-Myogenic Effects of TGFβ

4.1 Introduction and Rationale

Previously, we have shown that knockdown of SLK in normal mammary epithelial cells delayed TGFβ induced EMT, suggesting that SLK deletion antagonizes TGFβ signaling (Conway et al., 2017). This effect was found to be independent of the canonical TGFβ signaling pathway, as Smad3 was activated in SLK deficient cells. Exposure of myoblasts to TGFβ can significantly impair myoblast differentiation (D. Liu et al., 2001; D. Liu et al., 2004). This is relevant in the context of muscular dystrophy, as sustained levels of TGFβ promotes fibrosis and inhibits myoblast differentiation. Blocking TGFβ signalling in mouse models of muscular dystrophy decreased the progression of the disease (Accornero et al., 2014; Nelson et al., 2011). Therefore, inhibiting TGFβ signaling may be a therapeutic strategy in treating various muscle disorders, including muscular dystrophy. Given that SLK knockdown was sufficient to delay TGFβ induced EMT, we hypothesized that its deletion would block the anti-myogenic effects of TGFβ in myoblasts and restore myoblast differentiation.

4.2 Knockdown of SLK Protects Myoblasts from Anti-Myogenic Effects of TGFβ

We first tested the effect of SLK deletion on the anti-myogenic effects of TGFβ by knocking down SLK in C2C12 myoblasts under differentiation conditions in the presence of TGFβ. As before, both AdScramble and AdshSLK-infected cells did not shown any alterations in the induction of the myogenic transcriptional program following 4 days in differentiation media [Fig4.1A, lane1&2]. AdshScramble-infected cells treated with TGFβ showed a significant reduction in the expression of myogenin and myosin heavy chain, consistent with previous reports [Fig4.1, lane3]. Interestingly, SLK depleted cells had significantly higher levels of

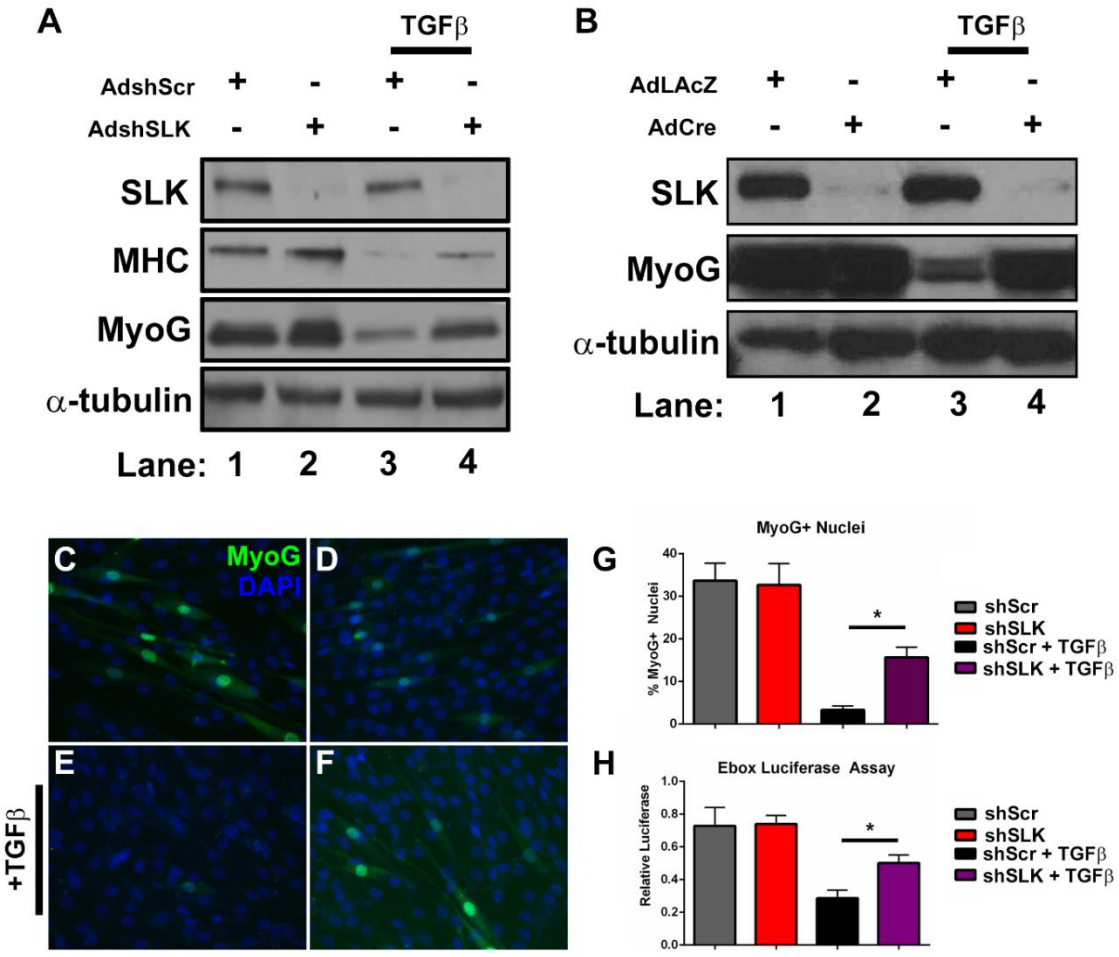
A
TGFβ
AdshScr + - + -
AdshSLK - + - +
SLK
MHC
MyoG
α-tubulin
Lane: 1 2 3 4
B
TGFβ
AdLAcZ + - + -
AdCre - + - +
SLK
MyoG
α-tubulin
Lane: 1 2 3 4
C
MyoG
DAPI
D
E
F
+TGFβ
G
MyoG+ Nuclei
% MyoG+ Nuclei
40
30
20
10
0
*
shScr
shSLK
shScr + TGFβ
shSLK + TGFβ
H
Ebox Luciferase Assay
Relative Luciferase
1.0
0.8
0.6
0.4
0.2
0.0
*
shScr
shSLK
shScr + TGFβ
shSLK + TGFβ

Figure 4.1: SLK Knockdown Protects Myoblasts from the Inhibitory Effect of TGFβ. (A) C2C12 myoblasts were infected with AdshScramble or AdshSLK virus and differentiated in the presence of 5ng/μL of TGFβ. Western blot analysis was used to assess expression of myogenic markers such as MF20 and MyoG. (B) SLK was knocked out of primary $SLK^{fl/fl}$ using AdCre myoblasts and differentiated with in the presence of TGFβ. In both cases (A&B), SLK deficiency increased the expression of MyoG and MHC following treatment with TGFβ. (C-F) MyoG levels were assessed on TGFβ treated and untreated cells. SLK knockdown samples treated with TGFβ had significantly more MyoG+ nuclei than treated controls (* $p<0.05$). (G) Quantification of MyoG+ nuclei from 3 independent experiments. (H) E-box luciferase reporter activity was decreased in the presence of TGFβ, but was rescued upon SLK knockdown averaged from 3 separate experiments (* $p<0.05$).

myogenic gene expression compared to treated Adshscramble controls [Fig4.1, lane4]. Similarly, SLK knockout in primary myoblasts restored myogenin levels in the presence of TGFβ [Fig4.1B]. Myogenin positive nuclei were similarly increased following SLK knockdown [Fig4.1C-G]. Consistent with these findings, we find that SLK knockdown cells can activate an E-box luciferase reporter in the presence of TGFβ compared to treated control cells [Fig4.1H]. Therefore, reducing SLK levels restores myogenic differentiation in the presence of TGFβ.

4.3 SLK Knockdown does not affect Canonical TGFβ Signalling

The canonical TGFβ signaling pathway has been shown to inhibit myogenic differentiation. Following phosphorylation, Smad3 binds to MyoD and MEF2C, preventing their association with co-activators and binding to their respective target sequences. We therefore assessed the activation of the canonical TGFβ signaling pathway following both AdshScramble and AdshSLK infections. Analysis of TGFβ stimulated cells showed no detectable changes in the activation of Smad2 or Smad3 following SLK knockdown [Fig4.2A]. Furthermore, Snai1 and Periostin were both induced similarly by TGFβ [Fig4.2A&B]. Activity of the Smad Binding Element (SBE) luciferase reporter was also not affected following SLK knockdown [Fig4.2C]. We then explored the possibility that SLK was responding to TGFβ stimulation. However, SLK kinase activity was unchanged following TGFβ stimulation [Fig4.2D]. Together, our data show that SLK does not respond to TGFβ stimulation and its knockdown does not prevent the activation of canonical TGFβ signalling and target gene expression.

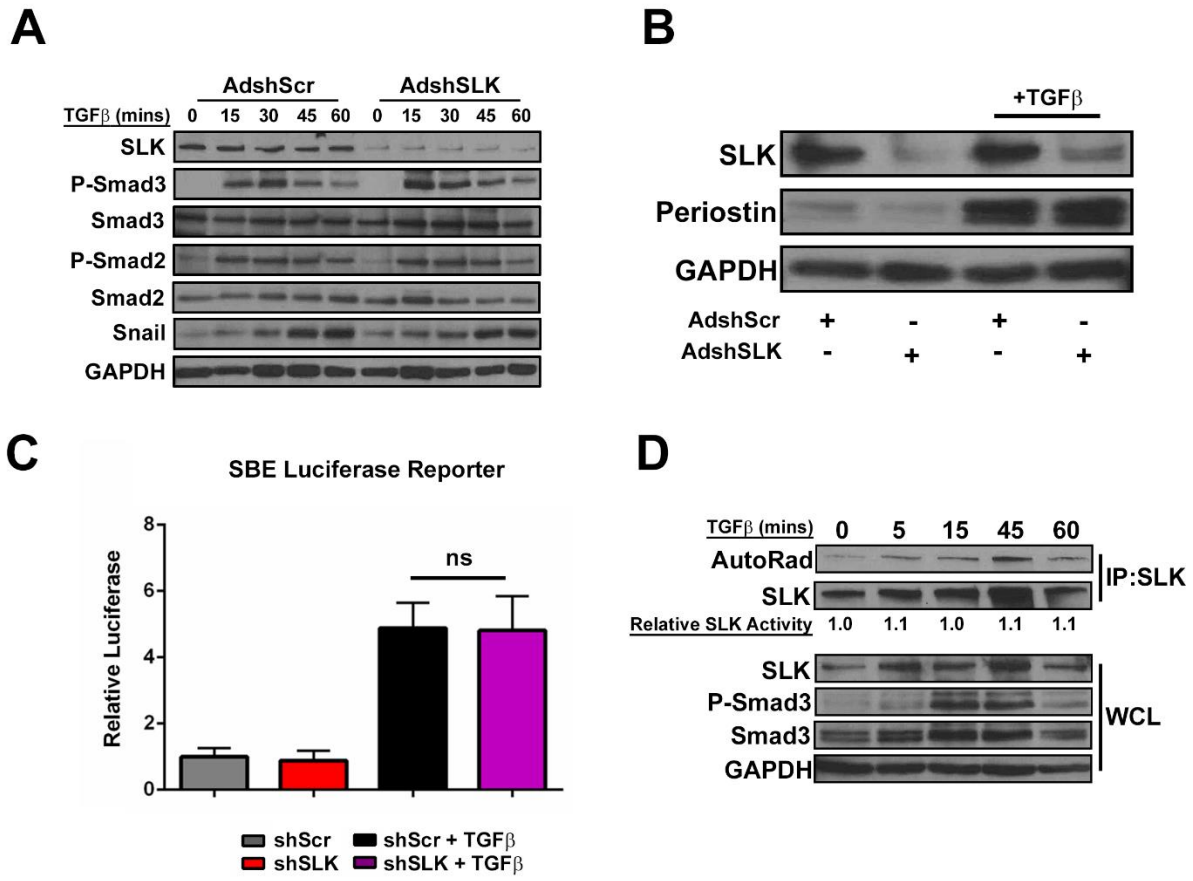

Figure 4.2: Canonical TGFβ Signaling is unaffected by the loss of SLK. (A) C2C12 myoblasts were infected with AdshScr or AdshSLK treated with TGFβ and samples were taken every 15 minutes for up to 1 hour. Canonical TGFβ pathway activity was determined by analyzing phospho-Smad2/3 levels as well as Snai1 expression. (B) Periostin levels were analyzed following 4 days of TGFβ treatment. Postn was similarly activated by TGFβ in AdshScr and AdshSLK samples. (C) Smad Binding Element (SBE) luciferase activity was activated by TGFβ similarly in both control and knockdown cells suggesting that no alterations TGFβ activation by SLK knockdown. (D) SLK kinase activity was normalized to levels immunoprecipitated from each sample. Activity was unchanged following treatment with TGFβ as determined by autoradiography.

4.4 RhoA-GTPase Activity and Phosphorylation are altered by SLK Levels

Previously, it has been shown that SLK can phosphorylate the RhoA-GTPase in smooth muscles cells downstream of angiotension II stimulation (Guilluy et al., 2008). RhoA has a complex role in myogenesis, with reports showing both a positive and negative effect on myogenic gene transcription (Carnac et al., 1998; Castellani, Salvati, Alema, & Falcone, 2006; Iwasaki et al., 2008; Wei et al., 1998). We speculated that SLK may be regulating RhoA phosphorylation in myoblasts, which may be contributing to the observed the enhanced differentiation of SLK-deficient cells

We first assessed normal RhoA Activity in cultured myoblasts. Upon SLK knockdown, we observed a significant reduction in RhoA activity [Fig4.3A]. Additionally, SLK depletion significantly reduces RhoA phosphorylation on serine 188 [Fig4.3A]. However, overexpression of an active SLK construct (YΔC) was insufficient to increase RhoA phosphorylation. Contrary to findings in smooth muscle, we could not readily detect binding between SLK and RhoA in proliferating or differentiating myoblasts [Fig4.3C].

The observation that SLK knockdown results in a significant downregulation in RhoA activity suggest that its inhibition enhances myogenesis in the presence of TGFβ. We predicted that over activation of RhoA would revert the rescue of myogenesis following SLK knockdown. Interestingly, the overexpression of the RhoA-N19 dominant negative mutant was sufficient to restore myogenin levels in the presence of TGFβ [Fig4.4A, Lane9]. However, overexpression of the active RhoA-V14 could not revert the rescue of differentiation following SLK knockdown

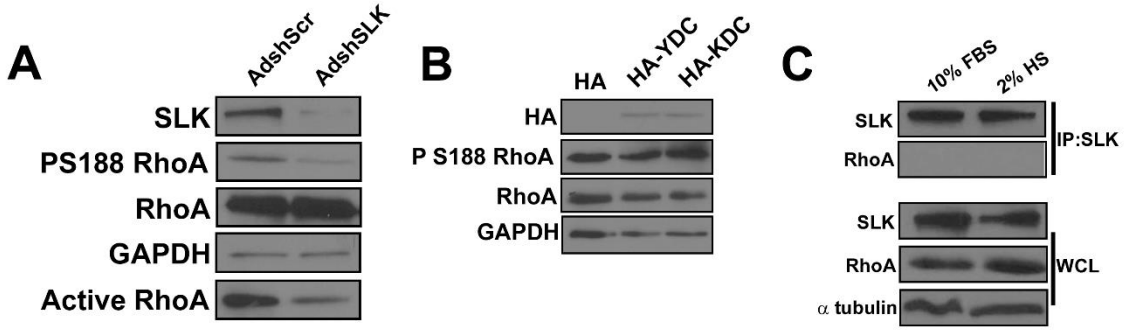

Figure 4.3: RhoA Activity and Phosphorylation is Decreased Following SLK Knockdown. (A) RhoA phosphorylation on serine 188 is reduced following SLK knockdown as determined by Western blot analysis. Rhotekin pulldown revealed decrease in RhoA activity in SLK deficient cells. (B) Overexpression of active and inactive SLK did not alter RhoA activity. (C) SLK IP in proliferating (10%FBS) and differentiating (2%HS) C2C12 samples. RhoA could not be co-immunoprecipitated in either sample indicating no binding between the two proteins in myoblasts.

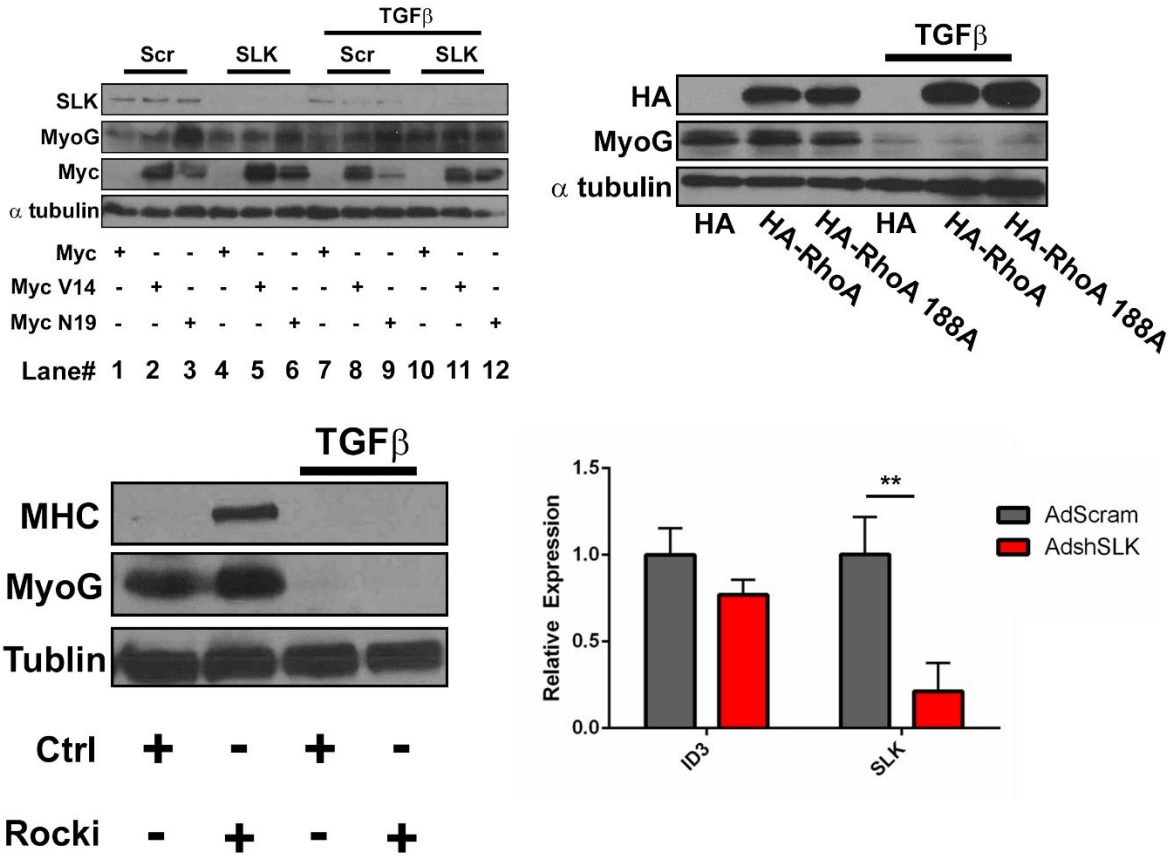

Figure 4.4: Active RhoA is not sufficient to Block the Pro-Myogenic Effects of SLK Knockdown. (A) Overexpression of a dominant negative RhoA (N19) was sufficient to increase differentiation. However, expression of an active RhoA (V14) could not reverse the rescue conferred by SLK knockdown. (B) Overexpression of RhoA-188A could not restore differentiation in TGFβ treated cells. (C) ROCK inhibition using Y27632 increases expression of Myogenin and MHC in normal cells, but could not increase its expression following treatment with TGFβ. (D) Expression of ID3 is unchanged in SLK deficient cells, suggesting no alterations in ROCK activity (** $p<0.01$).

[Fig4.4A]. Additionally, overexpression of a RhoA-188A mutant was also insufficient to increase myogenin levels following TGFβ treatment [Fig4.4B]. Pharmacoloigcla inactivation of the RhoA kinase ROCK using Y27632 (ROCKi) was previously shown to improve myogenic differentiation. We speculated that knockdown of SLK and the observed decrease in RhoA activity would also reduce ROCK activity in myoblasts to enhanced myogenic differentiation in the presence of TGFβ. Although ROCK inhibition alone was sufficient to improve myogenic differentiation, it could not restore the expression of myogenin or myosin heavy chain in the presence of TGFβ [Fig4.4C]. The promyogenic effects of ROCK inhibition has also been linked to the expression of Id3. However, SLK deficient myoblasts had no alterations in Id3 levels compared to controls [Fig4.4D]. Together, our data show that, although SLK knockdown leads to decreased RhoA activity, expression of active RhoA cannot to reverse the pro-myogenic effect of SLK knockdown following treatment with TGFβ. This also suggests that RhoA is not regulating myogenin expression downstream of TGFβ.

4.5 SLK Knockdown Increases p38 Activity in C2C12 Myoblasts

It was previously shown that SLK over-expression increased p38 activity in an ASK1 dependent manner. However, assessment of muscle lysates from SLK knockout mice revealed that SLK deficiency increases in p38 activity [Fig4.5A]. Many studies have shown a beneficial role for p38 in regulating myogenesis. For example, direct phosphorylation of E47 by p38 causes the formation of a MyoD-E47 heterodimer, activating genes involved in myoblast differentiation.

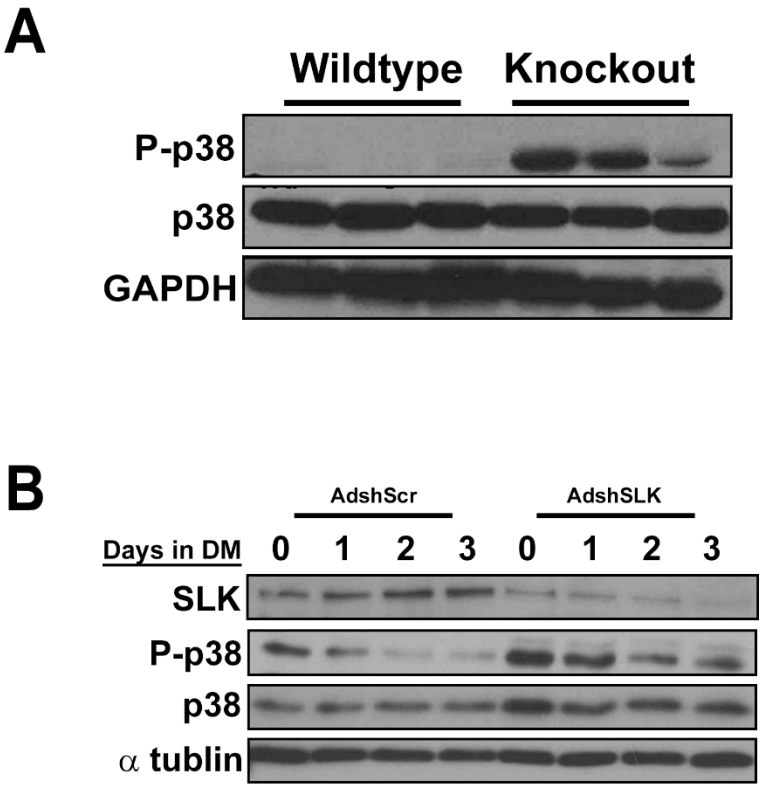

Figure 4.5: Activity of p38 is enhanced in SLK Knockout and Knockdown Samples. (A) Wildtype and SLK knockout muscles were blotted for active p38. Levels were significantly higher in SLK knockout, with wildtypes showing undetectable levels of active p38. (B) C2C12s were differentiated for 3 days following infected with AdshScramble or AdshSLK. Total Increase phosphor p38 was observed in SLK knockdown samples compared to controls, suggesting an increase in activity.

Therefore, we tested the effect of SLK deletion on p38 activity and myoblast differentiation. We assessed p38 activity in SLK deficient cells by knocking down SLK in differentiating myoblasts. Control cells showed high levels of phospho-p38 in proliferating cells, which steadily decreased over time in differentiation medium [Fig4.5A]. As seen *in vivo* we observed a significant increase in p38 phosphorylation across the time course following SLK knockdown [Fig4.5B]. These data suggest that SLK deficiency increases p38 activity in both cultured myoblasts and skeletal muscle.

4.6 Inhibition of p38 Blocks Myogenic Rescue in SLK Deficient Myoblast

Previous studies have shown that increased p38 activity can promote myogenic differentiation. Conversely, inhibition of p38 signaling impairs myoblast differentiation. Therefore, we tested whether increased p38 activity in SLK-deficient cells was responsible for the enhanced myogenic differentiation in the presence of TGFβ. We inhibited p38 using SB203580 in the presence or absence of TGFβ. The inhibition of p38 alone was sufficient to decrease differentiation in both AdScramble and AdshSLK infected cells [Fig4.6A]. More importantly, the inhibition of p38 was sufficient to prevent SLK deficient cells from differentiating in the presence of TGFβ. These findings suggest that the increased p38 activity following SLK knockdown plays a role in mediating the induction of differentiation in the presence of TGFβ. We next overexpressed active MKK6, an upstream activator of p38, and assessed differentiation. MKK6 expression on its own was sufficient to increase myoblast differentiation [Fig4.6B]. Interestingly, MKK6 expression was also sufficient to restore differentiation in the presence of TGFβ, suggesting that an increase in p38 activity can enhanced myogenesis in the presence of TGFβ. Furthermore, we analysed utrophin expression, as it has been previously shown to be

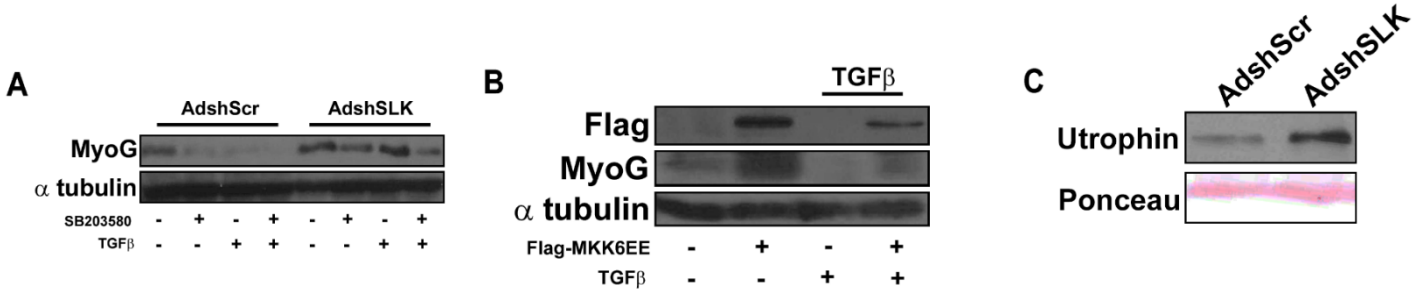

Figure 4.6: Inhibition of p38 reverts the Pro-myogenic Effect of SLK Knockdown. (A) Wildtype and SLK knockdown C2C12 myoblasts were treated with SB203580, TGFβ, or a combination of both in a four day differentiation assay. SB treatment was sufficient to block myogenesis and also further blocked the myogenic rescue conferred by SLK knockdown. (B) Expression of an active MKK6 mutant partially restored differentiation in the presence of TGFβ, but was less efficient than SLK knockdown. (C) Levels of utrophin are elevated in SLK knockdown cells.

regulated by p38 (Amirouche et al., 2013; Hadwen et al., 2018). Interestingly, levels of utrophin were elevated in SLK knockdown myoblasts [Fig4.6C].

4.7 Discussion and Interpretation of Results

TGFβ has been shown to inhibit myoblast differentiation. This is an important observation in muscular dystrophy, where elevated levels of TGFβ can contribute not only to fibrosis, but also function to inhibit muscle regeneration. Here, we show that the deletion of SLK is sufficient to overcome some of the anti-myogenic effects of TGFβ. Furthermore, we showed that SLK deletion results in an increase in p38 activity. Inhibition of p38 was sufficient to reverse the beneficial effects of SLK deletion. Additionally, activation or p38 by MKK6 was sufficient to restore differentiation in the presence of TGFβ. These findings will be beneficial in identifying new therapies for the treatment of muscular dystrophy.

Chapter 5 – Results:

SLK Expression and Function in Dystrophic Muscle

5.1 Introduction and Rationale

SLK deletion in cultured myoblasts results in a reduction in myoblast fusion without affecting the myogenic transcriptional program. Furthermore, deletion of SLK in skeletal muscle delays, but does not impair muscle regeneration. These results suggest that SLK is not absolutely essential for skeletal muscle formation or regeneration. Further work revealed that the knockdown of SLK can restore myogenic differentiation in the presence of TGFβ, suggesting that SLK is required for the TGFβ response. This observation is relevant in the context of muscular dystrophy, in which excess TGFβ signalling increases fibrosis and decreases myoblast differentiation. Therefore, we speculated that Myf5-Cre mediated deletion of SLK in the dystrophic *mdx* mouse model would increase myoblast differentiation and decrease the pathology associated sustained TGFβ signalling in muscular dystrophy. In order to test this, we examined the expression pattern of SLK in dystrophic muscle as well as the effect of crossing our muscle-specific SLK knockout with the *mdx* mouse strain.

5.2 SLK Levels are elevated in Regenerating Myofibers of Dystrophic Animals

To investigate the role of SLK in muscular dystrophy we analyzed the relative expression of SLK within the diaphragm of *mdx* muscles. Interestingly, SLK protein levels were elevated in *mdx* muscle compared to wildtype C57 controls, with no change in SLK kinase activity, as determined by autophosphorylation [Fig5.1A]. When diaphragm samples of the Golden Retriever Muscular Dystrophy (GRMD) animal model were analyzed similar increased levels of SLK were also observed, indicating that this phenomenon is translatable to different models of dystrophy and was not specific to the *mdx* mouse model [Fig5.1B]. SLK mRNA is also elevated in *mdx* muscle compared to C57 controls [Fig5.1C]. Throughout this analysis, the levels of

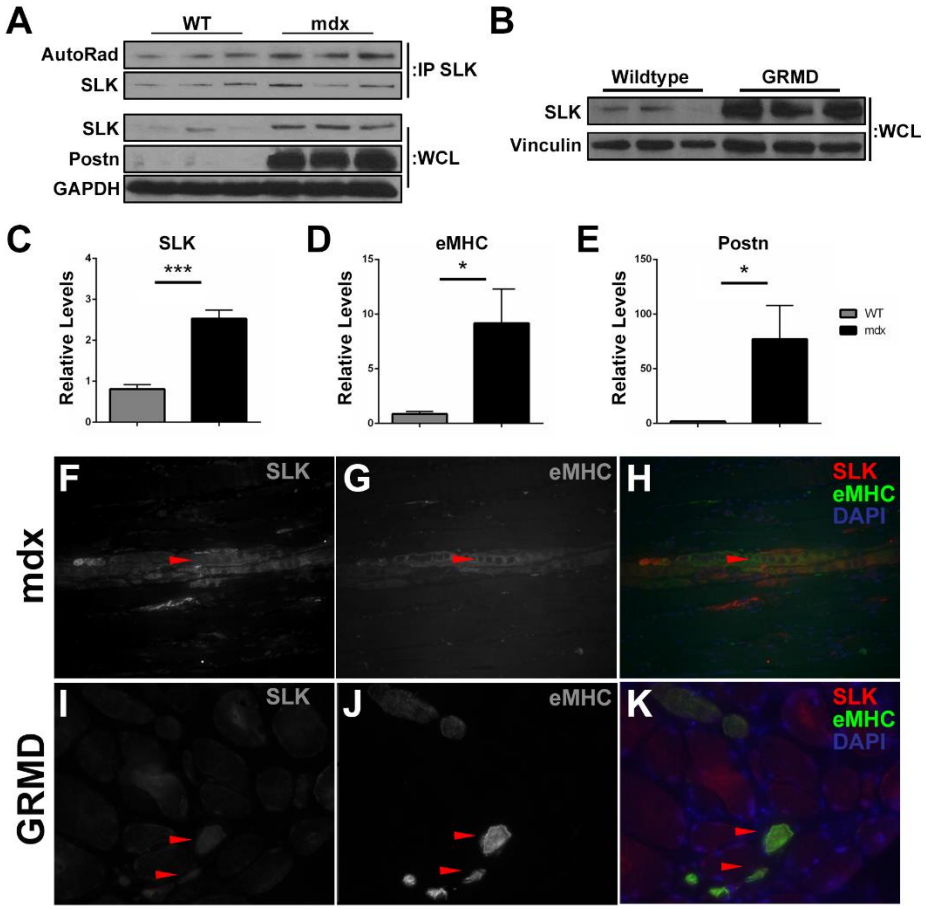
A
WT
mdx
AutoRad
SLK
:IP SLK
SLK
Postn
GAPDH
:WCL
B
Wildtype
GRMD
SLK
Vinculin
:WCL
C
SLK
***
Relative Levels
D
eMHC
*
Relative Levels
E
Postn
*
Relative Levels
WT
mdx
mdx
GRMD
F
SLK
G
eMHC
H
SLK
eMHC
DAPI
I
SLK
J
eMHC
K
SLK
eMHC
DAPI

Figure 5.1: Elevated SLK Expression in Regenerating Myofibers of Dystrophic Muscle. (A) SLK was immunoprecipitated from control and *mdx* muscle and subjected to *in vitro* kinase assays. No alterations in kinase activity were observed. Analysis of the WCL revealed that total SLK levels were elevated in *mdx* muscles. Periostin was used as a control to demonstrate the dystrophic phenotype. (B) Similar to *mdx*, muscles from GRMD have elevated SLK levels compared to wildtype controls. (C) Q-PCR analysis revealed a 2-fold increase in SLK mRNA, compared to 10 and 80-fold increase in eMHC (D) and Periostin (E), respectively (* $p<0.05$, *** $p<0.005$). Five independent samples were used for Q-PCR analysis. Co-staining for eMHC and SLK in the *mdx* (F-H) and GRMD (I-J) showed co-expression of both proteins.

embryonic Myosin Heavy Chain (eMHC) and Periostin (Postn) were consistently elevated in dystrophic muscle, demonstrating the induction both muscle regeneration and fibrosis [Fig5.1A, D&E].

The dystrophic muscle environment is composed of various cell types, such as regenerating myogenic cells as well as infiltrating immune cells and fibroblasts. Our prediction was that decreased expression of SLK in myoblasts would inhibit the anti-myogenic effects of TGFβ, increase myogenesis and thus enhance muscle function. As the increased SLK expression observed in the dystrophic muscle could be due to either regenerating myofibers or alternative cell populations of non-myogenic origin, we performed immunocytochemistry on tissue sections from *mdx* and GRMD muscle samples for SLK and eMHC. Interestingly, the most prominent staining for SLK was mostly co-localized with eMHC in both the *mdx* and GRMD models suggesting that regenerating fibers were the major cell type contributing to the increased expression levels of SLK [Fig5.1F-K]. Together, these results suggest that SLK is highly expressed within regenerating myofibers of dystrophic animals.

5.3 SLK Deletion in the *mdx* Background does exacerbate the Dystrophic Phenotype

After demonstrating that SLK was expressed within the myogenic tissue of dystrophic muscle sections we began crossing the SLK muscle knockout model with the *mdx* strain. As the deletion of SLK within skeletal muscle is sufficient to induce a mild myopathy, one possibility is that SLK ablation will exacerbate the pathology in *mdx* mice. This may then result in lethality, as is observed in other double knockout models of muscle dystrophy, such as the utrophin/dystrophin double knockout model. Conversely, the rescued myogenic differentiation observed downstream

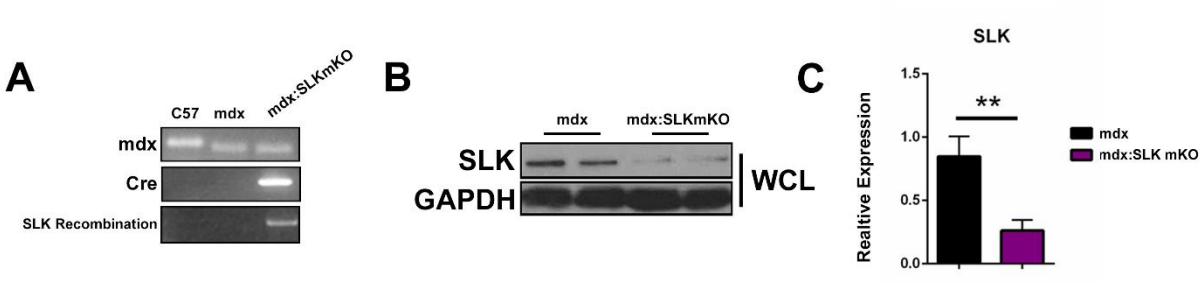

Figure 5.2: Deletion of SLK on an *mdx* Background. SLK muscle knockout mice were bred into the *mdx* background. (A) SLK recombination PCR revealed that deletion was efficient in Cre positive mice. SLK knockout was confirmed by both western blot (B) and Q-PCR (C) (** $P<0.01$). Five independent muscles were used for Q-PCR analysis of SLK expression.

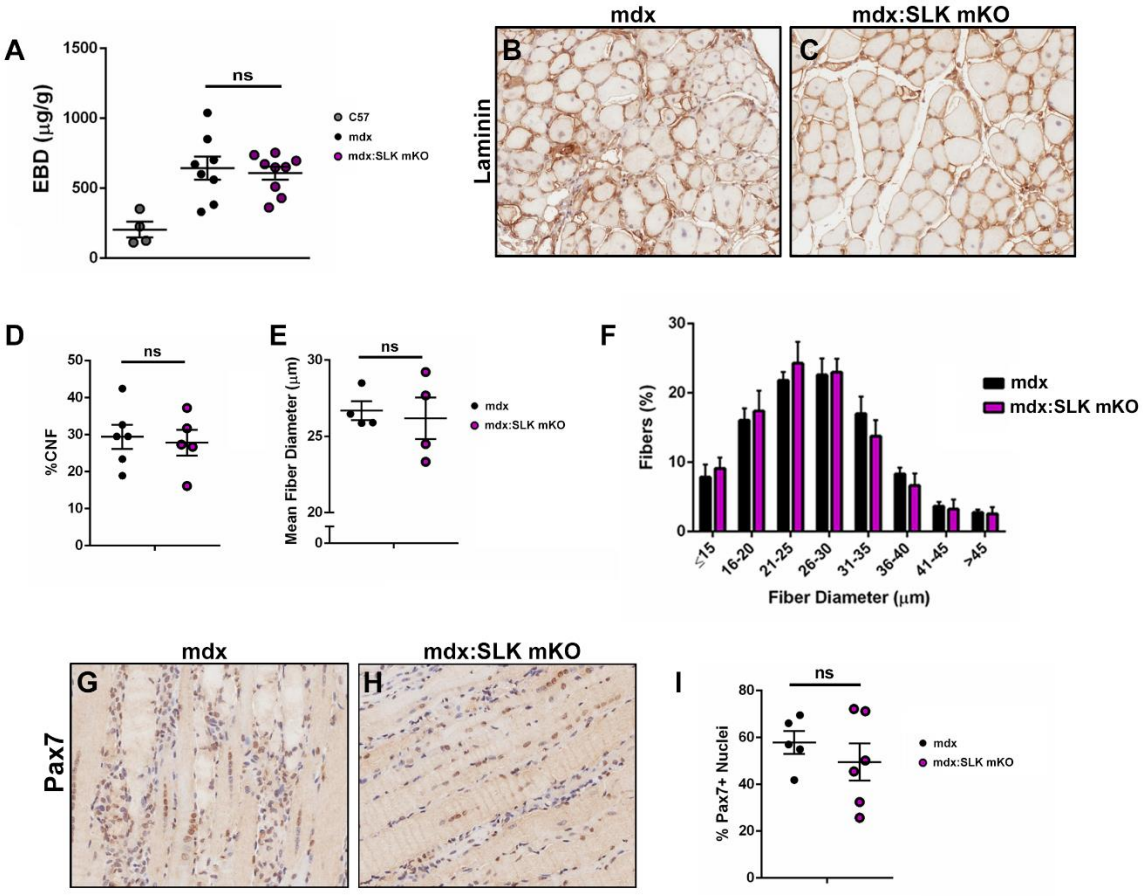

Figure 5.3: Myofiber Degeneration and Satellite Cell Activation are unchanged by SLK Deletion in *mdx* Mice. (A) Evan's blue dye (EBD) was injected into mice via intraperitoneal injection (n=4 C57, 8 *mdx*, 9 *mdx*:SLKmKO). Diaphragm muscles were ground and weighed and the amount of EBD was measured using absorbance. No differences were observed between *mdx* and *mdx*:SLK mKO. (B&C) Representative laminin stain on *mdx* and *mdx*:SLK mKO diaphragm sections. These images were used to calculate central nuclear fibers (%CNF) (D) and fiber diameter (E) (n=5/genotype). Fiber sizes were binned into groups to assess fiber size distribution (F). (G-I) Pax7 IHC on muscle sections for enumeration of Pax7+ nuclei were enumerated (n=5/genotype). No differences were observed between the genotypes, indicating no alteration in satellite cell activation in *mdx*:SLK mKO ($p<0.05$).

of TGFβ following SLK knockdown suggests that SLK deficient myoblasts may display enhanced differentiation compared to normal myoblasts, thus making SLK deletion beneficial to *mdx* muscle.

We first assessed the viability of a muscle specific deletion of SLK in the *mdx* background. We bred our Myf5-Cre SLK fl/fl mice into *mdx* background and assessed SLK deletion in adult muscle tissue. Recombination PCR performed on DNA extracted from skeletal muscle of Myf5-Cre/SLK$^{fl/fl}$ *mdx* mice (here after referred to as *mdx*:SLK mKO) showed the presence of the recombined PCR product [Fig5.2A]. Additionally, SLK protein and mRNA levels were significantly reduced in the *mdx*/SLK null mice compared to *mdx* alone [Fig5.2B&C]. The *mdx*:SLK mKO mice showed no alterations in viability and no indications of decreased lifespan and mice were born at the predicted ratios. These results indicate that SLK deficiency does not reduce survivability in *mdx* mice or exacerbate the *mdx* phenotype.

5.4 Terminal Differentiation is enhanced in *mdx*:SLK mKO mice

Myofiber degeneration in muscular dystrophy stimulates satellite cell activation and muscle regeneration. This progressive damage results in immune infiltration and fibrosis. Additionally, there is enhanced cytokine secretion in dystrophic muscle, such as higher levels of TGFβ. It has been shown that the increased levels of TGFβ in the dystrophic environment can inhibit satellite cell activation, proliferation and differentiation. Given that SLK knockdown restored myogenesis following TGFβ treatment in cultured myoblasts, we speculated that muscle regeneration would be improved following SLK deletion on an *mdx* background.

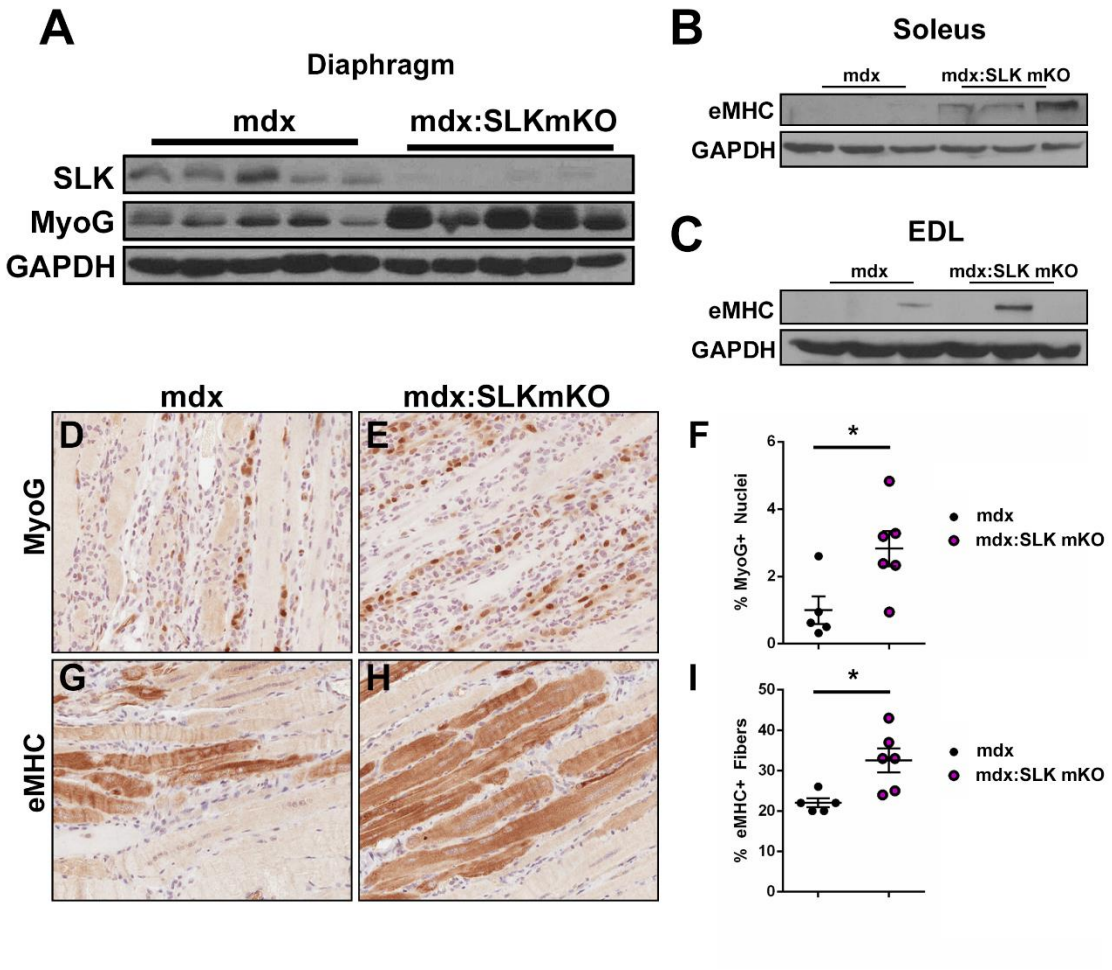

Figure 5.4: Markers of Terminal Differentiation are Elevated in *mdx*:SLK mKO. (A) Diaphragm muscle lysates form 3 month old *mdx* and *mdx*:SLK mKO mice were blotted and probed for Myogenin. Elevated levels of Myogenin were observed in *mdx*:SLK mKO muscle. (B) Similarly, elevated levels of eMHC were observed in the Soleus muscle of *mdx*:SLK mKO muscle. (C) EDL muscle lysates showed no marked difference between the genotypes in the levels of eMHC. (D-F) Myogenin IHC on diaphragm sections from *mdx* and *mdx*:SLK mKO mice (n=5/genotype). The number of MyoG positive nuclei was significantly elevated in sections from *mdx*:SLK mKO. (G-I) Similarly, the number of eMHC positive fibers was increased in *mdx*:SLK mKO compared to *mdx* muscle (n=5/genotype, * $p<0.05$).

We first characterized myofiber integrity of the *mdx*:SLK mKO using Evan's Blue Dye (EBD) uptake. Both *mdx* and *mdx*:SLK mKO showed a significant increase in the uptake of EBD compared to C57 controls, indicating enhanced permeability of the myofibers. However, the *mdx* and *mdx*:SLK mKO were not statistically different from each other, suggesting that there was no alteration in myofiber membrane integrity and myofiber necrosis between the two groups. We then assessed muscle regeneration by staining cross sections of diaphragms from both *mdx* and *mdx* SLK mKO with laminin [Fig5.3B&C]. These images were then used to calculated myofiber diameter and central nuclear fibers (CNF) [Fig5.3D-F]. Interestingly, both fiber diameter and number of CNF were similar between the groups in both the diaphragm [Fig5.3D&E]. No changes in fiber size distributions were noted between the groups [Fig5.3F]. The sections were stained for Pax7 and the number of Pax7-positive satellite cells were enumerated within each muscle section [Fig5.3G-I]. No significant changes were found in the percentage of cells expressing Pax7, indicating that satellite cells were activated and expanded in both groups. These results indicate that the satellite cell compartment and myofiber degeneration were not affected by SLK deletion.

In addition to inhibiting satellite cell activation, TGFβ also impairs myoblast differentiation. We therefore speculated that *mdx*:SLK mKO muscles may have a differentiation advantage compared to *mdx* alone. Therefore, we assessed the levels of the differentiation markers myogenin (MyoG) and embryonic myosin heavy chain (eMHC). Total levels of MyoG in the diaphragm were markedly elevated by western blot analysis in *mdx*:SLK mKO mice [Fig5.4A].

Additionally, the Soleus but not the EDL showed increased expression of eMHC compared to *mdx* controls [5.4B&C]. Supporting this, the number of MyoG positive cells was significantly

increased in the *mdx* SLK mKO mice compared to *mdx*, suggesting a greater number of differentiating cells within these muscles [Fig5.4D-F]. Furthermore, the number of eMHC myofibers was also significantly elevated [Fig5.4G-I], suggesting that SLK-deficient myoblasts may have an increased differentiation potential in an inflammatory environment.

5.5 Immune Infiltration, but not Fibrosis, is Reduced in *mdx*:SLK mKO Mice

A decrease in committed myogenic progenitors is a hallmark of dystrophic muscles. However, more deleterious aspects of the pathology, such as immune infiltration and fibrosis, contribute greatly to decreased muscle function in muscular dystrophy. Given that we observed an increase in regenerating fibers in *mdx* SLK:mKO mice we assessed fibrosis and immune infiltration.

Fibrosis was analyzed by Masson Trichome staining to visualize collagen deposition within skeletal muscle. As previously reported, *mdx* mice had significant collagen deposition (stained blue) [Fig5.5A]. However, surface area covered by collagen was unaffected in *mdx*:SLK mKO when compared to *mdx* controls at both 3 and 6 months of age [Fig5.5A-D]. We also analyzed levels of fibrotic markers (such as Perisotin and Vimentin) by Western blot [Fig5.5E], as well as additional markers by Q-PCR, such as collagen, connective tissue growth factor and fibronectin [Fig5.5F]. No significant differences in any of these markers were found between *mdx* and *mdx* SLK mKO muscles, indicating that SLK deletion in *mdx* mice does not decrease fibrosis.

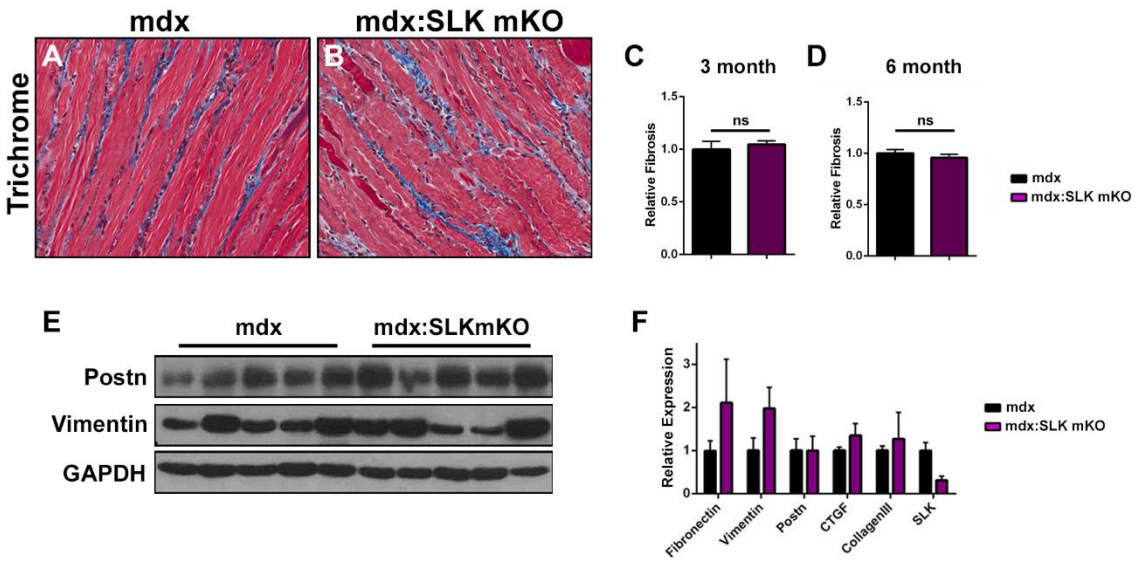

Figure 5.5: Fibrosis is unaffected by the deletion of SLK on an *mdx* Background. (A-D) Three and six month old diaphragm sections were stained with Masson Trichome to evaluate the collagen deposition (n=5/genotype). (E) Western blot analysis of Vimentin and Periostin showed equivalent levels between both *mdx* and *mdx*:SLK mKO. (F) mRNA levels of Fibronectin, Vimentin, Periostin, CTGF and Collagen were also unchanged (n=5/genotype, $p<0.05$).

Immune infiltration was assessed by immunohistochemistry for CD45 on diaphragm sections from *mdx* and *mdx* SLK mKO mice [Fig5.6A&B]. A significant reduction in the total number of CD45+ cells was observed in *mdx*:SLK mKO compared to *mdx* alone, indicating reduced infiltration of total leukocytes [Fig5.6C]. The overall proportion of macrophages (F480/CD11b double positive) present in the CD45+ cells in both *mdx* and *mdx* SLK mKO mice was not statistically different [Fig5.6D]. Studies have demonstrated that macrophage polarization has a significant impact on the inflammatory response and regeneration capacity. However, we did observe not any changes in the proportion of M1 or M2 positive cells between the two groups within the CD45+ population [Fig5.6E&F]. Therefore, although the total number of CD45+ cells is reduced in *mdx* SLK mKO mice, the proportion of total macrophages in each population, as well as the polarization, remains unchanged.

5.6 SLK Deficiency Protects the Soleus, but not EDL, from Contraction Induced Injury

Consistent muscle degeneration and fibrosis in muscular dystrophy leads to a reduction in muscle function. As we observed an increase in the amount of regenerating myofbers in the *mdx* mKO, we speculated that this would translate into improved of force generation. To analyze muscle force generation we dissected both the Soleus and EDL muscle, to evaluate muscle strength and integrity in both Type 1 and Type 2 muscle groups.

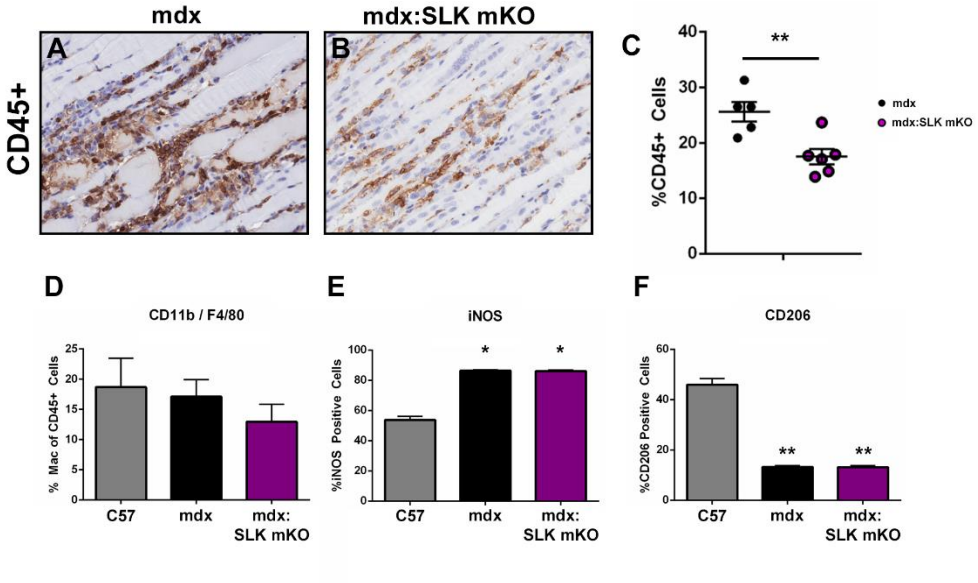

Figure 5.6: Decreased Leuocyte Infiltration in *mdx*:SLK mKO. (A-C) Diaphram *mdx* and *mdx*:SLK mKO muscles were stained for CD45 and the total number of positive cells were enumerated. *mdx*:SLK mKO had a significant reduction in the number of CD45+ cells (n=5/genotype, $p<0.05$). (D) Muscles were digested in collagenase B and flow cytometry was used to isolate CD45+/F4/80+/CD11b+ cells (p=5/genotype). (D) The proportion of CD45+ cells that were F4/80+/CD11b+ (macrophages) was unchanged between C57, *mdx* and *mdx*:SLK mKO mice. Macrophages were further characterized for M1 and M2 polarization by iNOS and CD206 staining (n=3/genotype) (E&F). Both *mdx* and *mdx*:SLK mKO showed similar polarization profiles of macrophages in 3 month old mice.

Consistent with previous findings, the EDL muscle from the *mdx* showed a significant increase in mass compared to wildtypes, which was also observed in the *mdx* SLK mKO [Fig5.7A]. As expected, EDL muscles from *mdx* mice had a significant reduction in isometric force compared to C57 control mice [Fig5.7B]. Isometric force measurements in *mdx* SLK mKO EDL muscles were similarly reduced from C57 controls, indicating no improvement in muscle function following SLK deletion [Fig5.7B]. We next performed eccentric muscle contraction analysis. Muscles were subjected to 7 consecutive contractions and maximal force production was measured at each time point. The EDL muscle from *mdx* showed a significant reduction at each contraction compared to wildtype controls [Fig5.7C]. EDL muscles from *mdx* SLK mKO were similarly affected, indicating that there was no protection from contraction induced injury.In contrast to the EDL, there was no observable alteration in Soleus muscle mass compared to non-dystrophic mice [Fig5.7D]. Although there was a significant reduction in force generation in the *mdx* Soleus the *mdx*:SLK mKO Soleus was not statistically different from *mdx* [Fig5.7E]. Similar to the Soleus, repeated eccentric contractions reduced the force generation in the *mdx* compared to C57 controls [Fig5.7F]. Surprisingly, in contrast to the EDL, repeated contraction in the *mdx*:SLK mKO did not show a reduction in force generation [Fig5.7F]. Collectively, these results demonstrate that SLK deficiency does not alter maximal specific force, but can protect some muscle groups from contraction induced injury. Other contractile properties remained unchanged between the genotypes [Table 5&6].

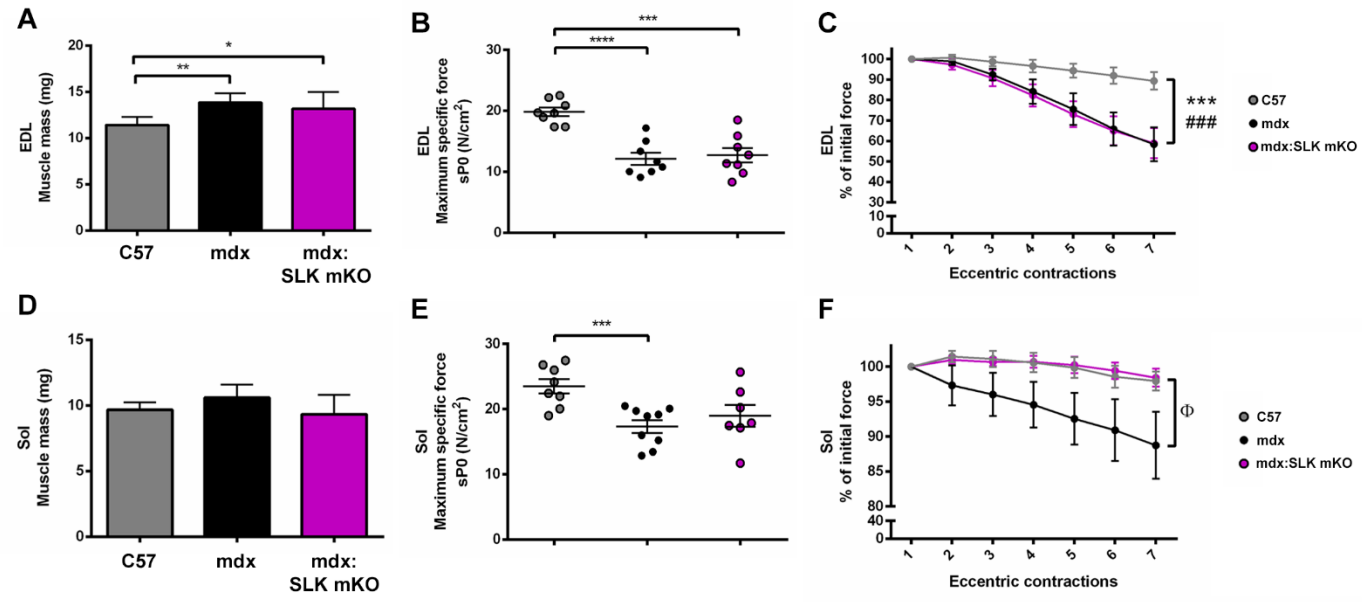
A
EDL
Muscle mass (mg)
C57
mdx
mdx:
SLK mKO
B
EDL
Maximum specific force
sP0 (N/cm²)
C
EDL
% of initial force
Eccentric contractions
C57
mdx
mdx:SLK mKO
D
Sol
Muscle mass (mg)
E
Sol
Maximum specific force
sP0 (N/cm²)
F
Sol
% of initial force
Eccentric contractions

Figure 5.7: Soleus Muscle from *mdx*:SLK mKO are protected from Eccentric Contraction Induced Injury. (A) EDL muscles were isolated from C57, mdx and mdx:SLK mKO mice and weighed. *Mdx* and *mdx*:SLK mKO had a similar increase in weight compared to C57 controls. (B) Isometric force was measured for the three genotypes. Both *mdx* and *mdx*:SLK mKO were similarly reduced compared to C57 controls (n=. (C) Eccentric contraction induced injury similarly reduced maximal force generation in *mdx* and *mdx*:SLK mKO. (D) Soleus muscles were weighed, with no observable change in weight between the genotypes. (E) Isometric force generation was significantly reduced in the *mdx* background compared to controls. *Mdx*:SLK mKO mice were not statistically different from either group. (F) *mdx* mice showed a dramatic decrease in maximal force generation following eccentric contraction induced injury which was not observed in *mdx*:SLK mKO, suggesting that *mdx*:SLK mKO soleus muscles are protected from eccentric contraction induced injury. Muscle weight and isometric force data are presented as +/- standard error of the mean (**P* < 0.05, ***P* < 0.01, ****P* < 0.005 and *****P* < 0.001). Eccentric contraction data are presented as means +/- standard errpr pf the mean. Significance denoted as * *mdx* significantly different from C57BL/10J , # *mdx*-SLK-mko significantly different from C57BL/10J and ϕ *mdx* significantly different from *mdx*-SLK-mko.

Table 5. Contractile and physical properties of EDL muscles.

Genotype	n	Muscle mass (mg)	±SD	Body weight (g)	±SD	L0 (mm)	±SD	TPT (ms)	±SD	1/2 RT (ms)	±SD
C57	8	11.4	±0.8	30.1	±2.9	12.9	±0.8	24	±3	19	±6
MDX	8	13.9	±1.0	31.3	±1.8	12.4	±0.5	25	±2	27	±7
MDX SLKmko	8	13.2	±1.8	30.3	±3.4	12.5	±0.6	27	±6	28	±4

Table 6. Contractile and physical properties of Sol muscles.

Genotype	n	Muscle mass (mg)	±SD	Body weight (g)	±SD	L0 (mm)	±SD	TPT (ms)	±SD	1/2 RT (ms)	±SD
C57	8	9.7	±0.5	30.1	±2.9	12.3	±0.8	51	±8	51	±8
MDX	8	10.6	±0.9	31.3	±1.8	12.2	±1.0	60	±7	72	±19
MDX SLK mko	8	9.3	±1.4	30.3	±3.4	12.4	±0.8	62	±7	68	±23

5.7 RhoA Activity is decreased in *mdx*:SLK mKO mice

Our previous data showed a reduction in RhoA activity and phosphorylation following SLK knockdown in C2C12 myoblasts. Although this did not contribute to the increased myogenesis observed following SLK knockdown, we investigated whether RhoA activity was affected in *mdx*:SLK mKO mice. Interestingly, in both *mdx* and GRMD muscle samples, RhoA levels and phosphorylation were elevated compared to controls [Fig5.8A&B]. Surprisingly, *mdx*:SLK mKO muscles showed decreased phosphorylation at Serine 188 and decrease total RhoA, but did not show any marked changes in RhoA GTPase activity [Fig5.8C].

5.8 Activity p38 is elevated in *mdx* SLK mKO mice

We have previously shown that SLK deletion in skeletal muscle leads to increased activity of the p38 kinase. Interestingly, inhibition of p38 prevents the induction of MyoG imparted by SLK knockdown in the presence of TGFβ. Given that we observed an increase in the myogenin and eMHC in *mdx*:SLK mKO muscles, we speculated that there was a similar increase in p38 activity in *mdx*:SLK mKO mice. Similar to previous findings, we observed elevated activity of p38 in skeletal muscle from the *mdx* and GRMD models [Fig5.9A&B]. Interestingly, total levels of p38 appeared to be higher in GRMD muscles compared to controls. We used western blot to analyze protein lysates from *mdx* and *mdx*:SLK mKO diaphragms. Our data show a significant increase in p38 activity in *mdx*:SLK mKO muscles compared to *mdx* controls, suggesting that the increased activity of p38 may be contributing to the enhanced regeneration [Fig5.9C]. Additionally, levels of utrophin were also elevated in *mdx*:SLKmKO muscle [Fig5.9D]. An increase in P-p38/MyoG double positive nuclei in the *mdx*:SLK mKO compared to *mdx* alone was also observed [Fig5.9E-F]. These findings demonstrate and increase in p38 activity.

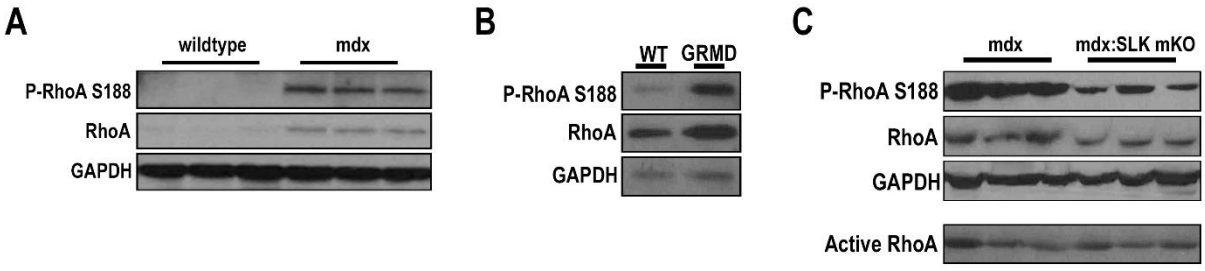

Figure 5.8: RhoA S188 Phosphorylation is decreased in *mdx*:SLK mKO. (A) RhoA phosphorylation and total levels are elevated in *mdx* muscle compared to wildtype control. (B) Similar to *mdx*, GRMD muscles also showed a dramatic elevation in both S188 phosphorylation and total levels of RhoA. (C) *mdx*:SLK mKO muscles had a decrease in both S188 phosphorylation and total levels of RhoA, but no alteration in RhoA-GTPase activity.

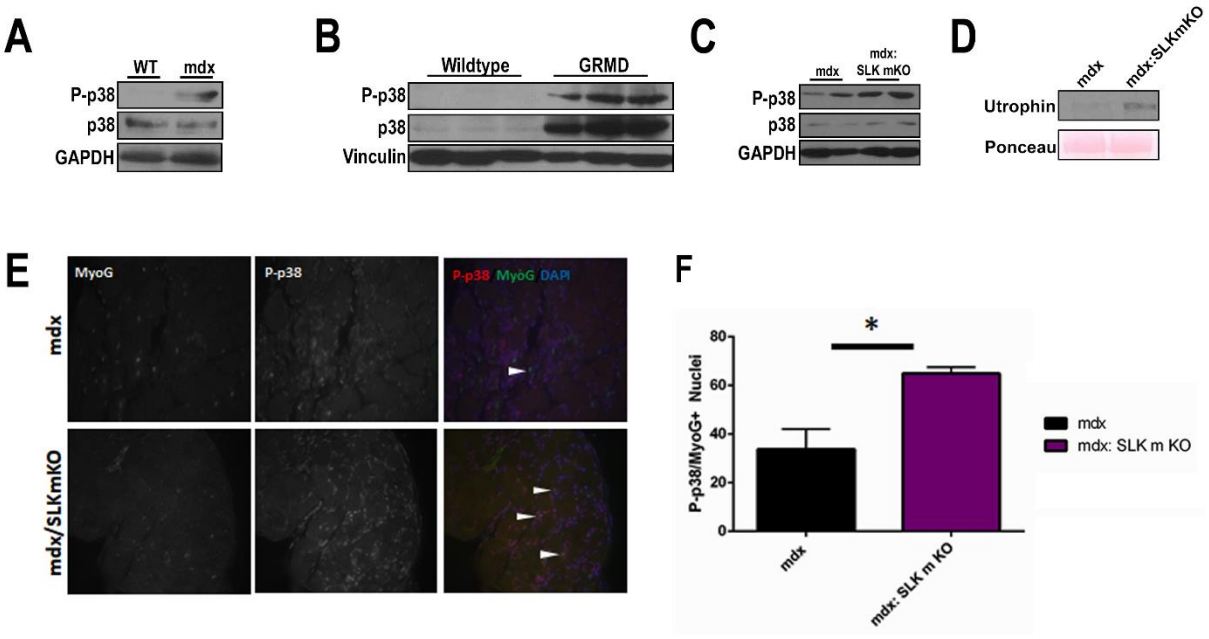

Figure 5.9: Elevated p38 Activity in *mdx*:SLK mKO. (A) Activity of p38 is elevated in *mdx* compared to C57 controls. (B) Similarly, p38 activity and levels are both elevated in GRMD muscles compared to wildtype controls. (C) *mdx*:SLK mKO mice have a significant increase in p38 activity compared to *mdx* alone. (D) Western blot for expression of utrophin shows upregulation in *mdx*:SLK mKO muscles compared to *mdx.* (E) IF for P-p38 and MyoG showing increased double positive nuclei (white arrows) in *mdx*:SLK mKO compared to mdx. (F) Quantification for percentage of double positive nuclei in (E) (* $p<0.05$).

5.9 Discussion and Interpretation of Results

Previously, we found that the knockdown of SLK was able to rescue differentiation in C2C12 and primary myoblasts treated with TGFβ in a p38 dependent mechanism. We speculated that this effect could be translated into the *mdx* model, where high levels of TGFβ impairs the myogenic potential of activated satellite cells. Prior to deleting SLK in the *mdx* model, we first analyzed SLK expression to ensure that it was indeed expressed within the myogenic precursors of *mdx* muscle. Surprisingly, we observed a dramatic increase in the levels of SLK which was found to be predominantly localized to regenerating myofibers. Deletion of SLK in the *mdx* background results in a significant increase in the levels of terminal differentiation markers, with no changes in myofiber damage or force generation. These findings suggest that the increase in terminal differentiation is not due to increase myofiber necrosis following SLK deletion, as uptake of EBD is not elevated by SLK deletion. Although fibrosis was unchanged in *mdx*:SLK mKO mice, the total level of CD45+ leukocytes was reduced suggesting an improvement in the pathological features of muscular dystrophy. Therefore, we concluded that muscle specific deletion of SLK could not fully restore muscle function in a dystrophic environment.

Chapter 6 – Discussion

6.1 Summary of Major Findings

Duchenne Muscular Dystrophy is a fatal X-linked inherited disorder characterized by severe muscle damage and loss of function (Flanigan, 2014). The underlying cardiomyopathy and respiratory problems associated with the disease lead to a dramatically decreased lifespan in patients suffering from the disorder. Identifying pathways regulating muscular dystrophy is required in order to develop novel therapies. Treatments targeting pathologies such as impaired muscle regeneration, increased immune infiltration and fibrosis have been shown to greatly enhance muscle function in DMD (Falzarano, Scotton, Passarelli, & Ferlini, 2015; Guiraud & Davies, 2017; Kim et al., 2015; Salmaninejad et al., 2018). In this study, we investigated the effect of a muscle specific SLK deletion on muscle development and regeneration as well as the potential for SLK deletion to restore terminal differentiation in muscular dystrophy. We observed that decreased levels of SLK protected myoblasts from the anti-myogenic effects of TGFβ, a cytokine elevated in DMD muscle. We have shown that SLK expression is significantly elevated within regenerating muscle tissue from both *mdx* and Golden Retriever Muscular Dystrophy models. Furthermore, we demonstrated that the deletion of SLK did not exacerbate the pathology of the *mdx* mouse, but rather increased myoblast differentiation and protected specific muscle groups from eccentric contraction induced injury. Here, we discuss the relevance of the major findings of this study as well as avenues of research that require future study to unravel the role of SLK in skeletal muscle physiology.

6.2 SLK in Myoblast Fusion and Muscle Regeneration

The differentiation of myoblasts into skeletal muscle requires a co-ordinated transcriptional response as well as the fusion of mono-nucleated cells into multi-nucleated myofibers (Hindi et al., 2013). The cascade of transcription factors is well defined and consists of various muscle

specific proteins such as MyoD and Myf5 and later the critical transcription factor myogenin (Bentzinger et al., 2012). Although the mechanisms regulating the differentiation of myoblasts into mature myofibers are well understood, the processes of myoblast fusion in mammalian cells are less characterized. In this study, we demonstrated that SLK deficiency results in decreased myoblast fusion and delayed muscle regeneration, but did not affect myoblast differentiation [Fig3.1&Fig3.14]. Many studies have identified various signalling kinases as being critical for myoblast fusion through knockdown and genetic knockout experiments. Examples of kinases shown to be involved in myoblast fusion are the Focal Adhesion Kinase (FAK) and Protein Kinase C Theta (PKC θ) (Madaro et al., 2011; Quach et al., 2009). Similar to SLK deletion, the reduction in the expression of both FAK and PKC θ results in decreased myoblast fusion without impacting the differentiation genetic program. These studies demonstrate that the processes of myoblast differentiation and fusion are two independent and parallel processes. Additionally, the deletion of these proteins from myoblasts only reduces and not completely inhibits cell-cell fusion, as evidenced by the sustained levels of syncytium formation in deleted myoblasts. *In vivo* deletion also decreased muscle regeneration and formation, but does not completely inhibit either process, similar to the genetic deletion of SLK. Given that SLK, FAK and PKC θ are not exclusively expressed in myogenic cells, and that their deletions do not completely inhibit cellular fusion, it is likely that their roles in myoblast fusion are not directly involved in syncytium formation itself. A more likely explanation is that these proteins mediate cytoskeletal remodeling and other processes such as cell migration, turnover of membrane proteins or gene expression that are not absolutely required for myoblast fusion. Indeed, the deficiency in FAK led to a reduction in β1D integrin and caveolin 3 expression, which were found to partially

mediate myoblast fusion (Quach et al., 2009). Further studies are required to determine the exact roles play by these proteins during myoblast fusion.

More recently, with the discovery of the muscle specific proteins Myomaker and Myomerger, it has become clear that cellular fusion-specific processes and proteins exist (Millay et al., 2013; Millay et al., 2014; Quinn et al., 2017). In contrast to SLK, deletion of Myomaker and Myomerger resulted in the complete absence of myoblast fusion as compared to a reduction. Although their specific functions remain somewhat elusive, the eventual identification of downstream pathways will no doubt clarify the role of many other proteins in the fusion process. Although SLK appears to be critical for myoblast fusion *in vitro,* muscle development and regeneration are not hindered by its deletion, suggesting that it is not essential for myoblast fusion *in vivo*.

Muscle regeneration is delayed, but not inhibited in SLK-null muscles [Fig3.14]. In addition to its role in myoblast fusion, we also demonstrated that SLK-deficient myoblasts show both decreased proliferation and migration compared to controls cells [Fig3.2]. One explanation for the decreased fiber size observed at 7 days post injury could be decreased proliferation of myogenic progenitors. However, the number of Pax7+ cells is not affected in SLK knockout muscles [Fig3.15]. In addition to proliferation, myoblast migration was also impaired following SLK knockdown. Therefore, SLK deficient muscle progenitors may be delayed in their recruitment to sites of injury, thus leading to the delayed muscle regeneration observed in SLK knockout muscles. As SLK has been shown to mediate various cellular functions, SLK could

also play a role in recognition, adhesion or membrane fusion depending on its cellular localization.

6.3 SLK's Role in Muscle Development and Myofiber Integrity

Previously, our lab generated a global SLK knock out model by replacing the 3' region of SLK with a LacZ fusion protein (gene trap) (Al-Zahrani et al., 2014) [Fig1.5]. This rendered SLK functionally null, as it could no longer phosphorylate target proteins. Mutant embryos homozygous for this allele were developmentally normal until E12.5. Beyond this time point, significant morphological defects were observed in mutant embryos. Cellular compartments such as the developing nervous system and skeletal muscles were smaller and less organized than wildtype controls. These findings made it difficult to determine the underlying cause of the developmental defects. Interestingly, we observed a significant decrease in placental vascularization, suggesting that SLK deficiency abrogates placental formation, essentially starving the mutant embryos. In our conditional Myf5-Cre:$SLK^{fl/fl}$ mice, Cre expression is detected early on during myogenic commitment and therefore the early muscle compartment would be deficient in SLK expression. Interestingly, in contrast to the global null model, there was no developmental delay in the expansion of the myogenic compartments as evidenced by staining with LacZ and Myosin Heavy Chain in ROSA26R reporter mice [Fig3.5]. These findings eliminate the possibility that the early embryonic deletion observed in our global null model was due to a deficiency in SLK within the myogenic compartment. Therefore, SLK expression is not required for the embryonic development of skeletal muscle.

The molecular mechanisms of SLK signalling have been predominantly studied in fibroblasts. In these cells, a role for SLK at the leading edge of migrating cells has been established. SLK has been shown to be activated downstream of FAK and Src signalling and to play a role in cell migration following scratch wounding *in vitro* (Wagner et al., 2008). In addition, SLK has been demonstrated to phosphorylate the adapter paxillin to induce focal adhesion turnover, a process necessary for cell motility (Quizi et al., 2013). This is of particular importance in developing myofibers as the components of the focal adhesion complex play a pivotal role not only in myoblast fusion, but also in the development and integrity of the costameres and attachment tendon (Peter, Cheng, Ross, Knowlton, & Chen, 2011; Quach & Rando, 2006). Costameres are active sites for signaling and sarcomere attachment to the ECM. Interestingly, our previous studies indicated that SLK localized with α actinin, a critical mediator of myofiber stability within the costamere (Storbeck et al., 2004). A more recent study supported these observations by demonstrating that SLK binds directly to α actinin-4 (Jaberi et al., 2015). Deletion or mutations of costamere-associated proteins result in an increase in central nuclei, decreased force generation and, in some cases, lethality. Our studies show that SLK-deficient muscles display altered localization of FAK and Paxillin, two important costamere proteins [Fig3.12]. Interestingly, vinculin localization was not affected, suggesting that SLK deletion might affect only a subset of costameric proteins. Nevertheless, this is likely to affect costameric signaling and to result in weaker attachment of the MTJ and the sarcomere. Based on our findings, SLK appears to be a regulator of myofiber integrity and stability. However, the phenotype observed following SLK deletion was much less severe than for other cytoskeletal regulators such as Talin and integrin linked kinase (ILK) (Conti, Monkley, Wood, Critchley, & Muller, 2009; Gheyara et al., 2007). This may be in part due to compensation from an alternative pathway that remains to

be uncovered. Nevertheless, SLK deficiency results in similar mis-localization of focal adhesion proteins within the myofiber. Further work is required in order to understand exactly how SLK contributes to the stability of this complex.

6.4 SLK Kinase Activity is required during Myoblast Differentiation

We have previously reported that over-expression of the truncated/inactive mutant of SLK, KΔC, prevents the fusion of C2C12 myoblasts (Storbeck et al., 2004). However, muscle-specific overexpression of a full length dominant negative SLK driven by the human skeletal actin promoter (HSA-K63R) results in enhanced muscle regeneration as well as an increase in the fusion index of isolated primary myoblasts (Storbeck et al., 2013). As SLK phosphorylation and activation requires homo-dimerization, binding of wildtype SLK to the K63R mutant would render the dimer inactive, suggesting that the K63R functions in a dominant negative fashion (Cybulsky, Guillemette, Papillon, & Abouelazm, 2017; Delarosa et al., 2011). Supporting this, HSA-K63R mice show reduced overall kinase activity. The conflicting results from the studies using the KΔC and K63R models made it necessary to design a muscle specific knockout of SLK to investigate the effect of SLK deficiency on skeletal muscle formation. The Myf5-Cre recombinase model was used to generate SLK muscle knockout mice in early muscle progenitors (E8.5 in the core muscles and 10.5 in limb muscles) (Sabourin & Rudnicki, 2000). Additionally, Pax7+ satellite cells arise from embryonic myoblasts, most of which express Myf5 during development (Gros et al., 2005). Therefore, our Myf5-Cre model would mediate deletion of SLK during early embryogenesis and in adult satellite cells. Surprisingly, deletion of SLK had no apparent effect on embryonic development, but caused a delay in muscle regeneration following cardiotoxin induced injury. These observations are in stark contrast to the enhanced regeneration observed in the HSA-K63R model, but similar to the decreased fusion observed after KΔC

overexpression in C2C12s. Similarly, SLK deletion significantly reduced primary myoblast fusion *in vitro*, while the HSA-K63R mice had an increased fusion index.

One possible explanation for these apparent inconsistencies is the expression pattern of the promoters used to drive K63R or Cre expression. Our *in vitro* and *in vivo* experiments performed here demonstrate that deletion of SLK prior to differentiation results in decreased myoblast fusion and delayed muscle regeneration, similar to the expression of the KΔC mutant (Storbeck et al., 2004). However, the HSA promoter is activated much later during differentiation and thus would not drive expression of K63R until terminal differentiation is initiated (Storbeck et al., 2013). These differences suggest that SLK activity is required in the early stages of differentiation, but needs to be downregulated as differentiation proceeds. In line with this observation, we have observed that levels of SLK are significantly lower in differentiated skeletal muscle compared to actively regenerating skeletal muscle [Fig3.13]. In addition, our assessment of SLK kinase activity in differentiating C2C12 myoblasts showed a decrease across a differentiation time course, further suggesting that SLK activity needs to be downregulated during myogenesis [Fig3.1]. Therefore, we would predict that deletion of SLK using the HSA-Cre recombinase would have a similar phenotype as that of the HSA-K63R. The generation of an inducible SLK knockout model using both the Pax7-Cre^{ErT} and the HSA-Cre^{ErT} would allow us to induce SLK deletion within the satellite cells and myofibers, respectively upon tamoxifen injection. Furthermore, the ability to induce SLK deletion would allow us to maintain its expression during embryonic development, thus allowing a more direct assessment of its functional role in adult tissue to be studied.

An alternate possibility for these divergent phenotypes is that SLK plays both kinase-dependent and -independent roles during the differentiation and the maturation process. Kinase-independent roles may include localization of binding partners to specific sub-cellular areas. The expression of a full length kinase dead SLK in differentiating cells would still allow any potential molecular scaffolding functions in the HSA-K63R model. However, in the SLK knockout model, both kinase-dependent and independent processes would be impaired during development and repair. The loss of possible scaffolding functions in the SLK knockout muscles likely leads to anchoring defects of focal adhesion proteins, as these were not observed in the HSA-K63R model. Additionally, there was no obvious increase in centrally located nuclei in the HSA-K63R model, indicating that there was no progressive muscle damage. We have previously shown that SLK knockdown, but not K63R overexpression, results in a decrease in TGFβ-mediated EMT demonstrating that kinase-independent roles for SLK exist (Conway et al., 2017). Recently, our lab has developed K63R knock-in mutation. This was designed using Crispr/Cas9 mediated editing of the SLK locus, with homologous recombination using a template DNA containing mutations necessary to generate the K63R mutant. To date, we have observed that heterozygous mice harbouring the K63R mutation are viable with no apparent defects. Assessing embryonic development of K63R homozygotes will begin to delineate between kinase-dependent and independent functions of SLK. If SLK primarily plays kinase independent functions within skeletal muscle we would not expect to see the myopathy observed in the Myf5-Cre:SLK$^{fl/fl}$ model. However, if its primary function in skeletal muscle is dependent on its kinase activity then we would anticipate a similar phenotype to develop.

6.5 SLK Inhibition in the Treatment of DMD

Current treatment options for muscular dystrophy alleviate the symptoms of DMD such as inflammation without correcting the underlying cause of the disease (Kim et al., 2015). However, recent advances in the field of genetic engineering have provided new tools for development of clinical therapies. For example, mini dystrophin replacement was effective at increasing muscle strength in *mdx* mice (Li et al., 2006). Clinical trials are currently in development for exon-skipping technologies with encouraging results (Charleston et al., 2018). More recently, Crispr/Cas9 mediated repair of mutations in mouse and dog models of muscular dystrophy have been successful at restoring dystrophin expression and reverting disease progression (Amoasii et al., 2018). Modified Crispr vectors have been designed to upregulate utrophin in *mdx* mice and curb disease progression without causing DNA damage, thus eliminating the possibility of aberrant repair occurring following Cas9 cleavage (Liao et al., 2017). However, patients suffering from DMD have progressive muscle wasting that is characterized by persistent immune infiltration and fibrosis, which itself can prevent the activation of endogenous satellite cells and muscle repair that cannot be readily reversed. Therefore, simply repairing the underlying mutation using approaches such as Crispr/Cas9 may not be useful alone and should therefore be performed in combination with additional therapies.

As SLK inhibition protects myoblasts from the anti-myogenic effects of TGFβ and increased differentiation in *mdx* mice, the therapeutic targeting of SLK within the myoblasts of DMD patients could provide the same beneficial effects. Modifying these cultured myoblasts using Crispr/Cas9 repair dystrophin mutations as well as rendering them deficient in SLK expression would therefore allow these cells to not only be resistant to the fibrotic environment via SLK

deletion, but also re-introduce dystrophin to DMD patients. Similar techniques could also be used to treat other muscular dystrophies using appropriate guide RNA sequences. Alternatively, transient downregulation of SLK activity using SLK specific inhibitors may also prove to be beneficial in increasing myoblast differentiation. However, prior to the use of broad SLK inhibitors in muscular dystrophy, the effect of SLK deletion on other cell types need to be examined. A large body of evidence suggests that SLK deficiency causes a decrease in cell motility and proliferation (O'Reilly et al., 2005; Wagner et al., 2008). Therefore, the use of an SLK inhibitor may be sufficient to reduce both of these properties in invasive cells types, such as fibroblasts and immune cells. Further *in vivo* experiments with specific inhibition of SLK in macrophages and fibroblasts will be useful to elucidate the possible side effects of SLK inhibitors in the dystrophic muscle.

SLK deletion in skeletal muscle resulted in a central nuclear myopathy characterised by decreased force generation. Therefore, inhibition of SLK in muscular dystrophy may affect myofiber stability. However, our results demonstrated that deletion of SLK using Myf5-Cre recombinase in the *mdx* model did not increase muscle degeneration, as myofiber permeability and force generation were not affected. These findings demonstrate that although normal muscle is affected by the loss of SLK, *mdx* mice do not show a compounded effect following SLK deletion. Myf5-Cre mediates deletion of SLK within developing skeletal muscles, thereby rendering the entire myogenic lineage, including myofibers, deficient in SLK expression. It is possible that the deletion of SLK early during embryogenesis affects myofiber stability. Therefore, satellite cell specific deletion of SLK using the Pax-Cre^{ErT} in lieu of the Myf5-Cre model would allow us to specifically delete SLK in muscle progenitor cells and preserve SLK

expression in the myofiber. The prediction would be increased myogenic differentiation without any effect on myofiber integrity. Additionally, using an inducible Pax7 and HSA Cre drivers would allow us to further delineate between a progenitor cell and myofiber effect of SLK deletion that cannot be readily delineated using the Myf5-Cre model.

Interestingly, we observed that SLK deletion in the *mdx* mouse protected the Soleus, but not the EDL, from contraction induced injury. A previous study by our lab showed that SLK was predominantly expressed within Type 1 fibers (Storbeck et al., 2004). Given that the Soleus is composed of mostly Type 1 fibers, one possibility is that SLK deletion in muscle groups expressing high levels of SLK is beneficial or more apparent. The EDL composed predominantly of fast twitch type II fibers may not display any obvious benefits. However, analysis of muscle groups from *mdx* mice revealed that there was no difference in expression of SLK between different muscle groups. Therefore, the difference in resistance to contraction induced injury may not be solely be attributed to differential fiber type expression of SLK. Another possibility is that the Soleus is less affected than the EDL in muscular dystrophy (Moens, Baatsen, & Marechal, 1993). This phenomenon had been previously reported by others. This would make the beneficial effects of SLK deletion more apparent in the Soleus. We observed a significant increase in the expression of embryonic myosin heavy chain (eMHC) in the soleus and diaphragm, but not the EDL, suggesting increased terminal differentiation in those muscle groups. Alternatively, the resistance to contraction induced injury observed may also be due to elevated utrophin expression observed due to increased p38 signalling. Nevertheless, SLK deletion renders some muscle groups resistant to injury in the *mdx* model.

6.6 SLK and p38 Signalling in Muscular Dystrophy

The activity of p38 has been shown to be critical for myoblast differentiation. Exogenous expression of p38 in rhabdomyosarcoma cells increased MyoD and MEF2 transcriptional activity, which stimulated terminal differentiation (Puri et al., 2000). In contrast, treatment of myoblasts with p38 inhibitors or specific deletion of p38α also decreased the expression of terminal differentiation markers (Wu et al., 2000; Zetser, Gredinger, & Bengal, 1999). Collectively, these results demonstrate that p38 activity has a pro-myogenic function. In addition to its role in myogenesis, p38 also upregulates cellular stress and apoptotic signaling (Wissing et al., 2014). As for muscle-specific deletion of SLK *in vivo*, the activity of p38 is also enhanced in cultured myoblast deficient for SLK, suggesting that enhanced p38 activity may enhanced terminal differentiation in SLK deficient myoblasts [Fig4.5]. Indeed, inhibition of p38 using SB203580 blocked myogenic induction conferred by SLK deletion in the presence of TGFβ [Fig4.6]. Similarly, enhancing p38 activity via the expression of an over-active MKK6 construct rescued myogenesis downstream of TGFβ, similar to an SLK knockdown [Fig4.6]. Together, these data suggest that SLK deficiency upregulates p38 activity, enhancing myogenesis.

Consistent with our results, a previous study reported enhanced levels and activity of p38 in animal models of muscular dystrophy (Wissing et al., 2014). However, this study determined that upon p38 deletion in the *mdx* mouse there was a significant reduction in fibrosis and improvement of many of the pathologies associated with the *mdx* mouse. Furthermore, overexpression of the active of MKK6 severely exacerbated the pathology of the *mdx* mouse. These results initially appear to conflict with our findings, in which p38 activity appears to be

beneficial to *mdx* muscles. However, this study also demonstrated a significant decrease in the activity of downstream apoptotic pathways following p38 deletion. Additionally, over activation of p38 through muscle specific expression of an active MKK6 construct increased myofiber necrosis as well as increased the activation of apoptotic pathways. The authors concluded that the decreased apoptosis downstream of p38 deletion was responsible for the rescue of the disease phenotype. Previous studies have demonstrated that increased SLK signalling results in increased apoptosis through various pathways (Cybulsky et al., 2010; Hao et al., 2006; Sabourin & Rudnicki, 1999; Sabourin et al., 2000). Therefore, SLK deletion may also decrease myofiber susceptibility to cell death. . In addition, the deletion of p38 in this model is driven by myosin-light chain Cre, which would inactivate p38 in myofibers but not in myoblasts. Therefore, p38 activity in myofibers may be primarily mediating a stress response, whereas its role in proliferating myoblasts is to mediate cellular differentiation. The expression of MKK6 was also driven on the same promoter, which could also explain the lack of beneficial effects of MKK6 expression of myogenesis. Finally, this study showed that treatment of mice with a p38 inhibitor, SB731445, resulted in similar effects as p38 deletion. However, given that drug treatments would not be selective to myoblast populations alone, these effects could be attributed to decreased p38 activity in infiltrating immune cells. Indeed, the activity of p38 has been shown play a role in the immune response, such as macrophage polarization. Therefore, although direct inhibition of p38 within myoblasts may be detrimental to muscle regeneration, inactivation in other cells types may actually promote muscle repair and restore muscle function. These studies highlight the necessity to consider both temporal and spatial activation of Cre-recombinase and inhibitors when designing and interpreting experimental results.

In addition to its role in apoptosis, p38 signalling has also been shown to be responsible for the self-renewal of satellite cells (Bernet et al., 2014). In aged skeletal muscles, satellite cells lose their capacity to expand and renew the stem cell population, leading to impaired muscle regeneration. This process was determined to be a cell autonomous effect as satellite cells from older mice transplanted into younger skeletal muscles failed to rescue the expansion defect. The activity of p38 in aged satellite cells was found to be elevated compared to satellite cells from younger mice. Partial inhibition of p38 using a low dose of SB203580 restored aged satellite cells asymmetric cellular division, whereas a higher dose blocked asymmetric division. Therefore, although necessary for myoblast differentiation, over activation of p38 results in decreased asymmetric cell division and reduces the expansion of the satellite cell compartment. Therefore, inhibition of SLK may lead to increase p38 activity, which could result in exhaustion of the satellite cell pool, thus exacerbating the disease state of muscle dystrophy. This could be further explored *in vivo* by performing repeated cardiotoxin injections in mice and assessing the repopulation of the satellite cell niche following resolution of muscle injury. Previous reports have shown that utrophin expression can be modulated through P-p38 activity via the stabilization or utrophin mRNA. Consistent with this, we observed an increase in utrophin levels possibly mediated through the same mechanism.

6.7 Indirect Role for SLK in TGFβ Signalling in Myoblasts

Previously, we demonstrated that SLK downregulation inhibited TGFβ induced EMT (Conway et al., 2017). This effect was found to be independent of the canonical Smad2/3 pathway. Similarly, SLK knockdown in C2C12 myoblasts blocked myogenic inhibition by TGFβ treatment independent of Smad2/3 phosphorylation [Fig4.1&Fig4.2]. SLK kinase activity was not altered by TGFβ stimulation, suggesting that SLK was not contributing to or directly

responding to a TGFβ induced response [Fig4.2]. One explanation for the rescue of myoblast differentiation in the presence of TGFβ is that SLK deletion independently increases p38 activity. This increased activity in p38 could stimulate the pro-myogenic effects without perturbing TGFβ signalling Indeed, activation of p38 signalling independently of SLK knockdown was sufficient to observe a similar phenotype and blocking p38 activity reverted the rescue conferred by SLK knockdown. Therefore, SLK might function to decrease myoblast differentiation through repression of a p38 signaling axis that, when activated, is sufficient to increase myoblast differentiation.

6.8 Uncovering Novel Phosphorylation Targets for SLK

Several SLK substrates have been identified. However, few have been physiologically validated. For example, our analysis of Paxillin phosphorylation on Serine 250, a previously identified target of SLK in fibroblasts, did not reveal any significant change between wildtype and knockout mice (Quizi et al., 2013). The phosphorylation of RhoA on Serine 188 was proposed to reduce RhoA-GTPase activity. However, in C2C12 myoblasts, decreased phosphorylation of Serine 188 leads to a reduction in RhoA activity (Guilluy et al., 2008). Decreased RhoA activity could be due to enhanced turnover of RhoA, as a decrease in Serine 188 phosphorylation also makes active GTP bound RhoA more susceptible to proteasome breakdown (Rolli-Derkinderen et al., 2005). Finally, another group has shown that SLK is capable of phosphorylating ASK1, an upstream regulator of p38 (Hao et al., 2006). The same group also found that SLK over expression increases ASK1 phosphorylation on a yet undetermined residue, and that this increase p38 phosphorylation. This is in direct contrast to what was observed in SLK knockout muscles where SLK deficiency led to a dramatic increase in p38 activity. One possibility is that the

phosphorylation of ASK1 may be inhibitory and thus deleting SLK enhances ASK1 and p38 activity, driving myoblast differentiation.

In an effort to uncover novel phosphorylation targets of SLK, our lab has recently designed mutations of the ATP binding pocket to accept an analogue of ATP (Y. Liu, Shah, Yang, Witucki, & Shokat, 1998). These mutations were previously characterized to accept a bulky N6-benzyl moiety. Essentially, only a kinase domain with the appropriate mutation can use this ATP analogue to phosphorylate substrate. The same N6-benzyl analogue has a thio-labelled tertiary phosphate. In this way, targets of the mutant SLK will be tagged with the thio-labelled phosphate, which can be detected using mass spectrometry. This method will be a useful tool to begin to elucidate novel phosphorylation targets of SLK *in vitro*. The findings of this study will no doubt yield results useful in determining new pathways regulated by SLK and will be essential in understanding its biological function.

6.9 Conclusion

In this study, we explored the role of SLK in skeletal muscle using a genetic knockout in early embryonic myoblasts. Our results demonstrate that SLK plays a role in myofiber stability and muscle regeneration, but is dispensable for overall skeletal muscle formation. Furthermore, we show that SLK deficiency is capable of restoring differentiation in the presence of TGFβ, which is in part mediated through a p38 dependent mechanism [Fig6.1]. Finally, we found that levels of SLK were elevated in dystrophic muscle and that muscle specific deletion of SLK in *mdx* mice was sufficient to increase terminal differentiation. These finds suggest that SLK inhibition may

be a useful therapeutic means to restore myoblast differentiation in skeletal muscle disorders where myoblast differentiation is impaired, such as muscular dystrophy and cachexia.

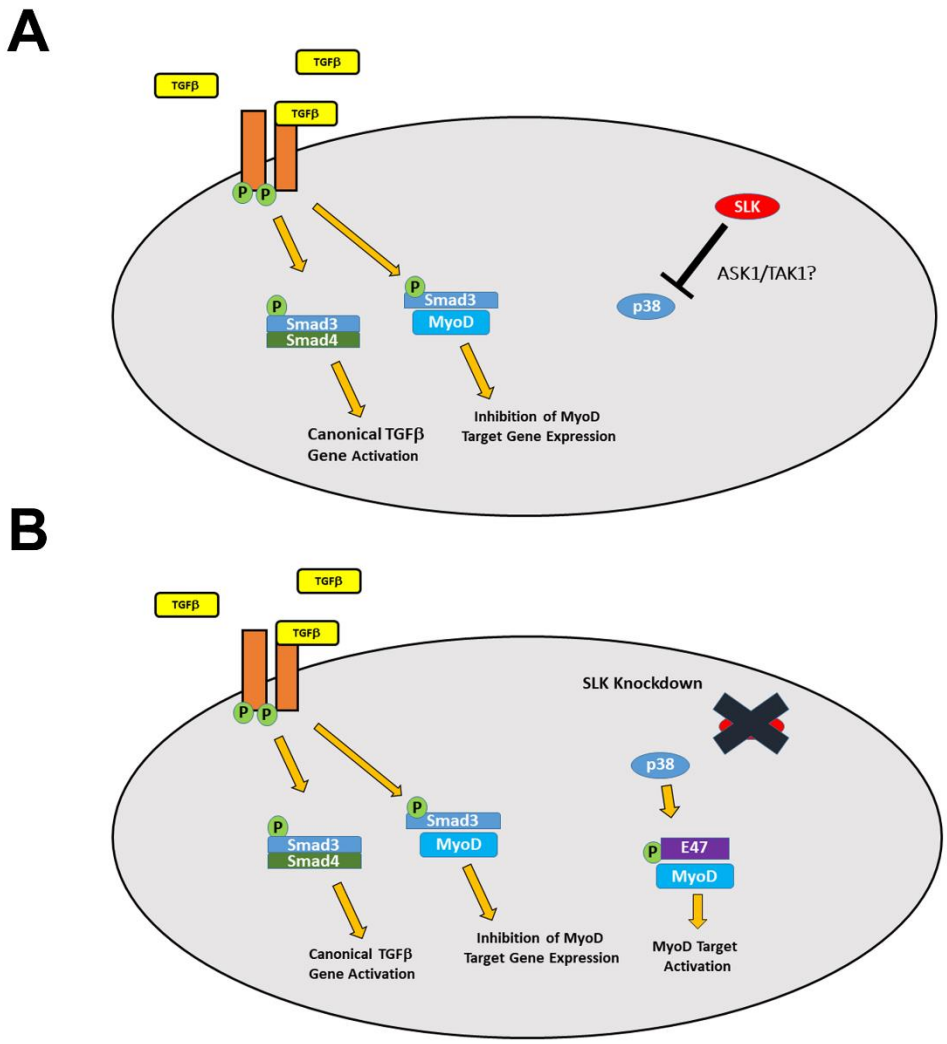

Figure 6.1: Model for Restoration of Differentiation following SLK Knockdown. (A) In wildtype myoblasts, treatment with TGFb increased both canonical Smad4 gene activation and inhibits myogenic differentiation through Smad3 association with MyoD. SLK maintains low activity of p38, possibly through inhibition of ASK1/TAK1. (B) Upon SLK knockdown, inhibition on p38 is relieved, resulting in increased phosphorylation of E47, leading to heterodimerization with MyoD. This leads to increased differentiation. However, the canonical role of Smad signalling is intact.

7.0 References

Abmayr, S. M., & Pavlath, G. K. (2012). Myoblast fusion: lessons from flies and mice. *Development, 139*(4), 641-656. doi:10.1242/dev.068353

Accornero, F., Kanisicak, O., Tjondrokoesoemo, A., Attia, A. C., McNally, E. M., & Molkentin, J. D. (2014). Myofiber-specific inhibition of TGFbeta signaling protects skeletal muscle from injury and dystrophic disease in mice. *Hum Mol Genet, 23*(25), 6903-6915. doi:10.1093/hmg/ddu413

Ait Mou, Y., Lacampagne, A., Irving, T., Scheuermann, V., Blot, S., Ghaleh, B., . . . Cazorla, O. (2018). Altered myofilament structure and function in dogs with Duchenne muscular dystrophy cardiomyopathy. *J Mol Cell Cardiol, 114*, 345-353. doi:10.1016/j.yjmcc.2017.12.008

Akita, Y., Ohno, S., Goto, J., Nakano, I., Takatsu, M., Sugita, H., & Suzuki, K. (1987). Diagnosis of Duchenne and Becker muscular dystrophies by DNA polymorphism. *Jinrui Idengaku Zasshi, 32*(2), 71-82. doi:10.1007/BF01893160

Al-Zahrani, K. N., Sekhon, P., Tessier, D. R., Yockell-Lelievre, J., Pryce, B. R., Baron, K. D., . . . Sabourin, L. A. (2014). Essential role for the SLK protein kinase in embryogenesis and placental tissue development. *Dev Dyn, 243*(5), 640-651.

Amirouche, A., Tadesse, H., Lunde, J. A., Belanger, G., Cote, J., & Jasmin, B. J. (2013). Activation of p38 signaling increases utrophin A expression in skeletal muscle via the RNA-binding protein KSRP and inhibition of AU-rich element-mediated mRNA decay: implications for novel DMD therapeutics. *Hum Mol Genet, 22*(15), 3093-3111. doi:10.1093/hmg/ddt165

Amoasii, L., Hildyard, J. C. W., Li, H., Sanchez-Ortiz, E., Mireault, A., Caballero, D., . . . Olson, E. N. (2018). Gene editing restores dystrophin expression in a canine model of Duchenne muscular dystrophy. *Science*. doi:10.1126/science.aau1549

Barthelemy, I., Pinto-Mariz, F., Yada, E., Desquilbet, L., Savino, W., Silva-Barbosa, S. D., . . . Butler-Browne, G. (2014). Predictive markers of clinical outcome in the GRMD dog model of Duchenne muscular dystrophy. *Dis Model Mech, 7*(11), 1253-1261. doi:10.1242/dmm.016014

Barthelemy, I., Uriarte, A., Drougard, C., Unterfinger, Y., Thibaud, J. L., & Blot, S. (2012). Effects of an immunosuppressive treatment in the GRMD dog model of Duchenne muscular dystrophy. *PLoS One, 7*(11), e48478. doi:10.1371/journal.pone.0048478

Bate, M. (1990). The embryonic development of larval muscles in Drosophila. *Development, 110*(3), 791-804.

Bate, M., & Rushton, E. (1993). Myogenesis and muscle patterning in Drosophila. *C R Acad Sci III, 316*(9), 1047-1061.

Bellini, M., Biagi, S., Stasi, C., Costa, F., Mumolo, M. G., Ricchiuti, A., & Marchi, S. (2006). Gastrointestinal manifestations in myotonic muscular dystrophy. *World J Gastroenterol, 12*(12), 1821-1828.

Bengtsson, N. E., Hall, J. K., Odom, G. L., Phelps, M. P., Andrus, C. R., Hawkins, R. D., . . . Chamberlain, J. S. (2017). Muscle-specific CRISPR/Cas9 dystrophin gene editing ameliorates pathophysiology in a mouse model for Duchenne muscular dystrophy. *Nat Commun, 8*, 14454. doi:10.1038/ncomms14454

Bentzinger, C. F., Wang, Y. X., & Rudnicki, M. A. (2012). Building muscle: molecular regulation of myogenesis. *Cold Spring Harb Perspect Biol, 4*(2). doi:10.1101/cshperspect.a008342

Bernet, J. D., Doles, J. D., Hall, J. K., Kelly Tanaka, K., Carter, T. A., & Olwin, B. B. (2014). p38 MAPK signaling underlies a cell-autonomous loss of stem cell self-renewal in skeletal muscle of aged mice. *Nat Med, 20*(3), 265-271. doi:10.1038/nm.3465

Bertini, E., D'Amico, A., Gualandi, F., & Petrini, S. (2011). Congenital muscular dystrophies: a brief review. *Semin Pediatr Neurol, 18*(4), 277-288. doi:10.1016/j.spen.2011.10.010

Bhowmick, N. A., Ghiassi, M., Bakin, A., Aakre, M., Lundquist, C. A., Engel, M. E., . . . Moses, H. L. (2001). Transforming growth factor-beta1 mediates epithelial to mesenchymal transdifferentiation through a RhoA-dependent mechanism. *Mol Biol Cell, 12*(1), 27-36. doi:10.1091/mbc.12.1.27

Bi, P., Ramirez-Martinez, A., Li, H., Cannavino, J., McAnally, J. R., Shelton, J. M., . . . Olson, E. N. (2017). Control of muscle formation by the fusogenic micropeptide myomixer. *Science, 356*(6335), 323-327. doi:10.1126/science.aam9361

Bladt, F., Riethmacher, D., Isenmann, S., Aguzzi, A., & Birchmeier, C. (1995). Essential role for the c-met receptor in the migration of myogenic precursor cells into the limb bud. *Nature, 376*(6543), 768-771. doi:10.1038/376768a0

Bour, B. A., Chakravarti, M., West, J. M., & Abmayr, S. M. (2000). Drosophila SNS, a member of the immunoglobulin superfamily that is essential for myoblast fusion. *Genes Dev, 14*(12), 1498-1511.

Braun, A., Bichlmaier, R., & Cleve, H. (1992). Molecular analysis of the gene for the human vitamin-D-binding protein (group-specific component): allelic differences of the common genetic GC types. *Hum Genet, 89*(4), 401-406.

Bulfield, G., Siller, W. G., Wight, P. A., & Moore, K. J. (1984). X chromosome-linked muscular dystrophy (mdx) in the mouse. *Proc Natl Acad Sci U S A, 81*(4), 1189-1192.

Burakov, A. V., Zhapparova, O. N., Kovalenko, O. V., Zinovkina, L. A., Potekhina, E. S., Shanina, N. A., . . . Nadezhdina, E. S. (2008). Ste20-related protein kinase LOSK (SLK) controls microtubule radial array in interphase. *Mol Biol Cell, 19*(5), 1952-1961. doi:10.1091/mbc.E06-12-1156

Burks, T. N., & Cohn, R. D. (2011). Role of TGF-beta signaling in inherited and acquired myopathies. *Skelet Muscle, 1*(1), 19. doi:10.1186/2044-5040-1-19

Cano, A., Perez-Moreno, M. A., Rodrigo, I., Locascio, A., Blanco, M. J., del Barrio, M. G., . . . Nieto, M. A. (2000). The transcription factor snail controls epithelial-mesenchymal transitions by repressing E-cadherin expression. *Nat Cell Biol, 2*(2), 76-83. doi:10.1038/35000025

Capote, J., Kramerova, I., Martinez, L., Vetrone, S., Barton, E. R., Sweeney, H. L., . . . Spencer, M. J. (2016). Osteopontin ablation ameliorates muscular dystrophy by shifting macrophages to a pro-regenerative phenotype. *J Cell Biol, 213*(2), 275-288. doi:10.1083/jcb.201510086

Carnac, G., Primig, M., Kitzmann, M., Chafey, P., Tuil, D., Lamb, N., & Fernandez, A. (1998). RhoA GTPase and serum response factor control selectively the expression of MyoD without affecting Myf5 in mouse myoblasts. *Mol Biol Cell, 9*(7), 1891-1902.

Castellani, L., Salvati, E., Alema, S., & Falcone, G. (2006). Fine regulation of RhoA and Rock is required for skeletal muscle differentiation. *J Biol Chem, 281*(22), 15249-15257. doi:10.1074/jbc.M601390200

Chal, J., & Pourquie, O. (2017). Making muscle: skeletal myogenesis in vivo and in vitro. *Development, 144*(12), 2104-2122. doi:10.1242/dev.151035

Charleston, J. S., Schnell, F. J., Dworzak, J., Donoghue, C., Lewis, S., Chen, L., . . . Mendell, J. R. (2018). Eteplirsen treatment for Duchenne muscular dystrophy: Exon skipping and dystrophin production. *Neurology, 90*(24), e2146-e2154. doi:10.1212/WNL.0000000000005680

Charrasse, S., Comunale, F., Grumbach, Y., Poulat, F., Blangy, A., & Gauthier-Rouviere, C. (2006). RhoA GTPase regulates M-cadherin activity and myoblast fusion. *Mol Biol Cell, 17*(2), 749-759. doi:10.1091/mbc.e05-04-0284

Chazaud, B., Sonnet, C., Lafuste, P., Bassez, G., Rimaniol, A. C., Poron, F., . . . Gherardi, R. K. (2003). Satellite cells attract monocytes and use macrophages as a support to escape apoptosis and enhance muscle growth. *J Cell Biol, 163*(5), 1133-1143. doi:10.1083/jcb.200212046

Christ, B., Jacob, M., & Jacob, H. J. (1983). On the origin and development of the ventrolateral abdominal muscles in the avian embryo. An experimental and ultrastructural study. *Anat Embryol (Berl), 166*(1), 87-101.

Cirak, S., Arechavala-Gomeza, V., Guglieri, M., Feng, L., Torelli, S., Anthony, K., . . . Muntoni, F. (2011). Exon skipping and dystrophin restoration in patients with Duchenne muscular dystrophy after systemic phosphorodiamidate morpholino oligomer treatment: an open-label, phase 2, dose-escalation study. *Lancet, 378*(9791), 595-605. doi:10.1016/S0140-6736(11)60756-3

Conti, F. J., Monkley, S. J., Wood, M. R., Critchley, D. R., & Muller, U. (2009). Talin 1 and 2 are required for myoblast fusion, sarcomere assembly and the maintenance of myotendinous junctions. *Development, 136*(21), 3597-3606. doi:10.1242/dev.035857

Conway, J., Al-Zahrani, K. N., Pryce, B. R., Abou-Hamad, J., & Sabourin, L. A. (2017). Transforming growth factor beta-induced epithelial to mesenchymal transition requires the Ste20-like kinase SLK independently of its catalytic activity. *Oncotarget, 8*(58), 98745-98756. doi:10.18632/oncotarget.21928

Cooper, B. J., Valentine, B. A., Wilson, S., Patterson, D. F., & Concannon, P. W. (1988). Canine muscular dystrophy: confirmation of X-linked inheritance. *J Hered, 79*(6), 405-408.

Cybulsky, A. V., Guillemette, J., Papillon, J., & Abouelazm, N. T. (2017). Regulation of Ste20-like kinase, SLK, activity: Dimerization and activation segment phosphorylation. *PLoS One, 12*(5), e0177226. doi:10.1371/journal.pone.0177226

Cybulsky, A. V., Takano, T., Papillon, J., Guillemette, J., Herzenberg, A. M., & Kennedy, C. R. (2010). Podocyte injury and albuminuria in mice with podocyte-specific overexpression of the Ste20-like kinase, SLK. *Am J Pathol, 177*(5), 2290-2299. doi:10.2353/ajpath.2010.100263

D'Angelo, M. G., Lorusso, M. L., Civati, F., Comi, G. P., Magri, F., Del Bo, R., . . . Bresolin, N. (2011). Neurocognitive profiles in Duchenne muscular dystrophy and gene mutation site. *Pediatr Neurol, 45*(5), 292-299. doi:10.1016/j.pediatrneurol.2011.08.003

Deconinck, A. E., Rafael, J. A., Skinner, J. A., Brown, S. C., Potter, A. C., Metzinger, L., . . . Davies, K. E. (1997). Utrophin-dystrophin-deficient mice as a model for Duchenne muscular dystrophy. *Cell, 90*(4), 717-727.

Deconinck, N., & Dan, B. (2007). Pathophysiology of duchenne muscular dystrophy: current hypotheses. *Pediatr Neurol, 36*(1), 1-7. doi:10.1016/j.pediatrneurol.2006.09.016

Delarosa, S., Guillemette, J., Papillon, J., Han, Y. S., Kristof, A. S., & Cybulsky, A. V. (2011). Activity of the Ste20-like kinase, SLK, is enhanced by homodimerization. *Am J Physiol Renal Physiol, 301*(3), F554-564. doi:10.1152/ajprenal.00062.2011

Derynck, R., Zhang, Y., & Feng, X. H. (1998). Smads: transcriptional activators of TGF-beta responses. *Cell, 95*(6), 737-740.

Desguerre, I., Mayer, M., Leturcq, F., Barbet, J. P., Gherardi, R. K., & Christov, C. (2009). Endomysial fibrosis in Duchenne muscular dystrophy: a marker of poor outcome associated with macrophage alternative activation. *J Neuropathol Exp Neurol, 68*(7), 762-773. doi:10.1097/NEN.0b013e3181aa31c2

Dietrich, S., Abou-Rebyeh, F., Brohmann, H., Bladt, F., Sonnenberg-Riethmacher, E., Yamaai, T., . . . Birchmeier, C. (1999). The role of SF/HGF and c-Met in the development of skeletal muscle. *Development, 126*(8), 1621-1629.

DiMario, J., Buffinger, N., Yamada, S., & Strohman, R. C. (1989). Fibroblast growth factor in the extracellular matrix of dystrophic (mdx) mouse muscle. *Science, 244*(4905), 688-690.

Dowling, P., Culligan, K., & Ohlendieck, K. (2002). Distal mdx muscle groups exhibiting up-regulation of utrophin and rescue of dystrophin-associated glycoproteins exemplify a protected phenotype in muscular dystrophy. *Naturwissenschaften, 89*(2), 75-78.

Dumont, N. A., Wang, Y. X., von Maltzahn, J., Pasut, A., Bentzinger, C. F., Brun, C. E., & Rudnicki, M. A. (2015). Dystrophin expression in muscle stem cells regulates their polarity and asymmetric division. *Nat Med, 21*(12), 1455-1463. doi:10.1038/nm.3990

Dutta, D., Anant, S., Ruiz-Gomez, M., Bate, M., & VijayRaghavan, K. (2004). Founder myoblasts and fibre number during adult myogenesis in Drosophila. *Development, 131*(15), 3761-3772. doi:10.1242/dev.01249

Falzarano, M. S., Scotton, C., Passarelli, C., & Ferlini, A. (2015). Duchenne Muscular Dystrophy: From Diagnosis to Therapy. *Molecules, 20*(10), 18168-18184. doi:10.3390/molecules201018168

Fayssoil, A., Nardi, O., Orlikowski, D., & Annane, D. (2010). Cardiomyopathy in Duchenne muscular dystrophy: pathogenesis and therapeutics. *Heart Fail Rev, 15*(1), 103-107. doi:10.1007/s10741-009-9156-8

Flanigan, K. M. (2014). Duchenne and Becker muscular dystrophies. *Neurol Clin, 32*(3), 671-688, viii. doi:10.1016/j.ncl.2014.05.002

Gheyara, A. L., Vallejo-Illarramendi, A., Zang, K., Mei, L., St-Arnaud, R., Dedhar, S., & Reichardt, L. F. (2007). Deletion of integrin-linked kinase from skeletal muscles of mice resembles muscular dystrophy due to alpha 7 beta 1-integrin deficiency. *Am J Pathol, 171*(6), 1966-1977. doi:10.2353/ajpath.2007.070555

Gildor, B., Massarwa, R., Shilo, B. Z., & Schejter, E. D. (2009). The SCAR and WASp nucleation-promoting factors act sequentially to mediate Drosophila myoblast fusion. *EMBO Rep, 10*(9), 1043-1050. doi:10.1038/embor.2009.129

Giordano, C., Mojumdar, K., Liang, F., Lemaire, C., Li, T., Richardson, J., . . . Petrof, B. J. (2015). Toll-like receptor 4 ablation in mdx mice reveals innate immunity as a therapeutic target in Duchenne muscular dystrophy. *Hum Mol Genet, 24*(8), 2147-2162. doi:10.1093/hmg/ddu735

Gros, J., Manceau, M., Thome, V., & Marcelle, C. (2005). A common somitic origin for embryonic muscle progenitors and satellite cells. *Nature, 435*(7044), 954-958. doi:10.1038/nature03572

Guerriero, V., Jr., & Florini, J. R. (1978). Stimulation by glucocorticoids of myoblast growth at low cell densities. *Cell Biol Int Rep, 2*(5), 441-446.

Guilluy, C., Rolli-Derkinderen, M., Loufrani, L., Bourge, A., Henrion, D., Sabourin, L., . . . Pacaud, P. (2008). Ste20-related kinase SLK phosphorylates Ser188 of RhoA to induce vasodilation in response to angiotensin II Type 2 receptor activation. *Circ Res, 102*(10), 1265-1274. doi:10.1161/CIRCRESAHA.107.164764

Guiraud, S., & Davies, K. E. (2017). Pharmacological advances for treatment in Duchenne muscular dystrophy. *Curr Opin Pharmacol, 34*, 36-48. doi:10.1016/j.coph.2017.04.002

Guo, C., Willem, M., Werner, A., Raivich, G., Emerson, M., Neyses, L., & Mayer, U. (2006). Absence of alpha 7 integrin in dystrophin-deficient mice causes a myopathy similar to Duchenne muscular dystrophy. *Hum Mol Genet, 15*(6), 989-998. doi:10.1093/hmg/ddl018

Hadwen, J., Farooq, F., Witherspoon, L., Schock, S., Mongeon, K., & MacKenzie, A. (2018). Anisomycin Activates Utrophin Upregulation Through a p38 Signaling Pathway. *Clin Transl Sci, 11*(5), 506-512. doi:10.1111/cts.12562

Hamer, P. W., McGeachie, J. M., Davies, M. J., & Grounds, M. D. (2002). Evans Blue Dye as an in vivo marker of myofibre damage: optimising parameters for detecting initial myofibre membrane permeability. *J Anat, 200*(Pt 1), 69-79.

Han, D. S., Yang, W. S., & Kao, T. W. (2017). Dexamethasone Treatment at the Myoblast Stage Enhanced C2C12 Myocyte Differentiation. *Int J Med Sci, 14*(5), 434-443. doi:10.7150/ijms.18427

Hao, W., Takano, T., Guillemette, J., Papillon, J., Ren, G., & Cybulsky, A. V. (2006). Induction of apoptosis by the Ste20-like kinase SLK, a germinal center kinase that activates apoptosis signal-regulating kinase and p38. *J Biol Chem, 281*(6), 3075-3084. doi:10.1074/jbc.M511744200

Haralalka, S., Shelton, C., Cartwright, H. N., Katzfey, E., Janzen, E., & Abmayr, S. M. (2011). Asymmetric Mbc, active Rac1 and F-actin foci in the fusion-competent myoblasts during myoblast fusion in Drosophila. *Development, 138*(8), 1551-1562. doi:10.1242/dev.057653

Heldin, C. H., Miyazono, K., & ten Dijke, P. (1997). TGF-beta signalling from cell membrane to nucleus through SMAD proteins. *Nature, 390*(6659), 465-471. doi:10.1038/37284

Heller, K. N., Montgomery, C. L., Janssen, P. M., Clark, K. R., Mendell, J. R., & Rodino-Klapac, L. R. (2013). AAV-mediated overexpression of human alpha7 integrin leads to histological and functional improvement in dystrophic mice. *Mol Ther, 21*(3), 520-525. doi:10.1038/mt.2012.281

Hindi, S. M., Tajrishi, M. M., & Kumar, A. (2013). Signaling mechanisms in mammalian myoblast fusion. *Sci Signal, 6*(272), re2. doi:10.1126/scisignal.2003832

Hodges, B. L., Hayashi, Y. K., Nonaka, I., Wang, W., Arahata, K., & Kaufman, S. J. (1997). Altered expression of the alpha7beta1 integrin in human and murine muscular dystrophies. *J Cell Sci, 110 (Pt 22)*, 2873-2881.

Hoffman, E. P., Brown, R. H., Jr., & Kunkel, L. M. (1987). Dystrophin: the protein product of the Duchenne muscular dystrophy locus. *Cell, 51*(6), 919-928.

Hoffman, E. P., & Kunkel, L. M. (1989). Dystrophin abnormalities in Duchenne/Becker muscular dystrophy. *Neuron, 2*(1), 1019-1029.

Hu, X. Y., Burghes, A. H., Ray, P. N., Thompson, M. W., Murphy, E. G., & Worton, R. G. (1988). Partial gene duplication in Duchenne and Becker muscular dystrophies. *J Med Genet, 25*(6), 369-376.

Hussein, M. R., Hamed, S. A., Mostafa, M. G., Abu-Dief, E. E., Kamel, N. F., & Kandil, M. R. (2006). The effects of glucocorticoid therapy on the inflammatory and dendritic cells in muscular dystrophies. *Int J Exp Pathol, 87*(6), 451-461. doi:10.1111/j.1365-2613.2006.00470.x

Ikeya, M., & Takada, S. (1998). Wnt signaling from the dorsal neural tube is required for the formation of the medial dermomyotome. *Development, 125*(24), 4969-4976.

Irwin, A. N., & Herink, M. C. (2017). Eteplirsen for the Treatment of Duchenne Muscular Dystrophy: Quality of Evidence Concerns-an Alternative Viewpoint. *Pharmacotherapy, 37*(10), e109-e111. doi:10.1002/phar.1996

Isaac, C., Wright, A., Usas, A., Li, H., Tang, Y., Mu, X., . . . Huard, J. (2013). Dystrophin and utrophin "double knockout" dystrophic mice exhibit a spectrum of degenerative musculoskeletal abnormalities. *J Orthop Res, 31*(3), 343-349. doi:10.1002/jor.22236

Itoh, S., Kameda, Y., Yamada, E., Tsujikawa, K., Mimura, T., & Kohama, Y. (1997). Molecular cloning and characterization of a novel putative STE20-like kinase in guinea pigs. *Arch Biochem Biophys, 340*(2), 201-207. doi:10.1006/abbi.1997.9893

Iwasaki, K., Hayashi, K., Fujioka, T., & Sobue, K. (2008). Rho/Rho-associated kinase signal regulates myogenic differentiation via myocardin-related transcription factor-A/Smad-dependent transcription of the Id3 gene. *J Biol Chem, 283*(30), 21230-21241. doi:10.1074/jbc.M710525200

Jaberi, A., Hooker, E., Guillemette, J., Papillon, J., Kristof, A. S., & Cybulsky, A. V. (2015). Identification of Tpr and alpha-actinin-4 as two novel SLK-interacting proteins. *Biochim Biophys Acta, 1853*(10 Pt A), 2539-2552. doi:10.1016/j.bbamcr.2015.06.005

Jarvinen, T. A., Kaariainen, M., Jarvinen, M., & Kalimo, H. (2000). Muscle strain injuries. *Curr Opin Rheumatol, 12*(2), 155-161.

Kablar, B., Asakura, A., Krastel, K., Ying, C., May, L. L., Goldhamer, D. J., & Rudnicki, M. A. (1998). MyoD and Myf-5 define the specification of musculature of distinct embryonic origin. *Biochem Cell Biol, 76*(6), 1079-1091.

Kassar-Duchossoy, L., Giacone, E., Gayraud-Morel, B., Jory, A., Gomes, D., & Tajbakhsh, S. (2005). Pax3/Pax7 mark a novel population of primitive myogenic cells during development. *Genes Dev, 19*(12), 1426-1431. doi:10.1101/gad.345505

Kim, S., Campbell, K. A., Fox, D. J., Matthews, D. J., Valdez, R., & STARnet, M. D. (2015). Corticosteroid Treatments in Males With Duchenne Muscular Dystrophy: Treatment Duration and Time to Loss of Ambulation. *J Child Neurol, 30*(10), 1275-1280. doi:10.1177/0883073814558120

Kim, S., Shilagardi, K., Zhang, S., Hong, S. N., Sens, K. L., Bo, J., . . . Chen, E. H. (2007). A critical function for the actin cytoskeleton in targeted exocytosis of prefusion vesicles during myoblast fusion. *Dev Cell, 12*(4), 571-586. doi:10.1016/j.devcel.2007.02.019

Kobayashi, Y. M., Rader, E. P., Crawford, R. W., & Campbell, K. P. (2012). Endpoint measures in the mdx mouse relevant for muscular dystrophy pre-clinical studies. *Neuromuscul Disord, 22*(1), 34-42. doi:10.1016/j.nmd.2011.08.001

Kornegay, J. N., Tuler, S. M., Miller, D. M., & Levesque, D. C. (1988). Muscular dystrophy in a litter of golden retriever dogs. *Muscle Nerve, 11*(10), 1056-1064. doi:10.1002/mus.880111008

Kuang, S., Kuroda, K., Le Grand, F., & Rudnicki, M. A. (2007). Asymmetric self-renewal and commitment of satellite stem cells in muscle. *Cell, 129*(5), 999-1010. doi:10.1016/j.cell.2007.03.044

Lafuste, P., Sonnet, C., Chazaud, B., Dreyfus, P. A., Gherardi, R. K., Wewer, U. M., & Authier, F. J. (2005). ADAM12 and alpha9beta1 integrin are instrumental in human myogenic cell differentiation. *Mol Biol Cell, 16*(2), 861-870. doi:10.1091/mbc.e04-03-0226

Lee, S. J., & McPherron, A. C. (2001). Regulation of myostatin activity and muscle growth. *Proc Natl Acad Sci U S A, 98*(16), 9306-9311. doi:10.1073/pnas.151270098

Lewis, I. (1966). Late-onset muscle dystrophy: oculopharyngoesophageal variety. *Can Med Assoc J, 95*(4), 146-150.

Li, S., Kimura, E., Ng, R., Fall, B. M., Meuse, L., Reyes, M., . . . Chamberlain, J. S. (2006). A highly functional mini-dystrophin/GFP fusion gene for cell and gene therapy studies of Duchenne muscular dystrophy. *Hum Mol Genet, 15*(10), 1610-1622. doi:10.1093/hmg/ddl082

Liao, H. K., Hatanaka, F., Araoka, T., Reddy, P., Wu, M. Z., Sui, Y., . . . Izpisua Belmonte, J. C. (2017). In Vivo Target Gene Activation via CRISPR/Cas9-Mediated Trans-epigenetic Modulation. *Cell, 171*(7), 1495-1507 e1415. doi:10.1016/j.cell.2017.10.025

Liu, D., Black, B. L., & Derynck, R. (2001). TGF-beta inhibits muscle differentiation through functional repression of myogenic transcription factors by Smad3. *Genes Dev, 15*(22), 2950-2966. doi:10.1101/gad.925901

Liu, D., Kang, J. S., & Derynck, R. (2004). TGF-beta-activated Smad3 represses MEF2-dependent transcription in myogenic differentiation. *EMBO J, 23*(7), 1557-1566. doi:10.1038/sj.emboj.7600179

Liu, Y., Shah, K., Yang, F., Witucki, L., & Shokat, K. M. (1998). Engineering Src family protein kinases with unnatural nucleotide specificity. *Chem Biol, 5*(2), 91-101.

Lluis, F., Ballestar, E., Suelves, M., Esteller, M., & Munoz-Canoves, P. (2005). E47 phosphorylation by p38 MAPK promotes MyoD/E47 association and muscle-specific gene transcription. *EMBO J, 24*(5), 974-984. doi:10.1038/sj.emboj.7600528

Long, C., Amoasii, L., Mireault, A. A., McAnally, J. R., Li, H., Sanchez-Ortiz, E., . . . Olson, E. N. (2016). Postnatal genome editing partially restores dystrophin expression in a mouse model of muscular dystrophy. *Science, 351*(6271), 400-403. doi:10.1126/science.aad5725

Lorts, A., Schwanekamp, J. A., Baudino, T. A., McNally, E. M., & Molkentin, J. D. (2012). Deletion of periostin reduces muscular dystrophy and fibrosis in mice by modulating the transforming growth factor-beta pathway. *Proc Natl Acad Sci U S A, 109*(27), 10978-10983. doi:10.1073/pnas.1204708109

Luhovy, A. Y., Jaberi, A., Papillon, J., Guillemette, J., & Cybulsky, A. V. (2012). Regulation of the Ste20-like kinase, SLK: involvement of activation segment phosphorylation. *J Biol Chem, 287*(8), 5446-5458. doi:10.1074/jbc.M111.302018

Madaro, L., Marrocco, V., Fiore, P., Aulino, P., Smeriglio, P., Adamo, S., . . . Bouche, M. (2011). PKCtheta signaling is required for myoblast fusion by regulating the expression of caveolin-3 and beta1D integrin upstream focal adhesion kinase. *Mol Biol Cell, 22*(8), 1409-1419. doi:10.1091/mbc.E10-10-0821

Massari, M. E., & Murre, C. (2000). Helix-loop-helix proteins: regulators of transcription in eucaryotic organisms. *Mol Cell Biol, 20*(2), 429-440.

Mauro, A. (1961). Satellite cell of skeletal muscle fibers. *J Biophys Biochem Cytol, 9*, 493-495.

McDonald, A. A., Hebert, S. L., Kunz, M. D., Ralles, S. J., & McLoon, L. K. (2015). Disease course in mdx:utrophin+/- mice: comparison of three mouse models of Duchenne muscular dystrophy. *Physiol Rep, 3*(4). doi:10.14814/phy2.12391

McGreevy, J. W., Hakim, C. H., McIntosh, M. A., & Duan, D. (2015). Animal models of Duchenne muscular dystrophy: from basic mechanisms to gene therapy. *Dis Model Mech, 8*(3), 195-213. doi:10.1242/dmm.018424

McPherron, A. C., Lawler, A. M., & Lee, S. J. (1997). Regulation of skeletal muscle mass in mice by a new TGF-beta superfamily member. *Nature, 387*(6628), 83-90. doi:10.1038/387083a0

Mendell, J. R., Rodino-Klapac, L. R., Sahenk, Z., Roush, K., Bird, L., Lowes, L. P., . . . Eteplirsen Study, G. (2013). Eteplirsen for the treatment of Duchenne muscular dystrophy. *Ann Neurol, 74*(5), 637-647. doi:10.1002/ana.23982

Millay, D. P., O'Rourke, J. R., Sutherland, L. B., Bezprozvannaya, S., Shelton, J. M., Bassel-Duby, R., & Olson, E. N. (2013). Myomaker is a membrane activator of myoblast fusion and muscle formation. *Nature, 499*(7458), 301-305. doi:10.1038/nature12343

Millay, D. P., Sutherland, L. B., Bassel-Duby, R., & Olson, E. N. (2014). Myomaker is essential for muscle regeneration. *Genes Dev, 28*(15), 1641-1646. doi:10.1101/gad.247205.114

Miskew Nichols, B., Aoki, Y., Kuraoka, M., Lee, J. J., Takeda, S., & Yokota, T. (2016). Multi-exon Skipping Using Cocktail Antisense Oligonucleotides in the Canine X-linked Muscular Dystrophy. *J Vis Exp*(111). doi:10.3791/53776

Miyazono, K. (2009). Transforming growth factor-beta signaling in epithelial-mesenchymal transition and progression of cancer. *Proc Jpn Acad Ser B Phys Biol Sci, 85*(8), 314-323.

Moens, P., Baatsen, P. H., & Marechal, G. (1993). Increased susceptibility of EDL muscles from mdx mice to damage induced by contractions with stretch. *J Muscle Res Cell Motil, 14*(4), 446-451.

Morales, M. G., Gutierrez, J., Cabello-Verrugio, C., Cabrera, D., Lipson, K. E., Goldschmeding, R., & Brandan, E. (2013). Reducing CTGF/CCN2 slows down mdx muscle dystrophy and improves cell therapy. *Hum Mol Genet, 22*(24), 4938-4951. doi:10.1093/hmg/ddt352

Morley, J. E., Baumgartner, R. N., Roubenoff, R., Mayer, J., & Nair, K. S. (2001). Sarcopenia. *J Lab Clin Med, 137*(4), 231-243. doi:10.1067/mlc.2001.113504

Nakao, A., Afrakhte, M., Moren, A., Nakayama, T., Christian, J. L., Heuchel, R., . . . ten Dijke, P. (1997). Identification of Smad7, a TGFbeta-inducible antagonist of TGF-beta signalling. *Nature, 389*(6651), 631-635. doi:10.1038/39369

Narola, J., Pandey, S. N., Glick, A., & Chen, Y. W. (2013). Conditional expression of TGF-beta1 in skeletal muscles causes endomysial fibrosis and myofibers atrophy. *PLoS One, 8*(11), e79356. doi:10.1371/journal.pone.0079356

Nelson, C. A., Hunter, R. B., Quigley, L. A., Girgenrath, S., Weber, W. D., McCullough, J. A., . . . Wentworth, B. M. (2011). Inhibiting TGF-beta activity improves respiratory function in mdx mice. *Am J Pathol, 178*(6), 2611-2621. doi:10.1016/j.ajpath.2011.02.024

O'Reilly, P. G., Wagner, S., Franks, D. J., Cailliau, K., Browaeys, E., Dissous, C., & Sabourin, L. A. (2005). The Ste20-like kinase SLK is required for cell cycle progression through G2. *J Biol Chem, 280*(51), 42383-42390. doi:10.1074/jbc.M510763200

Olson, M. F., Ashworth, A., & Hall, A. (1995). An essential role for Rho, Rac, and Cdc42 GTPases in cell cycle progression through G1. *Science, 269*(5228), 1270-1272.

Parr, B. A., Shea, M. J., Vassileva, G., & McMahon, A. P. (1993). Mouse Wnt genes exhibit discrete domains of expression in the early embryonic CNS and limb buds. *Development, 119*(1), 247-261.

Peladeau, C., Adam, N. J., & Jasmin, B. J. (2018). Celecoxib treatment improves muscle function in mdx mice and increases utrophin A expression. *FASEB J*, fj201800081R. doi:10.1096/fj.201800081R

Peter, A. K., Cheng, H., Ross, R. S., Knowlton, K. U., & Chen, J. (2011). The costamere bridges sarcomeres to the sarcolemma in striated muscle. *Prog Pediatr Cardiol, 31*(2), 83-88. doi:10.1016/j.ppedcard.2011.02.003

Porter, J. D., Khanna, S., Kaminski, H. J., Rao, J. S., Merriam, A. P., Richmonds, C. R., . . . Andrade, F. H. (2002). A chronic inflammatory response dominates the skeletal muscle molecular signature in dystrophin-deficient mdx mice. *Hum Mol Genet, 11*(3), 263-272.

Pourquie, O., Coltey, M., Breant, C., & Le Douarin, N. M. (1995). Control of somite patterning by signals from the lateral plate. *Proc Natl Acad Sci U S A, 92*(8), 3219-3223.

Pu, Q., Abduelmula, A., Masyuk, M., Theiss, C., Schwandulla, D., Hans, M., . . . Huang, R. (2013). The dermomyotome ventrolateral lip is essential for the hypaxial myotome formation. *BMC Dev Biol, 13*, 37. doi:10.1186/1471-213X-13-37

Puri, P. L., Wu, Z., Zhang, P., Wood, L. D., Bhakta, K. S., Han, J., . . . Wang, J. Y. (2000). Induction of terminal differentiation by constitutive activation of p38 MAP kinase in human rhabdomyosarcoma cells. *Genes Dev, 14*(5), 574-584.

Quach, N. L., Biressi, S., Reichardt, L. F., Keller, C., & Rando, T. A. (2009). Focal adhesion kinase signaling regulates the expression of caveolin 3 and beta1 integrin, genes essential for normal myoblast fusion. *Mol Biol Cell, 20*(14), 3422-3435. doi:10.1091/mbc.E09-02-0175

Quach, N. L., & Rando, T. A. (2006). Focal adhesion kinase is essential for costamerogenesis in cultured skeletal muscle cells. *Dev Biol, 293*(1), 38-52. doi:10.1016/j.ydbio.2005.12.040

Quinn, M. E., Goh, Q., Kurosaka, M., Gamage, D. G., Petrany, M. J., Prasad, V., & Millay, D. P. (2017). Myomerger induces fusion of non-fusogenic cells and is required for skeletal muscle development. *Nat Commun, 8*, 15665. doi:10.1038/ncomms15665

Quizi, J. L., Baron, K., Al-Zahrani, K. N., O'Reilly, P., Sriram, R. K., Conway, J., . . . Sabourin, L. A. (2013). SLK-mediated phosphorylation of paxillin is required for focal adhesion turnover and cell migration. *Oncogene, 32*(39), 4656-4663. doi:10.1038/onc.2012.488

Reuveny, M., Heller, H., & Bengal, E. (2004). RhoA controls myoblast survival by inducing the phosphatidylinositol 3-kinase-Akt signaling pathway. *FEBS Lett, 569*(1-3), 129-134. doi:10.1016/j.febslet.2004.05.035

Rolli-Derkinderen, M., Sauzeau, V., Boyer, L., Lemichez, E., Baron, C., Henrion, D., . . . Pacaud, P. (2005). Phosphorylation of serine 188 protects RhoA from ubiquitin/proteasome-mediated degradation in vascular smooth muscle cells. *Circ Res, 96*(11), 1152-1160. doi:10.1161/01.RES.0000170084.88780.ea

Roovers, K., Wagner, S., Storbeck, C. J., O'Reilly, P., Lo, V., Northey, J. J., . . . Sabourin, L. A. (2009). The Ste20-like kinase SLK is required for ErbB2-driven breast cancer cell motility. *Oncogene, 28*(31), 2839-2848. doi:10.1038/onc.2009.146

Rudnicki, M. A., Braun, T., Hinuma, S., & Jaenisch, R. (1992). Inactivation of MyoD in mice leads to up-regulation of the myogenic HLH gene Myf-5 and results in apparently normal muscle development. *Cell, 71*(3), 383-390.

Rudnicki, M. A., Schnegelsberg, P. N., Stead, R. H., Braun, T., Arnold, H. H., & Jaenisch, R. (1993). MyoD or Myf-5 is required for the formation of skeletal muscle. *Cell, 75*(7), 1351-1359.

Sabourin, L. A., & Rudnicki, M. A. (1999). Induction of apoptosis by SLK, a Ste20-related kinase. *Oncogene, 18*(52), 7566-7575. doi:10.1038/sj.onc.1203119

Sabourin, L. A., & Rudnicki, M. A. (2000). The molecular regulation of myogenesis. *Clin Genet, 57*(1), 16-25.

Sabourin, L. A., Tamai, K., Seale, P., Wagner, J., & Rudnicki, M. A. (2000). Caspase 3 cleavage of the Ste20-related kinase SLK releases and activates an apoptosis-inducing kinase domain and an actin-disassembling region. *Mol Cell Biol, 20*(2), 684-696.

Salmaninejad, A., Valilou, S. F., Bayat, H., Ebadi, N., Daraei, A., Yousefi, M., . . . Mojarrad, M. (2018). Duchenne muscular dystrophy: an updated review of common available therapies. *Int J Neurosci, 128*(9), 854-864. doi:10.1080/00207454.2018.1430694

Sassoon, C. S., Zhu, E., Pham, H. T., Nelson, R. S., Fang, L., Baker, M. J., & Caiozzo, V. J. (2008). Acute effects of high-dose methylprednisolone on diaphragm muscle function. *Muscle Nerve, 38*(3), 1161-1172. doi:10.1002/mus.21048

Schienda, J., Engleka, K. A., Jun, S., Hansen, M. S., Epstein, J. A., Tabin, C. J., . . . Kardon, G. (2006). Somitic origin of limb muscle satellite and side population cells. *Proc Natl Acad Sci U S A, 103*(4), 945-950. doi:10.1073/pnas.0510164103

Schultz, E., Gibson, M. C., & Champion, T. (1978). Satellite cells are mitotically quiescent in mature mouse muscle: an EM and radioautographic study. *J Exp Zool, 206*(3), 451-456. doi:10.1002/jez.1402060314

Schwander, M., Leu, M., Stumm, M., Dorchies, O. M., Ruegg, U. T., Schittny, J., & Muller, U. (2003). Beta1 integrins regulate myoblast fusion and sarcomere assembly. *Dev Cell, 4*(5), 673-685.

Seale, P., Sabourin, L. A., Girgis-Gabardo, A., Mansouri, A., Gruss, P., & Rudnicki, M. A. (2000). Pax7 is required for the specification of myogenic satellite cells. *Cell, 102*(6), 777-786.

Serra, F., Quarta, M., Canato, M., Toniolo, L., De Arcangelis, V., Trotta, A., . . . Naro, F. (2012). Inflammation in muscular dystrophy and the beneficial effects of non-steroidal anti-inflammatory drugs. *Muscle Nerve, 46*(5), 773-784. doi:10.1002/mus.23432

Sharp, N. J., Kornegay, J. N., Van Camp, S. D., Herbstreith, M. H., Secore, S. L., Kettle, S., . . . et al. (1992). An error in dystrophin mRNA processing in golden retriever muscular dystrophy, an animal homologue of Duchenne muscular dystrophy. *Genomics, 13*(1), 115-121.

Shin, J., Tajrishi, M. M., Ogura, Y., & Kumar, A. (2013). Wasting mechanisms in muscular dystrophy. *Int J Biochem Cell Biol, 45*(10), 2266-2279. doi:10.1016/j.biocel.2013.05.001

Sicinski, P., Geng, Y., Ryder-Cook, A. S., Barnard, E. A., Darlison, M. G., & Barnard, P. J. (1989). The molecular basis of muscular dystrophy in the mdx mouse: a point mutation. *Science, 244*(4912), 1578-1580.

Song, Y., Yao, S., Liu, Y., Long, L., Yang, H., Li, Q., . . . Zhang, N. (2017). Expression levels of TGF-beta1 and CTGF are associated with the severity of Duchenne muscular dystrophy. *Exp Ther Med, 13*(4), 1209-1214. doi:10.3892/etm.2017.4105

St Pierre, B. A., & Tidball, J. G. (1994). Differential response of macrophage subpopulations to soleus muscle reloading after rat hindlimb suspension. *J Appl Physiol (1985), 77*(1), 290-297. doi:10.1152/jappl.1994.77.1.290

Storbeck, C. J., Al-Zahrani, K. N., Sriram, R., Kawesa, S., O'Reilly, P., Daniel, K., . . . Sabourin, L. A. (2013). Distinct roles for Ste20-like kinase SLK in muscle function and regeneration. *Skelet Muscle, 3*(1), 16. doi:10.1186/2044-5040-3-16

Storbeck, C. J., Daniel, K., Zhang, Y. H., Lunde, J., Scime, A., Asakura, A., . . . Sabourin, L. A. (2004). Ste20-like kinase SLK displays myofiber type specificity and is involved in C2C12 myoblast differentiation. *Muscle Nerve, 29*(4), 553-564. doi:10.1002/mus.20000

Storbeck, C. J., Wagner, S., O'Reilly, P., McKay, M., Parks, R. J., Westphal, H., & Sabourin, L. A. (2009). The Ldb1 and Ldb2 transcriptional cofactors interact with the Ste20-like kinase SLK and regulate cell migration. *Mol Biol Cell, 20*(19), 4174-4182. doi:10.1091/mbc.E08-07-0707

Strunkelnberg, M., Bonengel, B., Moda, L. M., Hertenstein, A., de Couet, H. G., Ramos, R. G., & Fischbach, K. F. (2001). rst and its paralogue kirre act redundantly during embryonic muscle development in Drosophila. *Development, 128*(21), 4229-4239.

Tajbakhsh, S., Rocancourt, D., Cossu, G., & Buckingham, M. (1997). Redefining the genetic hierarchies controlling skeletal myogenesis: Pax-3 and Myf-5 act upstream of MyoD. *Cell, 89*(1), 127-138.

Tanabe, Y., Esaki, K., & Nomura, T. (1986). Skeletal muscle pathology in X chromosome-linked muscular dystrophy (mdx) mouse. *Acta Neuropathol, 69*(1-2), 91-95.

Taniguti, A. P., Pertille, A., Matsumura, C. Y., Santo Neto, H., & Marques, M. J. (2011). Prevention of muscle fibrosis and myonecrosis in mdx mice by suramin, a TGF-beta1 blocker. *Muscle Nerve, 43*(1), 82-87. doi:10.1002/mus.21869

Tatsumi, R., Anderson, J. E., Nevoret, C. J., Halevy, O., & Allen, R. E. (1998). HGF/SF is present in normal adult skeletal muscle and is capable of activating satellite cells. *Dev Biol, 194*(1), 114-128. doi:10.1006/dbio.1997.8803

Tidball, J. G. (1995). Inflammatory cell response to acute muscle injury. *Med Sci Sports Exerc, 27*(7), 1022-1032.

Tixier, V., Bataille, L., & Jagla, K. (2010). Diversification of muscle types: recent insights from Drosophila. *Exp Cell Res, 316*(18), 3019-3027. doi:10.1016/j.yexcr.2010.07.013

Tremblay, P., Dietrich, S., Mericskay, M., Schubert, F. R., Li, Z., & Paulin, D. (1998). A crucial role for Pax3 in the development of the hypaxial musculature and the long-range migration of muscle precursors. *Dev Biol, 203*(1), 49-61. doi:10.1006/dbio.1998.9041

Vieira, N. M., Elvers, I., Alexander, M. S., Moreira, Y. B., Eran, A., Gomes, J. P., . . . Zatz, M. (2015). Jagged 1 Rescues the Duchenne Muscular Dystrophy Phenotype. *Cell, 163*(5), 1204-1213. doi:10.1016/j.cell.2015.10.049

Villalta, S. A., Nguyen, H. X., Deng, B., Gotoh, T., & Tidball, J. G. (2009). Shifts in macrophage phenotypes and macrophage competition for arginine metabolism affect the severity of muscle pathology in muscular dystrophy. *Hum Mol Genet, 18*(3), 482-496. doi:10.1093/hmg/ddn376

Villalta, S. A., Rinaldi, C., Deng, B., Liu, G., Fedor, B., & Tidball, J. G. (2011). Interleukin-10 reduces the pathology of mdx muscular dystrophy by deactivating M1 macrophages and modulating macrophage phenotype. *Hum Mol Genet, 20*(4), 790-805. doi:10.1093/hmg/ddq523

Voit, A., Patel, V., Pachon, R., Shah, V., Bakhutma, M., Kohlbrenner, E., . . . Babu, G. J. (2017). Reducing sarcolipin expression mitigates Duchenne muscular dystrophy and associated cardiomyopathy in mice. *Nat Commun, 8*(1), 1068. doi:10.1038/s41467-017-01146-7

Waddell, D. S., Baehr, L. M., van den Brandt, J., Johnsen, S. A., Reichardt, H. M., Furlow, J. D., & Bodine, S. C. (2008). The glucocorticoid receptor and FOXO1 synergistically activate the skeletal muscle atrophy-associated MuRF1 gene. *Am J Physiol Endocrinol Metab, 295*(4), E785-797. doi:10.1152/ajpendo.00646.2007

Wagner, S., Storbeck, C. J., Roovers, K., Chaar, Z. Y., Kolodziej, P., McKay, M., & Sabourin, L. A. (2008). FAK/src-family dependent activation of the Ste20-like kinase SLK is required for microtubule-dependent focal adhesion turnover and cell migration. *PLoS One, 3*(4), e1868. doi:10.1371/journal.pone.0001868

Wei, L., Zhou, W., Croissant, J. D., Johansen, F. E., Prywes, R., Balasubramanyam, A., & Schwartz, R. J. (1998). RhoA signaling via serum response factor plays an obligatory role in myogenic differentiation. *J Biol Chem, 273*(46), 30287-30294.

Weiss, A., & Attisano, L. (2013). The TGFbeta superfamily signaling pathway. *Wiley Interdiscip Rev Dev Biol, 2*(1), 47-63. doi:10.1002/wdev.86

Weston, A. D., Sampaio, A. V., Ridgeway, A. G., & Underhill, T. M. (2003). Inhibition of p38 MAPK signaling promotes late stages of myogenesis. *J Cell Sci, 116*(Pt 14), 2885-2893. doi:10.1242/jcs.00525

Wissing, E. R., Boyer, J. G., Kwong, J. Q., Sargent, M. A., Karch, J., McNally, E. M., . . . Molkentin, J. D. (2014). P38alpha MAPK underlies muscular dystrophy and myofiber death through a Bax-dependent mechanism. *Hum Mol Genet, 23*(20), 5452-5463. doi:10.1093/hmg/ddu270

Wrana, J. L., Attisano, L., Carcamo, J., Zentella, A., Doody, J., Laiho, M., . . . Massague, J. (1992). TGF beta signals through a heteromeric protein kinase receptor complex. *Cell, 71*(6), 1003-1014.

Wu, Z., Woodring, P. J., Bhakta, K. S., Tamura, K., Wen, F., Feramisco, J. R., . . . Puri, P. L. (2000). p38 and extracellular signal-regulated kinases regulate the myogenic program at multiple steps. *Mol Cell Biol, 20*(11), 3951-3964.

Xu, L., Park, K. H., Zhao, L., Xu, J., El Refaey, M., Gao, Y., . . . Han, R. (2016). CRISPR-mediated Genome Editing Restores Dystrophin Expression and Function in mdx Mice. *Mol Ther, 24*(3), 564-569. doi:10.1038/mt.2015.192

Yamada, E., Tsujikawa, K., Itoh, S., Kameda, Y., Kohama, Y., & Yamamoto, H. (2000). Molecular cloning and characterization of a novel human STE20-like kinase, hSLK. *Biochim Biophys Acta, 1495*(3), 250-262.

Yamazaki, M., Minota, S., Sakurai, H., Miyazono, K., Yamada, A., Kanazawa, I., & Kawai, M. (1994). Expression of transforming growth factor-beta 1 and its relation to endomysial fibrosis in progressive muscular dystrophy. *Am J Pathol, 144*(2), 221-226.

Yu, L., Hebert, M. C., & Zhang, Y. E. (2002). TGF-beta receptor-activated p38 MAP kinase mediates Smad-independent TGF-beta responses. *EMBO J, 21*(14), 3749-3759. doi:10.1093/emboj/cdf366

Zetser, A., Gredinger, E., & Bengal, E. (1999). p38 mitogen-activated protein kinase pathway promotes skeletal muscle differentiation. Participation of the Mef2c transcription factor. *J Biol Chem, 274*(8), 5193-5200.

Zhang, Q., Vashisht, A. A., O'Rourke, J., Corbel, S. Y., Moran, R., Romero, A., . . . Sampath, S. C. (2017). The microprotein Minion controls cell fusion and muscle formation. *Nat Commun, 8*, 15664. doi:10.1038/ncomms15664

Zhang, Y. H., Hume, K., Cadonic, R., Thompson, C., Hakim, A., Staines, W., & Sabourin, L. A. (2002). Expression of the Ste20-like kinase SLK during embryonic development and in the murine adult central nervous system. *Brain Res Dev Brain Res, 139*(2), 205-215.

Zhapparova, O. N., Fokin, A. I., Vorobyeva, N. E., Bryantseva, S. A., & Nadezhdina, E. S. (2013). Ste20-like protein kinase SLK (LOSK) regulates microtubule organization by targeting dynactin to the centrosome. *Mol Biol Cell, 24*(20), 3205-3214. doi:10.1091/mbc.E13-03-0137

Zhou, L., Porter, J. D., Cheng, G., Gong, B., Hatala, D. A., Merriam, A. P., . . . Kaminski, H. J. (2006). Temporal and spatial mRNA expression patterns of TGF-beta1, 2, 3 and TbetaRI, II, III in skeletal muscles of mdx mice. *Neuromuscul Disord, 16*(1), 32-38. doi:10.1016/j.nmd.2005.09.009

Zhu, P., Wu, F., Mosenson, J., Zhang, H., He, T. C., & Wu, W. S. (2017). CRISPR/Cas9-Mediated Genome Editing Corrects Dystrophin Mutation in Skeletal Muscle Stem Cells in a Mouse Model of Muscle Dystrophy. *Mol Ther Nucleic Acids, 7*, 31-41. doi:10.1016/j.omtn.2017.02.007

Zhu, S., Goldschmidt-Clermont, P. J., & Dong, C. (2004). Transforming growth factor-beta-induced inhibition of myogenesis is mediated through Smad pathway and is modulated by microtubule dynamic stability. *Circ Res, 94*(5), 617-625. doi:10.1161/01.RES.0000118599.25944.D5